ADDIS ABABA UNIVERSITY

SCHOOL OF GRADUATE STUDIES

ADDIS ABABA INSTITUTE OF TECHNOLOGY

DEPARTMENT OF CIVIL ENGINEERING

MSc THESIS
ON

CLIMATE CHANGE IMPACT ASSESSMENT ON WATER RESOURCES AVALIBLITY

(A case study for the selected catchments in Upper Blue Nile Basin)

May, 2011

ADDIS ABABA UNIVERSITY
SCHOOL OF GRADUATE STUDIES
ADDIS ABABA INSTITUTE OF TECHNOLOGY

DEPARTMENT OF CIVIL ENGINEERING

MSc THESIS

ON

CLIMATE CHANGE IMPACT ASSESSMENT ON WATER RESOURCES AVALIBLITY

(A case study for the selected catchments in Upper Blue Nile Basin)

BY: DEREJE LIBEN SEGNI
ADVISOR: Dr. SEMU AYALEW MOGES

May, 2011

ADDIS ABABA UNIVERSITY
Addis Ababa Institute of Technology
Department of Civil Engineering

Climate Change Impact Assessment on Water Resource Availability in the Catchments of Upper Blue Nile Basin

Thesis Submitted to the School of Graduate Studies in Partial Fulfilment of the Requirements for the Degree of

Master of Science

In

Civil Engineering

By

Dereje Liben Segni

APPROVED BY BOARD OF EXAMINERS

Dr. Semu Ayalew	----------	----------
(Advisor)	Signature	Date
Dr. Ing. Dereje Hailu	----------	----------
(External Examiner)	Signature	Date
Dr. Daniel Fikre Silassie	----------	----------
(Internal Examiner)	Signature	Date
Ato Dereje Tadesse	----------	----------
(Chairman)	Signature	Date

Climate Change Impact Assessment on Water Resource Availability in the Catchments of Upper Blue Nile Basin

By Dereje Liben Segni

Thesis Submitted to the University of Addis Ababa, Addis Ababa Institute of Technology (AAIT) as a Partial fulfillment of the requirements for the Degree of Masters of Science in Civil Engineering, Major Hydraulics.

Addis Ababa University
Addis Ababa Institute of Technology
School of Post Graduate Studies

May, 2011

DECLARATION AND COPY RIGHT

Dereje Liben Segni, declare that this Thesis is my own original work and that it has not been presented and will not be presented by me to any other university for similar or any other degree award.

Signature_____

DEDICATION

I dedicate this work to my family, my friends and especially to my parents who are the reasons for who I am!

Acknowledgement

At first and at most I would like to thank the almighty God for giving me the courage and wisdom to reach this point in my life.

I would like to express my sincere gratitude to my advisor, Dr. Semu Ayalew, for his unreserved assistance, constructive and timely comments at all stages of my work and also for supplying me relevant materials to carry out the research. I should strongly appreciate his patienceful guidance in a lot of discussions we made on various problems I faced during the course of the work.

I am very grateful to Addis Ababa Institute of Technology, Department of Civil Engineering for allowing me to take part in the Master Program and for my employer Oromia Water Works Design and Supervision Enterprise for granting me by sponsoring and made my dream come true. I also wish to extend my deepest gratitude to Ato Girma Sanbata Deputy Head of Oromia Water, Mineral and Energy Bureau, for his contribution during the process of sponsorship award and for all his unlimited supports, without his encouragement and care this would not have happened.

I also acknowledge, Hydrology Department of the Ministry of Water and Energy and the National Meteorological Service Agency, who supplied me data free of charge.

I am also grateful to Mr. Yared Ashenafi, who helped me in the hydrological modeling part, who solved my problems when I got stuck at some critical points. I am very grateful to all my teachers who taught me from grass root to this level.

Last but not least I would like to thank my mother, Likitu Tuku, my sweet love Ayantu Abera and my sister Birhane Liben, who have been always encouraging my academic undertakings with prayer and moral inspiration.

Finally, I would like to express my warm feeling of appreciation and tank to my friends who helped me in all stages especially to Kumela Tufa, Demeke Amana, Taye Adugna, Daneil Shewangizaw, Tamiru Lamessa, Ashenafi Abraham and Bethlehem Tezera, who were spiritually with me, and gave me the strength to finalize my duties successfully. Thanks for your encouragement and true friendship! Your friendship meant a great deal to me.

Abstract

The purpose of this thesis is to assess the significance of the climate change impact on streamflow at local scale (catchment scale) for some selected catchments in Upper Blue Nile Basin. The five catchments included in the study were Koga, Birr, Muger, Guder and Didessa Rivers.

The Soil and Water Assessment Tool (SWAT) model is applied to study of the hydrology of the catchments and associated uncertainty with the simulated outputs. The SWAT model was calibrated for the period of 1992 to 2001 and validated for the period of 2001-2005. Model uncertainty was also done to establish the uncertainty bounds of the model, which is also the important boundary limit to evaluate the significance of the impact of climate change. The uncertainty analysis was done by using SUFI2 in SWAT-CUP. In the end, the climate change impact studies on water availability of the catchments were done based on the outputs of the Regional Climate Model (RegCM3) of emission scenario A1B.

Overall the calibration and validation of the model was good except for Didessa. It was also shown from the model uncertainties analysis that the percentage of the simulated data within the uncertainty bound is only 24% for Didessa and 20% for Guder (P-factor=0.24, 0.20) which are relatively poor for both catchments. But for other catchments the percentage of simulated flow within the uncertainty limit during calibration and verification is more than 40% (P-factor=0.4).

In general in all catchments; the impact of climate change may cause an increase in annual flow in both periods except in Koga and Didessa rivers. The estimation of the annual and monthly average flow volume changes in both period shows, the flow volume incremental range might be 48% to 185%. On the contrary, the decrement range flow in both rivers might be 0.33% to 6.7%.

According to the uncertainty analysis carried out, the significance of the climatic change impacts for all catchment was analyzed. As a result it might be possible to conclude that for all catchments the impacts were significant except for Muger. Therefore, it can be deduced that climate change impact for most of the study areas might be the most sensitive than the propagated uncertainty on catchments flow.

Acronyms

ARC SWAT – SWAT Integrated with Arc GIS

ARS - Agricultural Research Service

CN II – Moisture Condition Curve Number

DEM – Digital Elevation Model

DEW02 – Dew Point Temperature Calculator

GCM – General Circulation Model

GIS – Geographic Information Systems

GLUE-Generalized Likelihood Uncertainty Estimation

HRU – Hydrological Response Unit

IPCC – International Panel on Climate Change

ITCZ – Inter-Tropical Convergence Zone

MCMC- Markov Chain Monte Carlo

MoWE – Ministry of Water and Energy

MRS – Mean Relative Sensitivity

NMSA – National Metrological Services Agency

ParaSol- Parameter Solution

PET – Potential Evapotranspiration

RCM – Regional Climate Models

RCN-Runoff Curve Number

SCS – Soil Conservation System

SDSM – Statistical Downscaling Model

SRTM – Shuttle Radar Topographic Mission

SWAT – Soil and Water Assessment Tool

SWAT-CUP- Soil and Water Assessment Tool- Calibration and Uncertainty Programs Version 2

SUFI2- Sequential Uncertainty Fittings 2

WGEN – Weather Generator

95PPU - 95% Prediction Uncertainty

Table of Contents

List of Tables

List of Figures

1 INTRODUCTION

1.1 Background

Weather is the state of the atmosphere at a given time whilst climate is the average weather over a period of time (Thorpe, 2005). Despite the annual periodicity in weather patterns, the Earth's climate has changed many times during the planet's history, with events ranging from ice ages to long periods of warmth (Yehun, 2009). Climate changes have had visible impacts on the natural systems. However, its impact will be significant with the hydrological cycle. Climate related natural phenomenon disaster such as floods, droughts, landslides etc., and those occasioned by anthropogenic factors causing land degradation such as deforestation, poor agricultural practices, inappropriate land use systems, among others, causes devastating effects. The situation is aggravated by threats mainly provoked by human activities such as land use change and pollution. Among these activities, Climate change is mainly expected to aggravate current stresses on water resources availability. The potential effects on water resources due to global climate change in the past few decades have been of great concern. Since climate is an important variable for water resources availability.

The general impacts of climate change on water resources have been brought out by the Third Assessment Report of the Intergovernmental Panel on Climate Change. It indicates an intensification of the global hydrological cycle affecting both ground and surface water resources. Changes in the total amount of precipitation, its frequency and intensity have also been predicted. Such changes when on the surplus side may affect the magnitude and timing of runoff but shall create drought-like situations when these are on the deficit side. This change is expected to produce some detrimental environmental effects hence the growing interest of its effects on the hydrological cycle. This has spurred an interest into the possible effects on water resources on which many countries prefers for their development activities like Ethiopia. The impacts are also predicted to be dependent on the baseline condition of the water resources system and

the ability of water resource managers to respond to climate change in addition to pressures due to increase in demand due to population growth, technology, and economic, social and legislative conditions. The coping capacity of the societies shall vary with respect to their preparedness. Thus, climate change impacts are going to be most severe in the developing world, because of their poor capacity to adapt to climate variability (IPCC, 2007).

Scientists agreed that climate change have adverse impacts on socio-economic development of all nations. But the degree of the impact will vary across nations. It is expected that changes in the earth's climate will hit developing countries like Ethiopia first and hardest because their economies are strongly dependent on basic forms of natural resources mainly on agriculture and their economic structure is less flexible to adjust to such drastic changes (NMSA, 2001). Accordingly, it may have far reaching implications to Ethiopia for various reasons, mainly as its economy largely depends on agriculture and hence, its requirements (water).

1.2 Statement of the Problem

Water stress is one of several current and future critical issues facing Africa. About 25% of the contemporary African population experience water stress, while 69% live under conditions of relative water abundance (Vörösmarty et al., 2005 cited in Yehun, 2009). Water supplies from rivers, lakes and rainfall are characterized by their unequal natural geographical distribution and accessibility, and unsustainable water use. Climate change has the potential to impose additional pressures on water availability and accessibility (IPCC, 2007).

Therefore, the freshwater resource of the Upper Blue Nile River Basin is a fundamental basis for the economic growth and social development for communities in the basin and in the riparian countries of East Africa. However; the ongoing global climate change puts further constraint on the already limited water resources in the basin. Due to high temporal and spatial variability in rainfall, prolonged dry season, global environmental changes and population growth, there is serious pressure on the water resources with consequences for the many rural poor in the basin. Therefore, evaluation of water resources in light of future climate change is very important for sustainable planning and management of the water resources.

Accordingly, a number of studies were conducted on the Nile River. However, few studies investigated the impact of climate change on Upper Blue Nile River Basin. Among these, there is no sufficient literature published at catchment level. All studies focused on the whole basin, while the water resources planning and managements were carried out at catchment level. Therefore, assessing and evaluating the significance of climatic change impacts on water resource availability of the basin at catchment scale is crucial for the water resource developments.

1.3 Objective of the Study

The overall objective is to assess the significance and potential impacts of climatic change on water resources availability by assessing and evaluating the spatial & temporal variability of the impact of climate change on water resource under uncertainty condition.

The specific objectives include:

- ✓ Modeling of the hydrological processes/dynamics using Arc SWAT hydrologic model for simulating the flows from the catchments in the Basin.
- ✓ To calibrate and to verify the hydrological model to assess the impacts of climate change.
- ✓ To perform model uncertainty to establish the uncertainty bounds of the model by using SUFI2 in SWAT-CUP.

1.4 Limitations of the Study

World Meteorological Organization recommends a baseline period of at least 30 years against which future climate projection to be done. Owing to data constraint, this study considered 1991 to 2005 as a baseline period, which ought to be from 1961 to 2005.

Because of data constraint, the climatic variables data used to generate future scenarios are also insufficient since only for two periods of 2030s and 2090s, which should be 2030s, 2060s and 2090s.

The regional climatic model output used in scenario generation for this study is of a grid 50km by 50km, which is a little bit coarse and only A1B emission scenarios was used.

In addition, in this study the impact of climate change was assessed assuming the land cover will remain the same. However, in real world the land use/land cover is changing.

1.5 Overview of the Thesis

It comprises seven chapters, which are briefly outlined below.

Chapter 1: Introduction.

This chapter discusses the background information, problem statement, general and specific objectives, and limitations of the study. It brings to focus the problems experienced in this region in light of the changing environment and climate.

Chapter 2: Description of the study area.

A description of the study area is presented which includes rainfall, climate, topography and drainage network, catchment hydrology and land cover of the study areas.

Chapter 3: Literature review.

This chapter summarizes literature regarding hydrologic modeling for use in impact assessment. It explores the subject of climate changes and their future scenarios, and how these impact the functioning of the watershed. Various methodologies used in the construction of climate change scenarios are also mentioned.

Chapter 4: Methodology of the study followed for determination of impacts.

A step-by-step methodology is presented and the models used for this exercise are described. The climate change models and their uncertainties are mentioned.

Chapter 5: Data availability, processing and evaluations.

It describes the various data used in the study, their sources and the methods used for data quality control.

Chapter 6: Result and Discussion.

This chapter presents the outcome of model application to assess the impact of climate change. It gives a detailed account of the model set up, sensitivity of model parameters, calibration, validation and model prediction uncertainty.

Chapter 7: The last chapter includes conclusion and Recommendation

This chapter summarizes the contribution of this research and suggests related future research issues.

2 DESCRIPITION OF THE STUDY AREA

2.1 Location

The Nile River is the longest international river system in the world. It flows some 6700 km through ten countries before reaching the Mediterranean Sea. Its headwaters are in Lake Victoria about 4^{o}S latitude, and it flows mostly northward to its mouth at 32^{o} N latitude. It is formed by three tributaries, the Blue Nile, the White Nile, and the Atbara. The Blue Nile contributes about sixty percent of the total flow of the Nile, whereas the Baro-Akobo (Sobat) and Tekeze (Atbara) contribute slightly less than fifteen percent each (Eman S.A. Soliman et al., 2009).

Among the three tributaries of the Nile River the headwaters of all the tributaries of the Blue Nile are in the highlands of Ethiopia, and the bulk of their runoff (70% on average) occurs between July and September (Conway, 2000). Among the tributaries of the Blue Nile, the Upper Blue Nile of which the origin is high land of Ethiopia, which contributes more than 50% of the Nile's flow at High Aswan Dam is the most important (Conway, 2000). Therefore, this study focuses on the selected catchments of the Upper Blue Nile River Basin, which is known as Abbay Basin in Ethiopia, runs from its origin Lake Tana to the Sudanese border and eventually meets the White Nile River at Khartoum, Sudan.

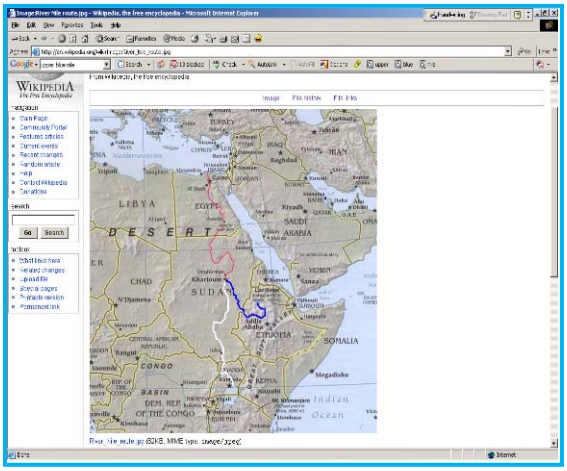

The basin lies in the west of Ethiopia, between 7^{0}45' and 12^{0}45' N, and 34^{0}05' and 39^{0}45' E and it covers an area of 176,000 km^{2} having 16 sub basins with total perimeter of about 2440 km. It is the largest in terms of volume of discharge, second largest in terms of area in the country.

Figure 2-1: Location Map of Nile River

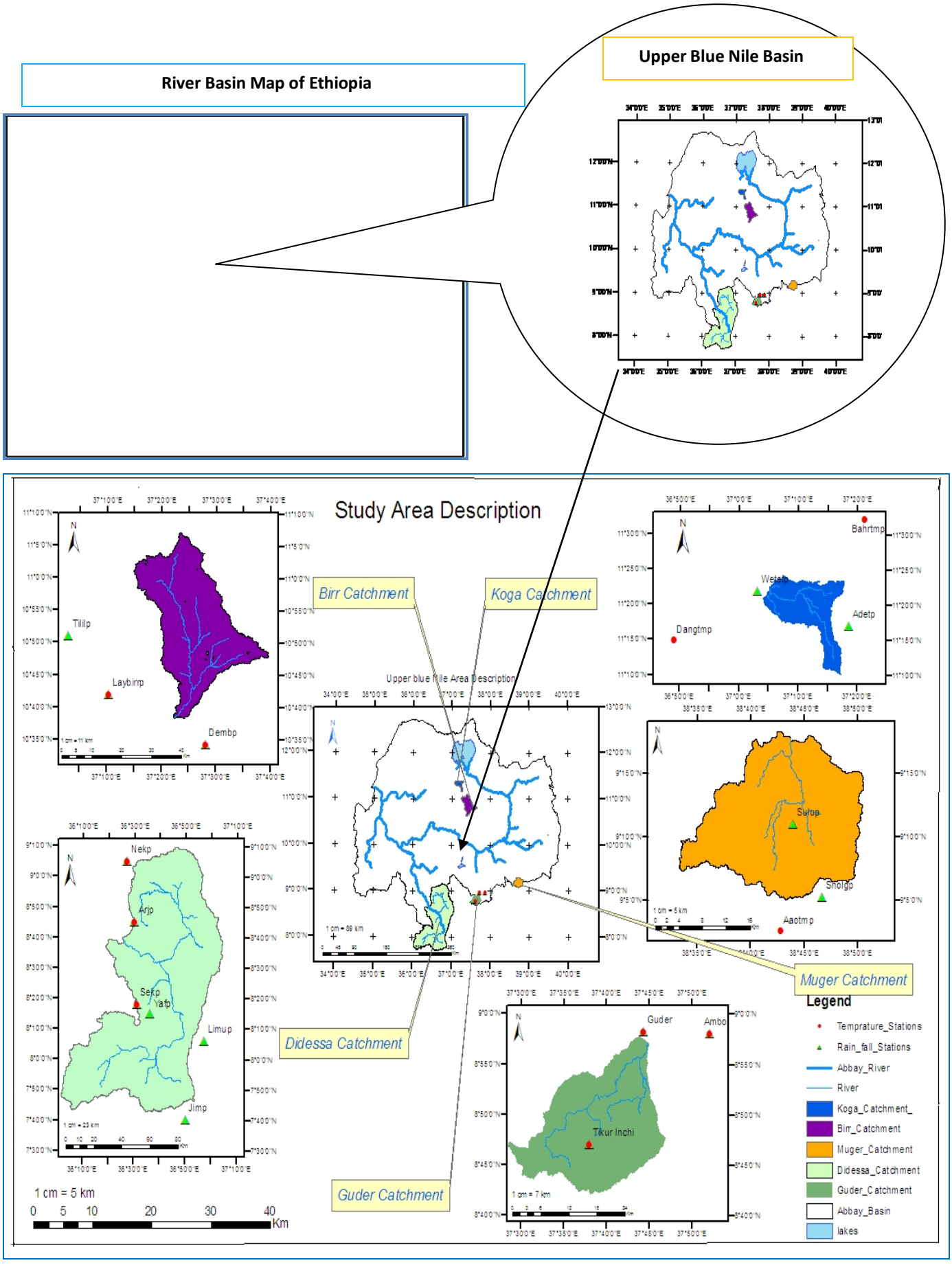

Figure 2-2: Study Area Descriptions

2.2 Topography

The topographic features of the Abbay basin vary between the highlands in the center and eastern part of the basin and the lowlands in the western part of the basin with altitude ranges from 498 up to 4261 masl. The Ethiopian highlands extend from 1500 masl up to as high as 4260 masl, with a slope of greater than 25 percent in the eastern part. Whereas the Ethiopian lowlands flatten 1000 masl to 500 masl with a slope of less than 7 percent, in Dinder and Rahad sub basins (Blue Nile Basin Atlas, 2009). The maps below in Figure 2.3 show the elevation of the basin.

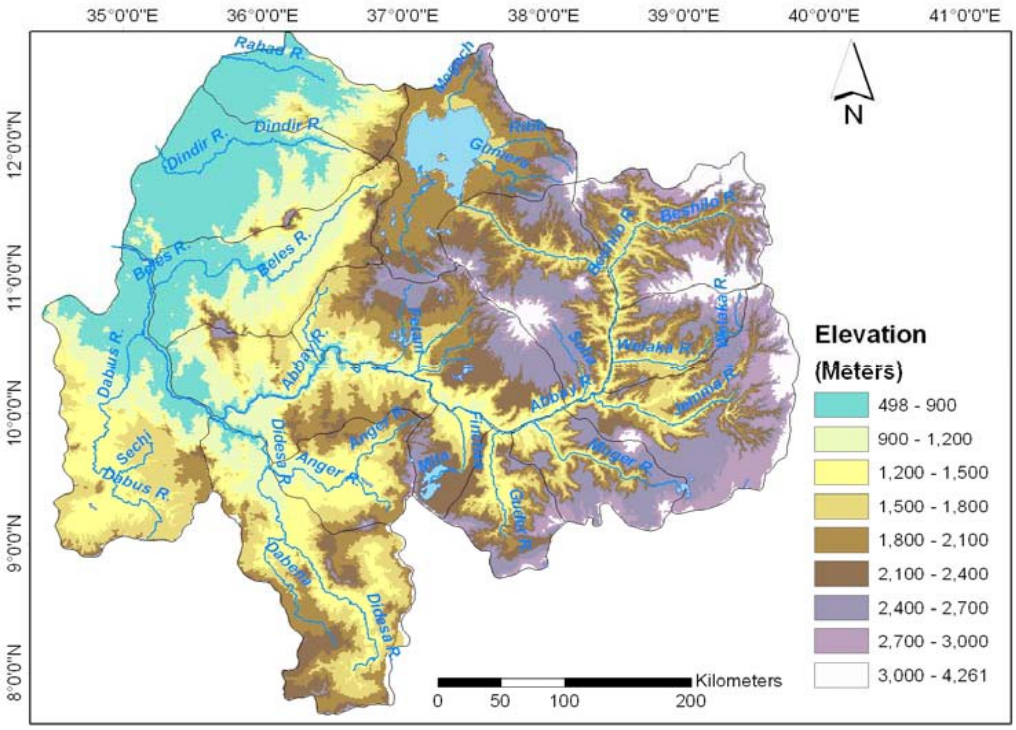

Figure 2-3: Topography of the Abbay Basin (source: Blue Nile Basin Atlas, 2009)

2.3 Climate

The climate of Ethiopia is mainly controlled by seasonal migration of Intertropical Convergence Zone (ITCZ) and its associated atmospheric circulation but the topography has also an effect on the local climate. The traditional climate

classification of the country is based on altitude and temperature shows the presence of five climatic zones namely: Wurch (cold climate at more than 3000 m altitude), Dega (temperate like climate-highland with 2500-3000 m altitude), Woina Dega (warm 1500-2500m altitude), Kola (hot and arid type, less than 1500 m in altitude), and Berha (hot and hyper-arid type) climate (NMSA, 2001). According to this classification, the majority part of the study area falls in Woina Dega and Kola climate however, small part of study area falls in Dega Zone.

The climate of Abbay basin is dominated by an altitude ranging from 590m to more than 4000m. The influence of this factor determines the rich variety of local climates ranging from hot to desert-like climate along the Sudan boarder with mean temperature of the coldest month above 18^{o}c, to temperate on the high plateau, and cold on the mountain peaks, with mean temperature of the warmest month below 10^{o}C.

2.3.1 Rainfall Distribution

The Ethiopian highlands having highest rainfall ranging from 1500 to 2200mm whereas lowlands having rainfall less than 1500mm. The lowest rainfall recorded less than 1000mm per annum in the Beshelo, Welaka, Jemma, Muger, Guder, and parts of Dinder and Rahad.

The annual precipitation increases from northeast to southwest over the basin. It varies between about 800mm to 2,220mm with a mean of about 1420mm (Blue Nile River Basin Master Plan, 1999). Most precipitation occurs in the wet (Kiremt) season (June through September), and the remaining precipitation occurs in the dry (Bega) season (October through January or February) and in the mild (Belg) season (February or March through May).

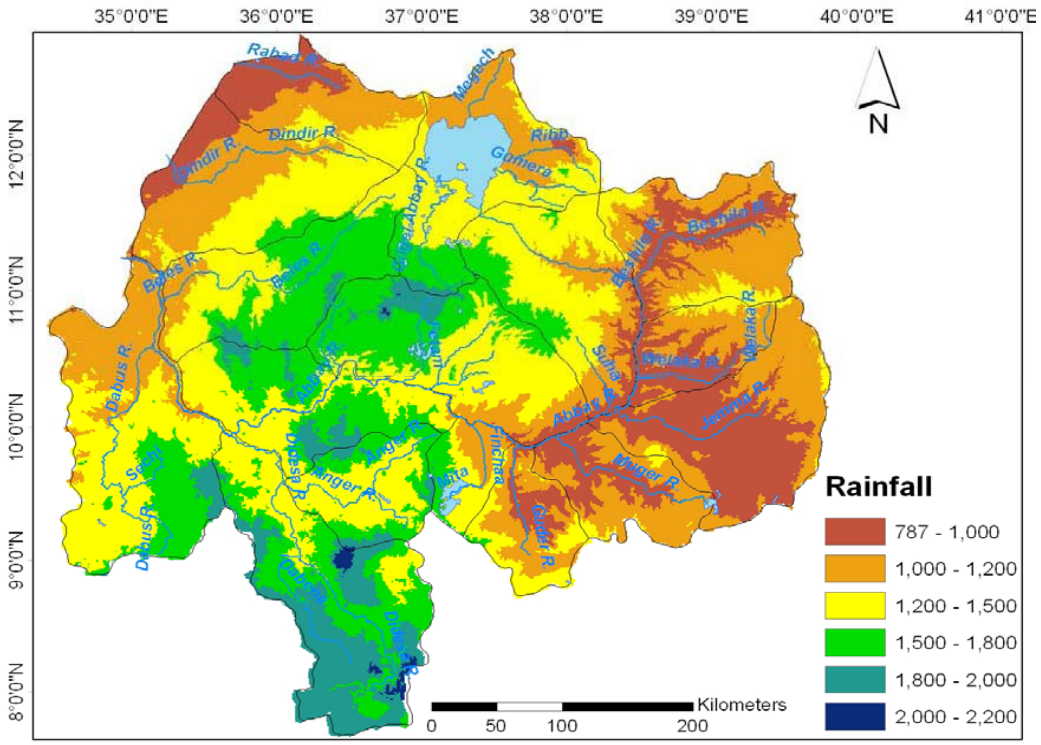

Figure 2-4: Rainfall Distribution in the Abbay Basin (Source: Blue Nile Basin Atlas, 2009)

2.3.2 Temperature

The highest temperature observed in the north western part of the basin, in parts of Rihad, Dinder, Beles and Dabus, the maximum temperature being 28°C-38°C and minimum temperature 15°C–20°C. Lower temperature observed in the highlands of Ethiopia in the central and eastern part of the basin. The maximum and minimum temperature ranges from 12°C–20°C and -1°C to 8°C respectively (Blue Nile Basin Atlas, 2009).

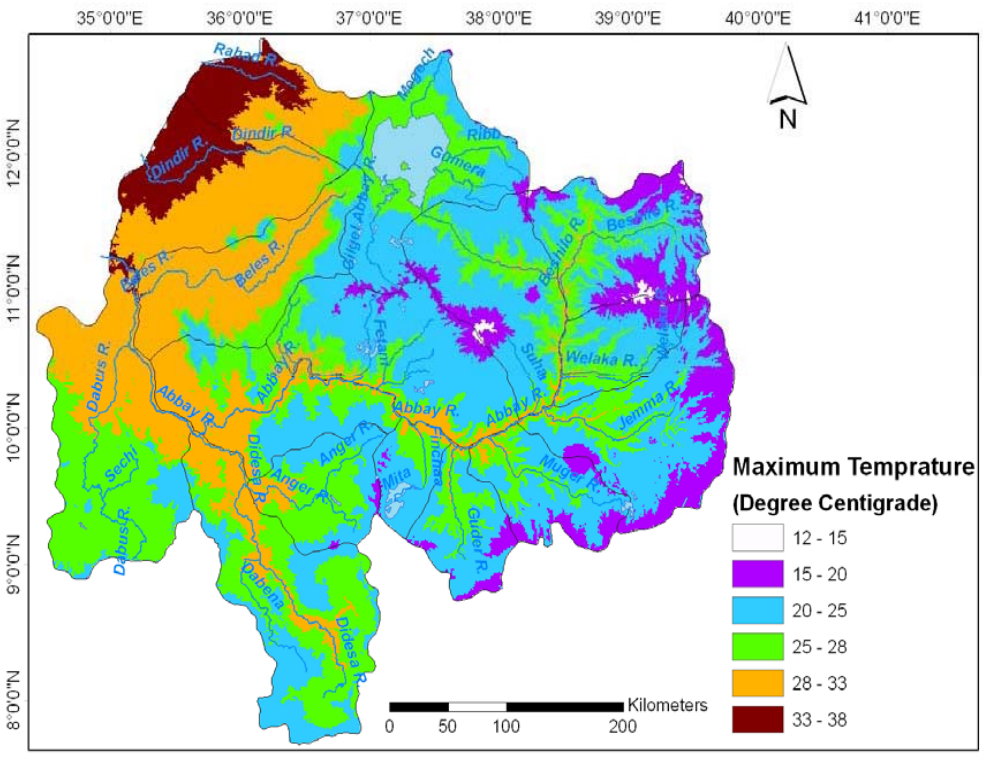

Figure 2-5: Maximum Temperature in the Abbay Basin (Source: Blue Nile Basin Atlas, 2009)

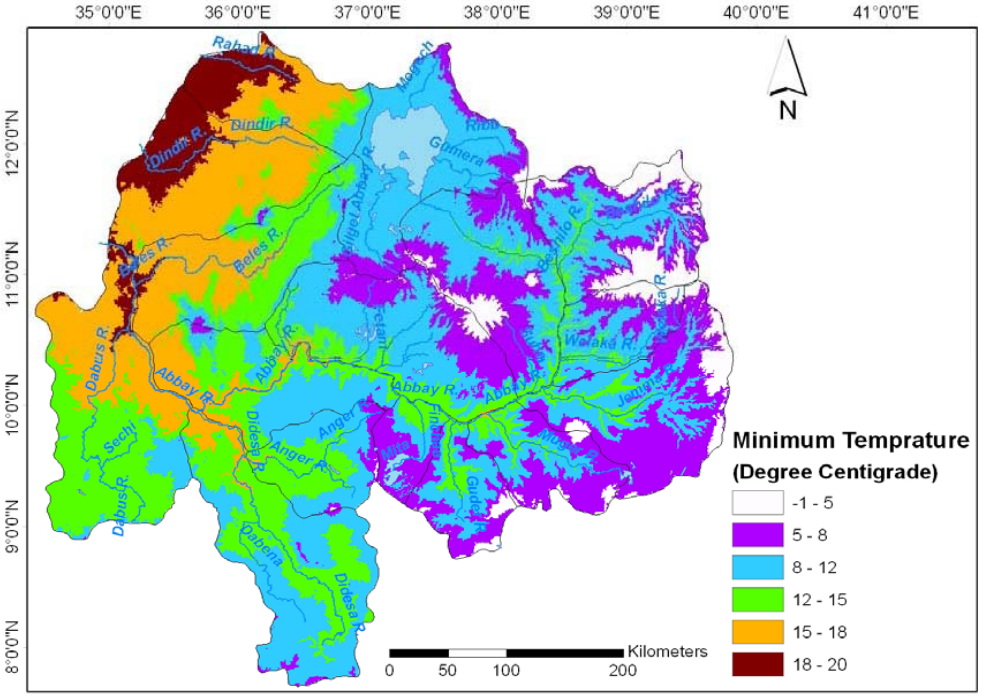

Figure 2-6: Minimum Temperature in the Abbay Basin (Source: Blue Nile Basin Atlas, 2009)

2.3.3 Evaporation

Potential Evatpotranspiration (PET) in the basin ranges between 1056 mm and 2232 mm per year. High PET is observed between 1800 mm and 2232 mm per year in North Western parts of the basin, in Dinder, Rahad, and parts of Beles and Didessa sub basins. The Eastern and southern parts having lower PET ranging between 1200 and 1800 mm per year and the lowest PET below 1200 mm per year observed in the parts of the highlands. This is highly correlated with the temperature.

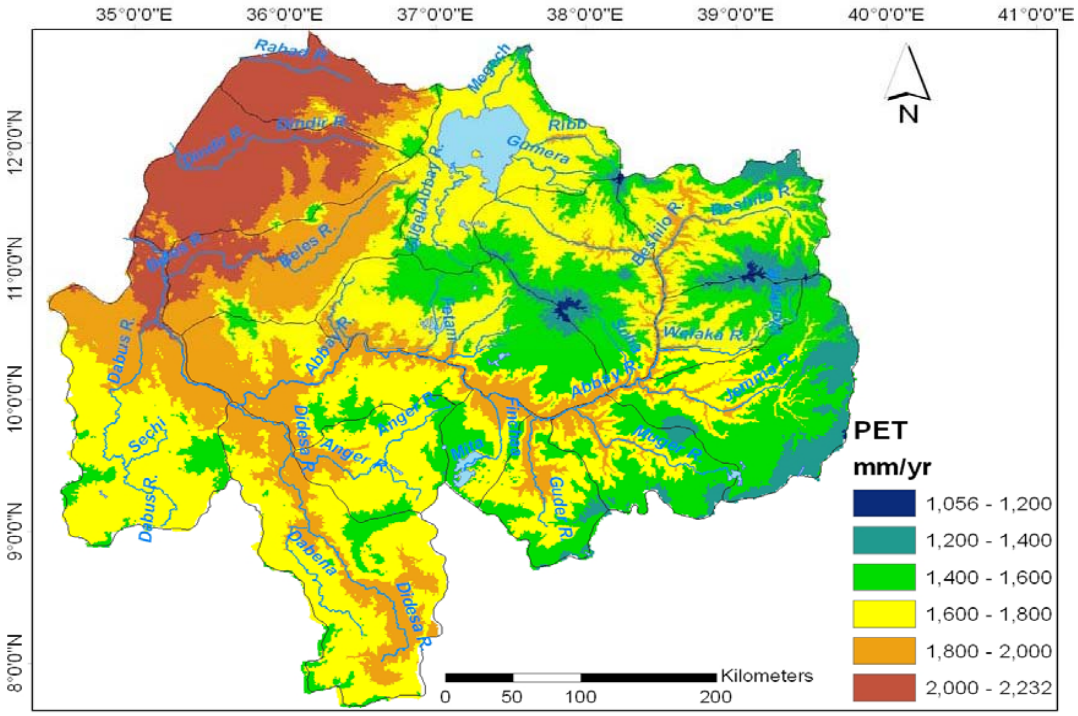

Figure 2-7: Potential Evapotranspiration in the Abbay Basin (Source: Blue Nile Basin Atlas, 2009)

2.4 Hydrology and Area of the Selected Catchments

More than 70% of annual flow in the Blue Nile results from the summer monsoon and is concentrated between July and October (Blue Nile Basin Atlas, 2009). This runoff flows directly to downstream countries due to the absence of storage in Ethiopia. Small tributaries in the mountainous region experience large fluctuations of stream flow due to the high seasonal variation of precipitation (UNESCO, 2004 cited Muluneh, 2008).

The flow of the Blue Nile is strongly seasonal because its runoff is primarily driven by monsoon precipitation.

The Abbay basin accounts for almost 17.1% of Ethiopia's land area, about 50% of its total average annual runoff and 25% of its population (Blue Nile Basin Master Plan, 1999). The Abbay Rivers has an average annual runoff of about 50 Billion Cubic Meter. And it also indicates there are sixteen subbasins in the River Basin, but only five of them are considered in this study as indicated in the Figure 2.2 & Table 2.1 with their corresponding aerial coverage. Runoff generation is high for Didessa catchment which has its head water in the area of highest rainfall in the Upper Blue Nile Basin and then diminishes in the Rahad and Dinder basins.

Depending on availability and accessibility of data and resource constraints, few catchments were used for this study from different geographic, climatic and topographic diversity of catchments with in the Upper Blue Nile Basin. The selected catchments are Koga, Birr, Didessa, Guder and Muger as listed in the table below.

Table 2-1: Major gauged rivers and areal coverage in the study area

No	Name of the River	UTM		Location of Gauged Station	Area in SQKMs
		X- Coordinate	Y-Coordinate		
1	Birr	323159	1177636	Jiga	978
2	Koga	287200	1257124	Merawi	244
3	Guder	362576	989468	Guder	524
4	Muger	470713	1027938	Chancho	489
5	Didessa	223228	952539	Arjo	9981
				Total	**12,216**

2.5 Land Use / Land Cover

The land cover for the basin is mainly characterized by dominantly cultivated, in the eastern part, and grass land, wood lands, and forest to the western part according to the Ministry of Water and Energy land cover classification.

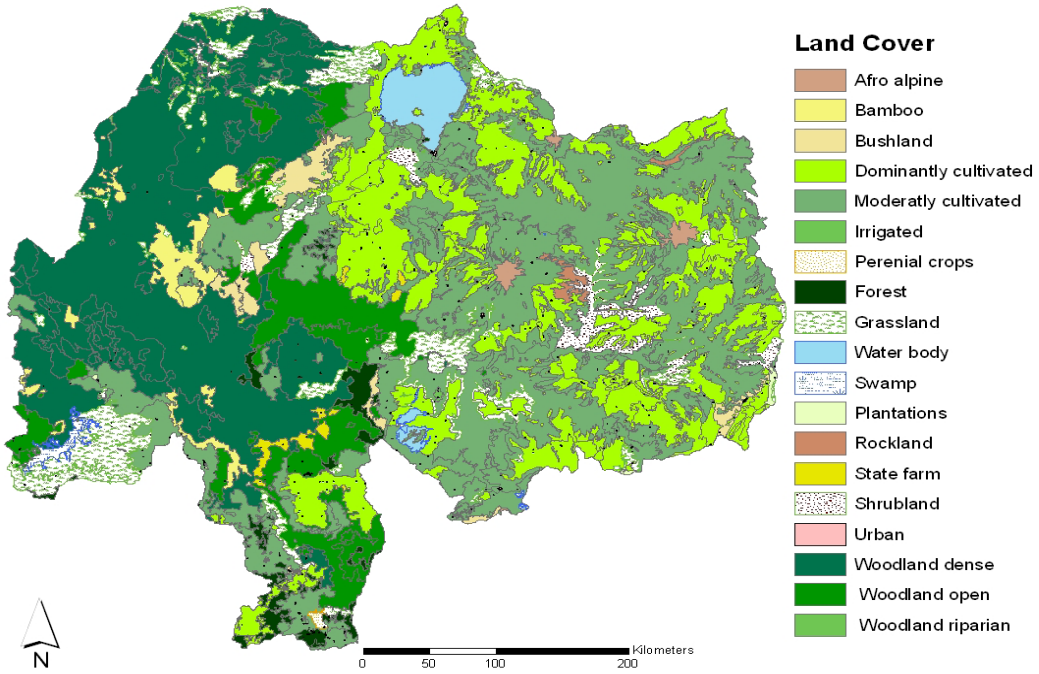

Figure 2-8: Land Cover in the Abbay Basin (Source: Blue Nile Basin Atlas, 2009)

2.6 Soil

The major dominant soil types in the basin are Alisols and Leptisols, followed by Nitosols, Vertisols, Cambrisols, Fluvisols and Luvisols.

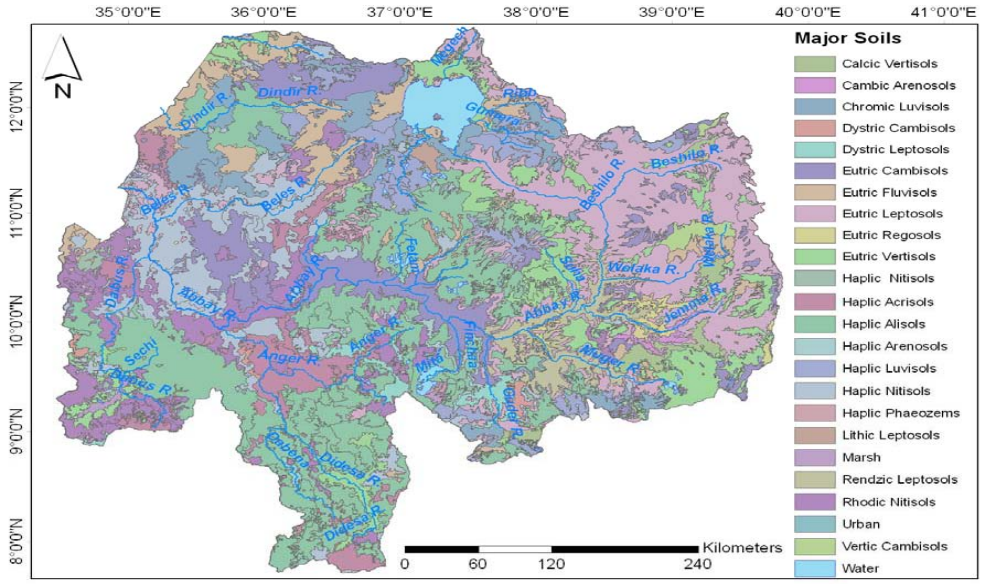

Figure 2.9: Major Soil types in Abbay Basin (source: Blue Nile Basin Atlas, 2009)

2.7 Geology

The geology of the basin having different formations such as Basalt, Alluvium, Lacustrine deposit, sand stone, granite and marbles(Blue Nile Basin Atlas, 2009). The dominant rock is Basalt (Tarmaber basalt, followed by Ashange basalt, and Amba Aiba basalt).

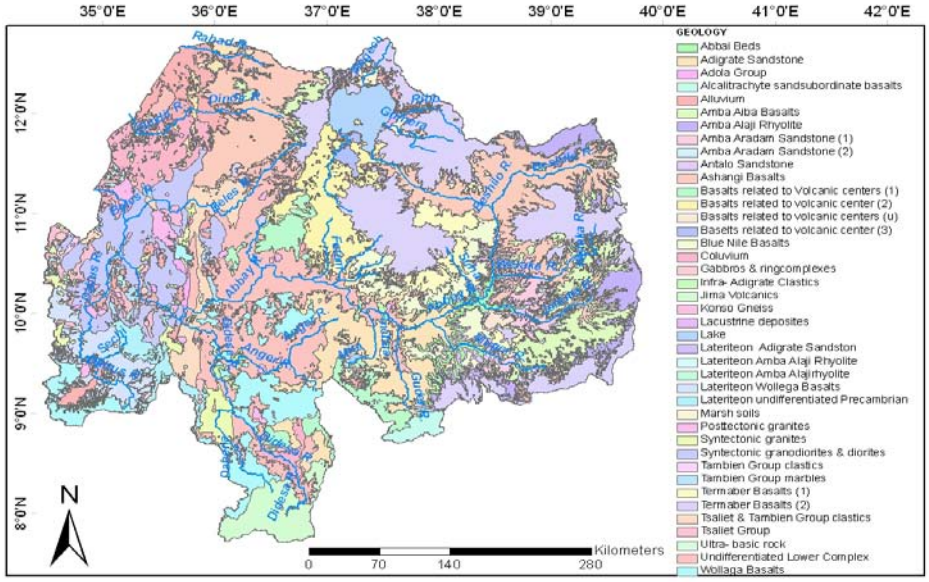

Figure 2.10: Geology of the Abbay Basin (Source: Abbay Basin Atlas, 2009)

2.8 Socio Economic and Administrative Aspect of the Basin

The administrative structure of the country is hierarchical, from Regional States, to zones, Weredas and Peasant Associations (PA) or Kebeles. According to the current regional structure, the basin covers three Regional States namely Amhara, Oromia, and Benishangul-Gumus Regional States.

According to Central Statically Authority report in 2007(CSA, 2007), from the total population of Ethiopia part of Blue Nile region by July 2008 is about 34.2% (Blue Nile Basin Atlas, 2009).

3 LITRATURE REVIEW

This section reviews three topics that are core to this research, namely hydrologic modeling, climate variability and related impacts and the previous studies related to the present research in the Upper Blue Nile Basin. Accordingly, an overview of the concept of climate change, application of hydrologic modeling for climate change impact assessment and the procedures used in different literature in climate change impact studies on water Resources are discussed below.

3.1 Climate change

3.1.1 Definition of Climate Change

A simple definition of the climate of a region is the average weather condition of a region over a long period of time. Therefore, it is safe to say that climate change is the change in the weather condition of a place over a long period of time. The IPCC (2007) defines climate change as "a change in the state of the climate that can be identified by changes in the average and/or the variability of its properties, and persist for an extended period of time, normally a decade or longer".

3.1.2 Global Climate Change

The subject on climate change has in the recent past attracted the attention of researchers in different fields ranging from engineering, physical science, to social science and politics. There is evidence that most of the warming observed over the last 50 years is attributable to human activities (IPCC, 2001). Human activities such as the usage of fossil fuels, changes in land use (e.g. deforestation), agriculture and industrial activities contribute to the emissions of greenhouse gasses thereby increasing the concentration of greenhouse gases in the atmosphere. Impacts of climate change observed around the world include among others the increase in surface temperature, sea-level rise; changes in precipitation and decrease in snow cover (IPCC, 2001).

Climate model projections with a transient 1% annual increase in greenhouse gas emissions show an increase in the global mean near-surface air temperature of 1.4 to 5.8°C, with a 95% probability interval of 1.7 to 4.9°C by 2100 (IPCC, 2001). This is likely to lead to a more vigorous hydrological cycle, with changes in precipitation and evapotranspiration rates that are regionally variable. These changes will in turn affect water availability and runoff and thus may affect the discharge regime of rivers.

3.1.3 Climate Variability and Change in Ethiopia

According to the Ethiopian National Meteorological Services Agency (NMSA, 2001) study for 42 meteorological stations, the country has experienced both dry and wet years over the last 50 years. Trend analysis of the annual rainfall showed there was a declining trend in the northern half of the country and southern Ethiopia while there is an increasing trend in the central part of the country.

Associated with rainfall and temperature change and variability, there was a recurrent draught and flood events in the country. There was also observation of water level rise and dry up of lakes in some parts of the region depending on the general trend of the temperature and rainfall pattern of the regions (Yehun, 2009).

The study of NMSA at the same year for 40 stations showed that there have been very warm and very cold years. However the general trend showed there was an increase in temperature over the last 50 years. The average annual minimum temperature over the country has been increasing by about 0.25^0c every ten years while average annual maximum temperature has been increasing by about 0.1^0c. The study also noted that the minimum temperature is increasing at a higher rate than the maximum temperature.

3.1.4 Climate Change and Related Impacts

There are many different ways in which climate change may affect catchment behavior, such as changes in rainfall totals, seasonality and intensity, effects on temperatures, radiation and evaporation, and effects on drainage density.

Many studies show the importance of linkages between climate change and hydrological regimes and how these impact on the water resources. Climate affects all aspects of the hydrologic cycle namely rainfall, runoff and evaporation. Changes in these components in turn affect the water availability and variability worldwide.

In general, water is involved in all components of the climate system. Therefore, climate change affects water through a number of mechanisms. Although climate change is expected to affect many sectors of the natural and man-made sectors of the environment, water is considered to be the most critical factor associated with climate change impacts (Yehun, 2009). Therefore, it is very important to make evaluations of the expected impact on the hydrology and water resources due to expected climate changes regardless of the direction of the change.

3.1.5 Impact Assessment Methodology and Modelling the Climate

In order to establish the possible effect of climate change on an exposed unit, in this case streamflow, a climate change impact assessment is executed. The usual approach used in hydrological impact studies which is essentially an estimation of what might happen under specific climate scenarios with the assumption that non-climatic factors are held constant. There is a general methodology to carry out investigation as to the effects of climate change on stream flow which tends to follow a general framework consisting of several steps.

This step includes using climate scenarios to derive a plausible future climate which of recent times is taken from GCM projections, downscaling techniques to obtain weather data at the local level and hydrological models to simulate hydrological conditions.

GCM are computer-run mathematical representation of the physical and dynamic processes of the atmosphere, ocean, cryosphere, land surface and their interactions. GCM divides the earth's surface into a series of horizontal boxes called grids which are separated by lines similar to longitude and longitude. The size of the box determines the resolution. The vertical layers of a GCM represent different level in the atmosphere

and depths in the ocean (Gleick et al., 2002). Most GCMs have a horizontal resolution of between 250 and 600 km, and 10 to 20 vertical layers in the atmosphere. A typical ocean model has a horizontal resolution of 125 to 250 km and a resolution of 200 to 400 m in the vertical (IPCC, 2001). Their resolution is thus quit coarser relative to the scale needed by impact assessors.

3.1.6 Downscaling

GCMs have coarse spatial resolution or large grid size (for example around 200km) which makes it difficult to predict regional and local climate which is often affected by forcing and circulation such as topography that occurs at a smaller scale and cannot be detected by the GCM.

In an attempt to resolve the inadequacy of GCMs projections on a small scale, regional climate models were developed and further research is continuing so as to develop model to predict climate at finer resolution.

Notwithstanding the limitation of these models to simulate local and regional climate, their output have been much used in regional and local climate impact assessment through the use of downscaling techniques.

These techniques enhance the regional information provided by GCM in order to provide fine scale climate information. According to Mearns et al., (2003) these techniques can be classified into three categories such as:

1. High resolution and variable resolution “time-slice” Atmosphere GCM
2. Regional climate models.
3. Empirical/statistical and statistical/dynamical methods.

3.1.7 Climate Scenarios

In order to have a basis for assessing future impacts of climate change it is vital to obtain a quantitative description of the changes in climate to be expected. The IPCC (2007) states that though there is increasing confidence among atmospheric scientist that increased concentration of greenhouse gas in the atmosphere will increase global temperature, there is much less confidence of the change in climate at the regional or

local level (e.g. river catchment or at the scale of farm) where climate change will be felt. There is no method to providing confident predictions of climate change at these scales; hence an alternative approach was developed which specify a number of plausible future trends. These are term climate scenarios which IPCC (2001) defines as "*a plausible representation of future climate that has been constructed for the explicit use in investigating the potential consequences of anthropogenic climate change".* The IPCC claims that climate scenarios should represent future conditions that accounts for both human-induced climate change and natural climate variability. Climate scenarios aids in climate projection which refers to the description of the response of the climate system to a scenario of greenhouse gas and aerosol, as simulated by a climate model. The assumptions of climate scenarios includes future trends in energy demand, emission of greenhouse gases, land use changes as well as assumptions about the behavior of the climate system over long time scale. A number of possible scenarios exist due to the uncertainties which encompass the assumption.

Generally, three main types of climate scenarios have been used in climate change impact assessment studies namely incremental scenarios which adjust the baseline climate according to anticipated future changes, analogue scenarios which uses analogs of a changed climate from the past record or from other regions and climate model based scenarios which use climate prediction from GCMs. The later is the most commonly used method to develop climate scenarios for quantitative impact assessment since GCMs are the most advance tool currently available for simulating the response of the global climate system to changes in atmospheric composition.

3.1.8 Regional Climate Models

GCMs and regional climate models (RCMs) are important tools and are preferred for use in the assessment of impacts of climate change (IPPC, 2001). The RCMs have a higher resolution than GCMs and are constructed for limited areas. Local climate change is influenced greatly by local features such as mountains, which are not well represented in GCMs because of their coarse resolution. Thus, RCMs may provide more

credible information on climate change than GCMs, especially in regions with very heterogeneous terrain, but would still contain the uncertainties inherent in GCMs. This is because they are constrained by boundary conditions of GCMs in which they are nested.

One of the methods used for scenario generation is to estimate average annual changes in precipitation and temperature using one or more RCMs or GCMs, and then use these estimates to adjust the observed time series of precipitation and temperature. Hypothetical scenarios using personal estimates or historical measurements of change, instead of GCM or RCM results, can also be generated using this procedure. One difficulty in this approach is that of maintaining consistency in adjusting variable by variable or a combination of variables. The other disadvantage of this approach is that it accounts only for changes in the mean of the time series and that it does not provide for a change in the variance. Changes in variability are important in determining the frequency of extreme climate events (Katz and Brown, 1992). Precipitation and temperature change fields imposed on the historical time series is one of the approaches used by IPCC for impact assessment (IPCC, 2001).

Other methods of creating climate change scenarios use techniques of downscaling GCM outputs, such as regression methods; weather pattern-based approaches (e.g., Wilby, 1995) and stochastic weather. Downscaling of climate information from GCMs is an important exercise for hydrologic modeling which requires input data at high spatial and temporal resolutions. Also, use of outputs from RCMs nested within GCM is also preferred because its resolution is much closer to that of landscape-scale hydrology. The challenge is that the RCMs require considerable computing resources. The nested regional climate modeling technique consists of using initial conditions, time dependent lateral meteorological conditions and surface boundary conditions to drive high resolution RCMs. The driving data is obtained from GCMs (or analyses of observations) and can include GHG and aerosol forcing (IPCC, 2001). They can provide high resolution (up to 10 to 20 km or less) and multi-decadal simulations and are capable of describing climate feedback mechanisms acting at the regional scale. An important advantage of dynamical models is that they account for local conditions, which may include changes in land-surface vegetation or atmospheric chemistry in physically consistent ways.

3.1.9 Climate Change Uncertainty

One of the major challenges both for climate modelers and users of climate change information is how to deal with uncertainty. Sources of uncertainty, which are not exclusive to climate change, are numerous, such as lack of information or knowledge, natural variability and processes that are essentially unpredictable. In climate change, rather than adopting a best or worst case scenario or an average of scenarios, it is commonly preferred to use a set of alternative scenarios and also from different GCMs or RCMs. This helps to explore a whole range of plausible scenarios, thus addressing the uncertainty of climate change and its impacts in a more effective way. Accurate predictions will never be achieved given the complexity of the earth-ocean-atmosphere processes coupled to greenhouse gas emissions, land surface modifications and some feedback mechanisms which cannot be adequately modeled. Types and methods used in climate scenario generation also factor the prediction uncertainty. Thus, using RCMs scenarios is somewhat better than in accommodating uncertainty than GCMs.

3.2 Hydrologic Modelling

A hydrologic model involves the application of mathematical expressions that define quantitative relationships between inputs (e.g. flow-forming factors) and outputs (e.g. flow characteristics). The scope of hydrologic modeling and its applications has broadened dramatically over the past decades. It is related to the spatial processes of the hydrologic cycle and is often used to estimate basin water resources as well as for impact assessment or more precisely water resources management. Many hydrologic models have been developed in the past and more are being developed and they are used to determine the performance of watersheds under inevitable land use changes, climate change, and increased climate variability. This is done in the form of sensitivity analysis where baseline conditions of climate and streamflow are established, and then used to compare the effect on streamflow due to changes in precipitation, temperature and other climate variables.

Hydrologic models are classified based on different criteria however the most convenient classification distinguishes between empirical, conceptual and physic-based models. Empirical models use statistical relationship to relate climate inputs to hydrological properties such as a regression analysis. The physic-based or water balance model uses equations to simulate the movement of water throughout the system until it leaves. On the other hand, the conceptual model attempts to give an idealistic representation of the catchment determining the water balance at different time scale through the use of parameters.

They are further classified as either lumped or distributed. Lumped (or homogeneous) models treat the catchment as a single unit. They provide no information about the spatial distribution of inputs and outputs, and simulate only the gross, spatially averaged response of the catchment. Conversely, distributed (or heterogeneous) models represent the catchment as a system of interrelated subsystems –both vertically and horizontally. Thus, distributed models can be considered as an assemblage of sub catchments arranged either in series or as a branched network (O' Loughlin et al., 1996 cited Swat theoretical documentation, 2005). They have been widely used in impact studies and normally require calibration using observed data from the catchment.

3.2.1 Hydrologic Model Selection

There are a range of possible model structures within each class of models. Hence, choosing a particular model structure for a particular application is one of the challenges of the model user community. Beven (2001) suggested four criterions for selecting model structures as below.

1. Consider models which are readily available and whose investment of time and money appeared worthwhile.
2. Decide whether the model under consideration will produce the outputs needed to meet the aims of a particular project.
3. Prepare a list of assumptions made by the model and check the assumptions likely to be limiting in terms of what is known about the response of the catchment. This

assessment will generally be a relative one, or at best a screen to reject those models that are obviously based on incorrect representations of the catchment processes.

4. Make a list of the inputs required by the model and decide whether all the information required by the model can be provided within the time and cost constraints of the project.

Therefore, a semi distributed physically based hydrological model SWAT is selected for this particular study by considering the factors stated above and it is a basin scale model used to simulate rainfall-runoff to predict the future climatic variation impacts.

3.3 Soil and Water Assessment Tool (SWAT)

It is a river basin model developed by Dr. Jeff Arnold for the United States Department of Agriculture (USDA) Agricultural Research Service (ARS) (Arnold et al., 1995). The current version of SWAT (SWAT2005) is a continuation of roughly thirty years of non-point source modeling experience. The model is comprehensive and was developed to assess the impact of land management practices on water, sediment and agricultural chemical yields in large complex basins with varying soil types, land use and management conditions. The inbuilt algorithms of SWAT model are useful tools for generating missing climate data for basins. The SWAT model is a physically based semi distributed hydrologic model requiring comprehensive input data. Currently the model is being applied worldwide with reported success. The use of SWAT model in USA, to support Total Maximum Daily Load analysis, as well as, in studies of climate change, hydrologic processes, land use change and water use and water quality applications, increased (Gassman et al. 2005). Recently, SWAT model has been also applied in catchments of Nilotic countries including Tanzania, Kenya, Ethiopia, Rwanda, Uganda and Burundi for various applications (Guithi, 2006).

It is a basin scale, continuous time model that operates on a daily/sub daily time step and is designed to predict the impact of management on water, climate, sediment, and agricultural chemical yields in ungauged watersheds.

The hydrologic model is based on a water balance equation for soil water content as follows (Arnold et al., 1995):

$$Sw = Sw_i + Pt - Qt - ET - SP - Q_R \quad \text{----------eqn. (1)}$$

Where **Sw** is the soil water content for the current day,

Sw_i is the soil water content for the previous day, Pt is precipitation,

Qt is surface runoff, ET is Evapotranspiration,

SP is percolation or seepage, and Q_R is return flow.

3.4 Previous Studies

Previous studies which examined the impacts of climate change on water resources in the Nile Basin (Conway and Hulme 1993, 1996; Conway 2005) have mostly focused on the changes in runoff and their consequences for the economies of downstream countries. However, climate change can affect multiple features of water resources, e.g., quantity and quality, high- and low-flow extremes, timing of events, water temperature, etc. All these aspects affect livelihoods in the basin but have not received attention in planning for future water allocation and design of water infrastructure yet. Also from the literature, it was clear that several attempts evaluated the sensitivity of the Nile discharge to the temperature changes (or evaporation) and precipitation. Probably the first of these studies was by Kite and Waititu (1981) cited in Guithi (2006) who looked at the Nzoia River, a tributary of Lake Victoria, using the Sacramento Watershed catchment model. They found that the streamflow is highly sensitive to precipitation (i.e. a 10% increase in precipitation caused a 40% increase in the runoff, in other words, the relationship is non-linear). Similar results were reported by several authors for the Blue Nile (e.g. Conway and Hulme, 1996).

Many researchers attempted to address the impact of future climate change on the Nile flows, using GCMs for a large set of SRES emissions scenarios (Conway, 2000). As previously mentioned, the impact of climate change on water resources sparks interest

as such numerous studies were done to quantify the impact of this phenomenon on water resources of the whole Nile River Basin.
But recently, some studies focus on Upper Blue Nile Basin, which emerges from highland of Ethiopia, of many catchments with in basin using different approaches.

The impact of climate change on water resources of Lake Tana-sub basin will be significant. If the temperature is increased by 2^{o}_{C} and there is no change in rainfall the mean annual flow will be decreased by 11.3%. But if the rainfall is decreased by 10% and 20% the decrease in runoff will be 29.3% and 44.6% respectively. On the other hand, if the rainfall is increased by10%and 20%, the mean annual runoff will increase by 6.6% and 32.5%respectivly. And it was concluded as the basin is more sensitive to change in rainfall than temperature (Tarekegn and Tadege, 2006).

A more recent study by Kedir (2008) assessed the change in climate on Gilgel Abbay catchment in Upper Blue Nile Basin using HBV Hydrological modeling and transient scenarios from GCMs by statistical downscaling methods. Studies in the Gilgel Abbay river watershed reveals that the result of downscaled precipitation does not manifest a systematic increase or decrease in all future time horizons for both A2 and B2 scenarios unlike that of minimum and maximum temperature. And the result from synthetic (hypothetical) scenario indicates that the Catchment is sensitive to climate change especially in rainfall than change temperature.
And also, a recent study by Muluneh (2008) based on hypothetical climate change scenario and using HBV hydrological model. The assessment was done on selected 10 catchments of the basin for the hypothetical scenario within the range of (-30 to +30) for both precipitation and PET. Evaluation of water resource change shows that for both scenarios impact assessment of Chacha is the most sensitive catchment followed by catchments Sechi, Birr, Guder, G/Belese, Teme, Muger, Koga, Neshi, and Little Anger. And from the sensitivity map developed for the whole Basin Jemma, Dabus, part of Belese, Woleka, Wonbera and Beshilo are a special and overstress sensitive subbasins, however; Fincha, Anger and Tana sub basins have relaxed water resource change sensitivity.

At the last by Yehun (2009) using SDSM downscaled climate outputs were used as an input to the SWAT model and used to assess the impact of climate change on the Gilgel Abbay River and Lake Tana basin. The result reveals that the impact of climate change may cause a decrease in monthly flow volume up to 46% in the 2020s and increase up to 135% in the 2080s. It is observed that climate change has negligible effect on the low flow condition of the river. Seasonal flow volume may show increase up to 136% and 36% for Belg and Kiremt respectively. It is observed that there may be a net annual increase in flow volume in Gilgel Abbay River due to climate change.

3.5 Uncertainty Analysis

Most important issue with calibration of watershed models is that of uncertainty in the predictions. Watershed models suffer from large model uncertainties. These can be divided into: conceptual model uncertainty, input uncertainty, and parameter uncertainty.

1. Conceptual model uncertainty (or structural uncertainty)
2. Input uncertainty is as a result of errors in input data such as rainfall, and more importantly, extension of point data to large areas in distributed models.
3. Parameter uncertainty

Another uncertainty worth mentioning is that of "modeler uncertainty". It has been shown before that the experience of modelers could make a big difference in model calibration. The packages like SWAT-CUP can help decrease modeler uncertainty by removing some probable sources of modeling and calibration errors. On a final note, it is highly desirable to separate quantitatively the effect of different uncertainties on model outputs, but this is very difficult to do. The combined effect, however, should always be quantified on model outputs (Abbaspour, 2007).

3.5.1 SWAT-CUP2

SWAT-CUP is an interface that was developed for SWAT. Using this generic interface, any calibration/uncertainty or sensitivity program can easily be linked to SWAT. This is

demonstrated by the program links GLUE, Parasol, SUFI2, and MCMC procedures to SWAT. In this particular study it was preferred to use sequential uncertainty fittings (SUFI2). It is automated model calibration requires that the uncertain model parameters are systematically changed, the model is run, and the required outputs (corresponding to measured data) are extracted from the model output files. The main function of an interface is to provide a link between the input/output of a calibration program and the model.

3.5.2 Conceptual Basis of the SUFI-2 Uncertainty Analysis Routine

In SUFI-2, parameter uncertainty accounts for all sources of uncertainties such as uncertainty in driving variables (e.g., rainfall), conceptual model, parameters, and measured data. The degree to which all uncertainties are accounted for is quantified by a measure referred to as the *P-factor*, which is the percentage of measured data bracketed by the 95% prediction uncertainty (95PPU). As all the processes and model inputs such as rainfall and temperature distributions are correctly manifested in the model output (which is measured with some error)-the degree to which we cannot account for the measurements - the model is in error; hence uncertain in its prediction. Therefore, the percentage of data captured (bracketed) by the prediction uncertainty is a good measure to assess the strength of our uncertainty analysis. The 95PPU is calculated at the 2.5% and 97.5% levels of the cumulative distribution of an output variable obtained through Latin hypercube sampling, disallowing 5% of the very bad simulations. As all forms of uncertainties are reflected in the measured variables (e.g., discharge), the parameter uncertainties generating the 95PPU account for all uncertainties. Breaking down the total uncertainty into its various components is highly interesting, but quite difficult to do.

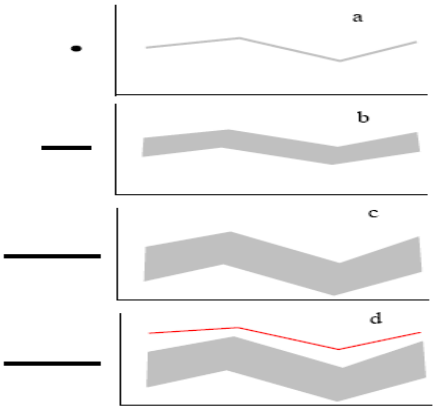

Figure 3-1: *A conceptual illustration of the relationship between parameter uncertainty and prediction uncertainty (source: Abbaspour et al., 2007)*

Another measure quantifying the strength of a calibration/uncertainty analysis is the R-factor, which is the average thickness of the 95PPU band divided by the standard deviation of the measured data. SUFI-2, hence seeks to bracket most of the measured data with the smallest possible uncertainty band. The concept behind the uncertainty analysis of the SUFI-2 algorithm is depicted graphically in Figure 3.2. This Figure illustrates that a single parameter value (shown by a point) leads to a single model response (Fig. 3.2a), while propagation of the uncertainty in a parameter (shown by a line) leads to the 95PPU illustrated by the shaded region in Figure 3.2b. As parameter uncertainty increases, the output uncertainty also increases (not necessarily linearly) (Fig. 3.2c). Hence, SUFI-2 starts by assuming a large parameter uncertainty (within a physically meaningful range), so that the measured data initially falls within the 95PPU, then decreases this uncertainty in steps while monitoring the P-factor and the R-factor.

In each step, previous parameter ranges are updated by calculating the sensitivity matrix (equivalent to Jacobian), and equivalent of a Hessian matrix, followed by the calculation of covariance matrix, 95% confidence intervals of the parameters, and correlation matrix. Parameters are then updated in such a way that the new ranges are always smaller than the previous ranges, and are centered on the best simulation (Abbaspour et al., 2007).

The goodness of fit and the degree to which the calibrated model accounts for the uncertainties are assessed by the above two measures. Theoretically, the value for *P-factor* ranges between 0 and 100%, while that of *R-factor* ranges between 0 and infinity. A *P-factor* of 1 and *R-factor* of zero is a simulation that exactly corresponds to measured data. The degree to which we are away from these numbers can be used to judge the

strength of our calibration. A larger *P-factor* can be achieved at the expense of a larger *R-factor*.

Hence, often a balance must be reached between the two. When acceptable values of R-factor and P-factor are reached, then the parameter uncertainties are the desired parameter ranges. Further goodness of fit can be quantified by the R^2 and/or Nash-Sutcliff (NS) coefficient between the observations and the final "best" simulation. It should be noted that we do not seek the "best simulation" as in such a stochastic procedure the "best solution" is actually the final parameter ranges.

If initially we set parameter ranges equal to the maximum physically meaningful ranges and still cannot find a 95PPU that brackets any or most of the data, for example, if the situation in Figure 3.2d occurs, then the problem is not one of parameter calibration and the conceptual model must be re-examined.

4 METHODOLOGY

4.1 Climate Change Scenarios

The climate change scenarios produced for this study were based on the outputs of RegCM version 3 results that were established on the A1B emission scenarios. As the objective here is to get indicative future climate ensembles, the scenarios available were only for maximum temperature, minimum temperature, and precipitation values. The rest of the climate variables were assumed to be constant. The outputs of RegCM3 model for the A1B emission scenarios were used to produce the future scenarios. The Regional Climatic Model was adopted to downscale the global outputs of the GCM model into the local watershed scale. For this study the climate scenarios are availed by the Civil Engineering Department of Addis Ababa Institute of Technology through my advisor.

The available future time scales were divided into two periods of 10 years.

4.2 Hydrologic Model Using SWAT

The climate change impact assessment on water resources can be best handled through simulation of the hydrological conditions that shall prevail under the projected weather conditions in an area. Such a treatment is essential because of the fact that the hydrological response is a highly complex process governed by a large number of variables such as terrain, land use, soil characteristics and the state of the moisture in the soil.

The reasons why SWAT Model was selected for this study in addition to the reasons stated in section 3.2.1 are the model is physically based, spatially distributed, and it belongs to the public domain. Moreover, it simulates hydrological outputs based on a changed climate if the changes in the climate parameters are given as an input to the model. This makes the model suitable for the proposed task.

A head of that, the Arc GIS 9.3 integrated SWAT interface called the Arc SWAT model provides a user friendly GUI that ease the use of the model. These qualities of the model satisfy the selection criteria discussed in section 3.2.1. The model has also been tested in different watersheds and reported to be able to well explaining watershed hydrological processes: the case studies in section 3.4, as examples, which justify the possible use of this model in the study area. A strong interest of testing suitability of different physically based models such as SWAT in different Upper Blue Nile watersheds was also another ground for the selection.

Arc SWAT (Arc GIS SWAT) is a complete preprocessor, interface and post processor of SWAT version 2005. It has been developed as an extension of Arc GIS 9.3 by Blackland Research Center, a Texas Agricultural Experiment Station part of Texas A & M University. Being in the Arc GIS 9.3 environment; the model provides the tools for delineating the watershed, defining the land use and soil, editing the model data bases, defining the weather stations, parameterzing and editing the inputs, running the model, reading and mapping the results, and calibrating the simulation results. The SWAT water balance model is one such model and has been used in the present study to carry out the hydrologic modeling for the selected catchments. The model simulates the hydrologic cycle at daily/sub-daily time steps. For this study the most recent version called *"ArcSWAT-2.3.4 for SWAT 2005 – Blackland Research Center – Ver. Beta 0.04"* was used.

4.2.1 Approach in Arc Swat Model

SWAT is a continuous time model that operates on a daily/sub-daily time steps. It is physically based and can operate on large basins for long periods of time (Arnold et al., 1995). The basic model inputs are rainfall, maximum and minimum temperature, radiation, wind speed, relative humidity, land cover, soil and topographic datas.
Watersheds can be subdivided into catchments and further into hydrologic response units (HRUs) to account for differences in soils, land use, crops, topography, weather, etc. The model has a weather generator that generates daily values of precipitation, air

temperature, solar radiation, wind speed, and relative humidity from statistical parameters derived from average monthly values.

SWAT splits hydrological simulations of a watershed into two major phases: the land phase and the routing phase. The difference between the two lies on the fact that water storage and its influence on flow rates is considered in channelized flow (Neitsch (a) et al. 2002).

In the land phase of the hydrologic cycle, runoff is predicted separately for each Hydrologic Response Unit (HRU) and routed to obtain the total runoff for the watershed.

The model computes surface runoff volume either by using modified SCS curve number method or the Green & Ampt infiltration method. Once the loadings (water, sediment, nutrients and pesticides) to the main channel are determined, they are routed through the stream network of the watershed.

Flow is routed through the channel using a variable storage coefficient method or the Muskingum routing method. SWAT has three options for estimating potential evapotranspiration: Hargreaves, Priestley-Taylor, and Penman-Monteith. The model also includes controlled reservoir operation and groundwater flow model. The detailed and complete descriptions are given in the SWAT theoretical documentation (Neitsch (a) et al. 2002). The important equations used by the model are discussed as follows.

4.2.2 Weather Generator Data Preparation

SWAT requires daily values of precipitation, maximum and minimum temperature, solar radiation, relative humidity and wind speed. The climatic data collected from all meteorological stations in the study area have; however, too many missing data. As SWAT has a built in weather generator called WGEN (Richardson et al., 1984 cited Zeray, 2006) that is used to fill the gaps, all the missing values were filled with a missing data identifier, -99.

The weather generator first independently generates precipitation for the day. Maximum temperature, minimum temperature, solar radiation and relative humidity are then generated based on the presence or absence of rain for the day. Finally, wind

speed is generated independently. For the sake of data generation, weather parameters were developed by using the weather parameter calculator PCPSTAT and dew point temperature calculator DEW02, which were downloaded from the SWAT website.

The PCPSTAT program reads daily values of solar radiation (calculated from daily sunshine hours), maximum and minimum temperatures, precipitation, relative humidity, and wind speed data. It then calculates monthly daily averages and standard deviations of all variables as well as probability of wet and dry days, skew coefficient, and average number of precipitation days in the month. The DEW02 programs reads daily values of relative humidity, and maximum and minimum temperature values and calculates monthly average dew point temperatures.

4.2.3 Watershed Delineation

The Arc GIS tool in Arc SWAT partitions watersheds into a number of hydrologically connected subbasins based on flow directions and accumulations. The catchment and subbasins delineation was carried out based on an automatic delineation procedure using a Digital Elevation Model (DEM) to define the location of the stream network.

The catchments have been divided into sub-basins using an arbitrarily selected threshold value. These threshold values used on the DEM of the respective river basins during the process of automatic delineation provides the number of sub basins that the river basin got sub-divided into as a result of this threshold (which basically controls the drainage density of the artificially constructed drainage system and thereby the number of sub-basins).

Generally, the smaller the threshold area, the more detailed are the drainage networks, and the larger are the number of subbasins and HRUs. However, this needs more processing time and space. As a result, an optimum size of a watershed that compromises both was selected. In addition to those defined by the model itself, five catchment outlets were manually added at the gauging stations, which were later used as a point of calibration and validation of the simulated flows. As a result five catchments namely, Koga, Birr, Guder, Muger and Didessa, were delineated. The total

area of the catchments as obtained from the automatic delineation has also been provided.

4.2.4 Determination of Hydrologic Response Units (HRU's)

The subbasin delineation was followed by the determination of HRUs, which are unique soil and land use combinations within a subbasin modeled regardless of their spatial positioning. This describes better the hydrologic water balance and increases the accuracy of load predictions (Zeray, 2006). SWAT predicts the land phases of the hydrologic cycle separately for each HRU and routes to obtain the total loadings of the catchment. The HRUs was determined by assigning only one HRU for each catchment considering the dominant soil/land use combinations. This has resulted in optimum number of HRUs in each of the catchments which makes the automatic calibration trial easier.

4.2.5 Flow Simulation

In SWAT, surface runoff amounts can be estimated using either the SCS curve number Method (SCS 1972) (Eq. 4-1) or the Green & Ampt infiltration method. In this study, the SCS curve number method was used. It is an empirical model that estimates the amounts of runoff under varying land use and soil types. The SCS curve number (CN) is a function of the soil's permeability, land use and antecedent soil water conditions.

$$Qsurf = \left[\frac{(Rday - I_a)2}{(Rday - Ia + S)}\right] \text{----------Eq. 4-1}$$

Where: Q_{surf} is accumulated runoff or rainfall excess (mm water),

R_{day} is rainfall depth for the day (mm water),

I_a is an initial abstraction which includes surface storage, interception and infiltration prior to runoff (mm water),

S is a retention parameter (mm water).

The retention parameter varies spatially due to changes in soils, land use, management and slope and temporally due to changes in soil water content. It is mathematically expressed as:

$$S = 25.4\left[\frac{1000}{CN} - 10\right]$$ ----------Eq. 4-2

Where: CN is the curve number for the day.

CN = f (land use, practice, soil permeability, soil hydrologic group)

For the definition of the soil hydrologic groups, the model uses the U.S. Natural Resource Conservation Service (NRCS) classification, which classifies soils into four hydrologic groups (A, B, C, & D) based on infiltration characteristics of the soils. Group A, B, C and D soils have high, moderate, slow, and very low infiltration rates with low, moderate, high, and very high runoff potential, respectively. The initial abstraction, I_a, is commonly approximated as 0.2S and the equation becomes:

$$Qsurf = \left[\frac{(Rday - 0.2S)^2}{Rday - 0.8S}\right]$$ ----------Eq.4.3

4.2.6 Potential Evapotranspiration (PET)

SWAT provides three methods that can be used to calculate potential evapotranspiration (PET). These are the Penman-Monteith method, the Priestley-Taylor method and the Hargreaves method. The model can also read in daily PET values if the user prefers to apply a different potential evapotranspiration method. The three PET methods vary in the amount of required inputs. The Penman-Monteith method requires solar radiation, air temperature, relative humidity and wind speed. The Priestley-Taylor method requires solar radiation, air temperature and relative humidity. The Hargreaves method requires air temperature only.

In this study, among the three methods, Penman-Monteith Method was used to estimate PET values.

4.2.7 Groundwater

SWAT assumes two layers of aquifers while simulating the groundwater balance; namely a shallow-unconfined aquifer, and a deep-confined aquifer. The unconfined shallow aquifer is contributes to flow in the main channel or reach of the sub basin, whereas the deep confined aquifer assumed to contribute to stream flows outside the watershed (Arnold et al. 1995).

The volume of water available in the shallow aquifer is governed by the recharge from the top soil profile (recharge), the flow into the main stream channels or reach (base flow), the movement into the overlying unsaturated zone (revap), and the flow to the deep aquifer (deep percolation). The details of the methodology are described in the SWAT Theoretical Documentation, version 2005. Evaporation, pumping withdrawals, seepage to the deep aquifer, and water uptake from the shallow aquifer by deep rooted plants is also components of the groundwater.

The water balance for a shallow aquifer in SWAT is calculated as:

$$aq_{sh,i} = aq_{sh,i-1} + w_{rchrg} - Q_{gw} - w_{revap} - w_{deep} - w_{pump,sh} \quad \text{----------Eq. 4-4}$$

Where: $aq_{sh,i}$ is the amount of water stored in the shallow aquifer on day i (mm),

$aq_{sh,i-1}$ is the amount of water stored in the shallow aquifer on day i-1 (mm),

w_{rchrg} is the amount of recharge entering the aquifer on day i (mm),

Q_{gw} is the groundwater flow, base flow, into the main channel on day i (mm),

w_{revap} is the amount of water moving into the soil zone in response to water deficiencies on day i (mm),

w_{deep} is the amount of water percolating from the shallow aquifer into the deep aquifer on day i (mm), and

$w_{pump,sh}$ is the amount of water removed from the shallow aquifer by pumping on day i (mm).

Base flow occurs only when the amount of water stored in the shallow aquifer exceeds a threshold volume of water. Similarly, deep percolation happens only when the amount of water stored in the shallow aquifer exceeds a threshold value.

4.2.8 Channel Routing

The second phase of the SWAT hydrologic simulation, the routing phase, consists of the movement of water, sediment and other constituents (e.g. nutrients, pesticides) in the stream network. As an optional process, the change in channel dimensions with time due to down cutting and widening is also included.

Similar to the case for the overland flow, the rate and velocity of flow is calculated by using the Manning's equation. The main channels or reaches are assumed to have a trapezoidal shape by the model. Two options are available to route the flow in the channel networks: the variable storage and Muskingum methods. Both are variations of the kinematic wave model. While calculating the water balance in the channel flow, the transmission and evaporation are also well considered by the model.

The variable storage method uses a simple continuity equation in routing the storage volume, whereas the Muskingum routing method models the storage volume in a channel length as a combination of wedge and prism storages. In the latter method, when a flood wave advances into a reach segment, inflow exceeds outflow and a wedge of storage is produced. As the flood wave recedes, outflow exceeds inflow in the reach segment and a negative wedge is produced. In addition to the wedge storage, the reach segment contains a prism of storage formed by a volume of constant cross-section along the reach length. In this study, the variable storage method was adopted.

4.3 SWAT Model Setup for the Study Area

The SWAT model was set up using data described in section 4.2.2 above and the SWAT-Arc GIS (Arc SWAT) interface. The interface helped to create the stream network, delineate the catchment boundary from the DEM and further subdivide the catchment into subbasins. The land cover and soil layers were used to generate HRUs. The climatic data was also integrated spatially to assign these data as the main drivers of the model to the various subbasins.

The model setup steps are described below.

- ✓ The first step was to load the Digital Elevation Model in the Arc SWAT interface.
- ✓ A mask of the catchments was used to focus the watershed area. This is however not a necessary step if the general location of the catchments are known.
- ✓ The stream network was generated by use of a threshold area that defines the origin of a stream. The smaller the number, the more detailed the stream network generated by the interface.
- ✓ The locations of the five river gauging locations were added as subbasin outlets. This was to ensure that the model calibration was done at their exact locations. Once the entire watershed outlet is selected, the subbasins are delineated and their parameters calculated. The subbasins are shown in Fig. 6.1-5.
- ✓ Next, the landuse and soil maps are loaded. The lookup table for each map is also loaded in order for the interface to know which codes or names to assign to the different categories. Once the land use and soil map have been loaded and reclassified, an overlay is done, resulting in landuse/soil distribution within the subbasins.
- ✓ The HRUs were then created by applying Dominant landuse, soil and slope. The number of subbasins and HRUs in each sub basin are given in Table 5.2.
- ✓ Then, the climatic data (observed rainfall and temperature) are loaded and the interface assigns the different weather station data sets to the subbasins in the watershed.
- ✓ At the final step, the SWAT input files are built and the model is ready to run.

4.4 Model Calibration and Validation

4.4.1 Base Flow Separation

For the sake of comparisons of water balance statistics of simulated and observed flows, the total gauged streamflow data should be separated into surface and base flow components. Thus, baseflow was separated from streamflow using an automated base flow separation and recession analysis techniques (Arnold et al. 1995). The automated

base flow separation and recession analysis technique uses a dos based software called Baseflow-program found from the SWAT website.

4.4.2 Sensitivity Analysis

Sensitivity analysis is a technique of identifying the responsiveness of different parameter involving in the simulation of a hydrological process. For big hydrological models like SWAT, which involves a wide range of data and parameters in the simulation process, calibration is quite a cumbersome task. Even though, it is quite clear that the flow is largely affected by curve number, for example in the case of SCS curve number method, this is not sufficient enough to make calibration as little change in other parameters could also change the volumetric, spatial, and temporal trend of the simulated flow. Hence, sensitivity analysis is a method of minimizing the number of parameters to be used in the calibration step by making use of the most sensitive parameters largely controlling the behavior of the simulated process (Zeray, 2006). This appreciably eases the overall calibration and validation process as well as reduces the time required for it.

The sensitivity analysis was undertaken by using a built-in tool in SWAT2005 that uses the Latin Hypercube One-factor-At-a-Time (LH-OAT) design method.

It was carried out prior to the calibration exercise. This method combines the 'One-factor-At-a Time' (OAT) design and the Latin Hypercube (LH) sampling by taking the LH samples as initial points for a OAT design. Thus, ensuring that the full range of all parameters have been sampled with the precision of an OAT design. This leads to a robust and efficient sensitivity analysis method. For m intervals in the LH method and p parameters, a total of m*(p+1) runs are required.

The analysis was carried out against the measured streamflow. The objective function (i.e. the sum of the squared errors between the observations and the simulations) is calculated during each run. The effect of a change of a parameter value on this objective function is then calculated. The parameters are ranked with decreasing sensitivity according to the mean relative sensitivity (MRS) of the parameters, and their category

of sensitivity was also defined based on the Lenhart et al. (2002) classification (cited Zeray, 2006). He divided sensitivity into four classes: small to negligible (0≤MRS<0.05), medium (0.05≤MRS<0.2), high (0.20≤MRS<1.0), and very high (MRS≥1.0). The analysis involved a total of 26 parameters. The list and definitions of parameters involved in sensitivity analysis are shown in Annex 2.2.

4.4.3 Model Evaluation Methods

The performance of SWAT was evaluated using statistical analyses to determine the quality and reliability of the predictions when compared to observed values. Summary statistics included the mean and standard deviation (SD), which were used to assess SWAT's ability to reproduce the distribution of the observed data and to assess the variability between the observed and simulated data. The goodness-of-fit measures used were the coefficient of determination (R^2; Eq. (4.7)) and the Nash- Sutcliffe efficiency (E_{NS}) value (Eq. (4.8)) (Nash and Sutcliffe, 1970). The R^2 and E_{NS} values are explained in Eqs. (4.7) and (4.8) respectively,

$$R^2 = \frac{\left[\sum_{i=1}^{n}(q_{si}-\overline{q}_s)(q_{oi}-\overline{q}_o)\right]^2}{\sum_{i=1}^{n}(q_{si}-\overline{q}_s)^2\sum_{i=1}^{n}(q_{oi}-\overline{q}_o)^2} \text{----------} Eq4.7$$

Nash and Sutcliffe simulation efficiency, E_{NS}, indicates the degree of fitness of the observed and simulated plots with the 1:1 line (Santhi *et al.* 2002). It is calculated as follows with the same variables defined above:

$$E_{NS} = 1 - \frac{\sum_{i=1}^{n}(q_{oi}-q_{si})^2}{\sum_{i=1}^{n}(q_{oi}-\overline{q}_o)^2} \text{----------} Eq4.8$$

E_{NS} can have values ranging from -∞ to 1. If the simulation is accurate, E_{NS} is equal to one. If the accuracy of the simulation results is smaller than the average value of the measured variables, then E_{NS} will have a negative value.

The sum is taken over the whole period of the data used for calibration. A value closer to unity, means the model explains the variance better. A negative modeling efficiency

means that the model prediction is worse than simply using the mean of the observed flows.

4.4.4 Model Calibration

Calibration is tuning of model parameters based on checking results against observations to ensure the same response over time. This involves comparing the model results to recorded streamflows. In this process, model parameters varied until recorded flow patterns are accurately simulated. Storm (1996) distinguished three types of calibration methods: the manual trial-and-error method, automatic or numerical parameter optimization method; and a combination of both methods. According to the authors, the manual calibration is the most common and especially recommended in cases where a good graphical representation is strongly demanded for the application of more complicated models. However, it is very cumbersome, time consuming, and requires experience.

Automatic calibration makes use of a numerical algorithm in the optimization of numerical objective functions. The method undertakes a large number of iterations until it find the best parameters. The third method makes use of combination of the above two techniques regardless of which comes first. For this study, combining of the two methods was considered.

The manual calibration of this study was done based on the procedures recommended in SWAT user manual: first calibration of the water balance followed by that of temporal flow. Water balance calibration normally takes care of the overall flow volume and its distribution among the different hydrologic components, whereas temporal flow calibration is concerned about the flow time lag and the hydrograph shape.

As discussed in the previous section (section 4.4.1), the gauged flow was separated into surface flow and baseflow components for the water balance comparisons. The calibration was commenced by the yearly average of the total water yield. Sensitive parameters found from the sensitivity analysis (section 4.4.2) were varied within their ranges till the volume is adjusted to the required quantity. The parameters varied were taken according to their relative sensitivity. This process continued by taking

consecutive parameters till the volume simulated is within $\pm$15% of the gauged flow volume.

The surface runoff adjustment was then followed by that of the baseflow. The same approach was followed as above being the adjustment made to the most sensitive parameters affecting the baseflow: the threshold water depth in the shallow aquifer for flow (GWQMN), the deep aquifer percolation fraction (Rchrg_dp), and the groundwater Revap coefficient (GW_REVAP). Each time the baseflow calibration is finalized, the surface runoff volume was also checked as adjustment of the baseflow parameters can also affect the surface runoff volume.

The same procedure was also followed to calibrate the water balance of the monthly flows too. After each calibration, the regression coefficient (R^2), and the Nash and Sutcliffe (1970) simulation efficiency (ENS) were also checked in accordance to Green et al. (2006) recommendation ($R^2 > 0.5$ and ENS > 0.4).

After the water balance calibration was completed, automatic calibration was continued for its temporal trend to take care of the inconsistency occurred in the patterns of the simulated and gauged flows.

The auto calibration was carried out for each of the sub watersheds independently. Even though long years of historical records were available, only part of it was used in the simulation due to a large number of missing values. The calibration was done using historical records of eight years for most catchments and six years for the Koga catchment. However, the simulation was run for ten and eight years respectively, where the first two years were used to "warm-up" the model. "Warming-up" is the very essential part of the simulation process that ensures the establishment of the basic flow conditions for the simulations to follow by bringing the hydrologic processes to an equilibrium condition.

For this study, the criteria of $E_{NS} > 0.4$ and $R^2 > 0.5$ were chosen to assess how well the model performed (Green et al., 2006) with results greater than 0.4 and 0.5 for E_{NS} and R^2, respectively, meaning that the model performed satisfactorily and results below those numbers intending that the model did not perform well. Santhi et al. (2001a, b)

used criteria of $R^2 > 0.6$ and $E_{NS} > 0.5$ to determine how well the model performed. Chung et al. (1999, 2002) cited in Guithi (2006) used standards of $E_{NS} > 0.3$ and $R^2 > 0.5$ to determine if the model results were satisfactory.

Calibration parameters that impact runoff, and, therefore water quality values, include the SCS runoff curve number for moisture condition II (CN2), the soil evaporation compensation factor (ESCO), the surface runoff lag time (SURLAG), and Available soil water capacity (SOL-AWC). The CN2 parameter was originally set a value of 81 as recommended by the USDA-SCS National Engineering Handbook (USDA-SCS, 1972) for these hydrologic groups. The other parameters (SURLAG, ESCO, and SOL_AWC) used SWAT's default values (4 days, 0.95, and 0, respectively).

4.4.5 Auto Calibration-Sensitivity Analysis Tool

Using only manually calibrated parameter values in the auto calibration process is as follows. First the parameters are manually calibrated for the time period of choice until the model simulation results are acceptable as per water balance comparisons. Next, the final parameter values that were manually calibrated are used as the initial values for the auto calibration procedure. Maximum and minimum parameter value limits are used to keep the output values within a reasonable value range. Finally, the auto calibration tool is run with the optimal fit values to provide the best fit between the measured and simulated data as determined by the E_{NS} values and how reasonable the values are.

The auto calibrated determined parameter values can then be adjusted to ensure that they are reasonable. The user has a large role in determining if the values are realistic for their application and can override the output manually. Each sub watershed's optimum parameter's value for a maximum E_{NS} value was determined using SWAT's embedded auto calibration tool for two time periods (1994-2001 and 2002- 2005) except for Koga (1996-2001 and 2002-2005) run on a daily time step. The maximum number of trials allowed was 20,000 before optimization was terminated with the complex shuffling set at 97.5% probability.

The final simulation parameter values, as a combination of auto calibration values and manually adjusted values, per catchments are used as final calibrated parameters.

Accordingly, calibration was done at five gauging stations namely Guder, Muger, Koga, Birr and Didessa. The model was calibrated for the period 1992 to 2001 with the first two years as the "warm up" period. Thus, only results for the period 1994-2001 were used in the evaluation of the calibration.

4.4.6 Model Verification

Model Verification is comparison of the model outputs with an independent data set without making further adjustments. The process continues till simulation of validation-period streamflows confirm that the model performs satisfactorily. In the validation process, data for a period of three to four years was used in all catchments to evaluate the model accuracy. The statistical criteria used during the calibration procedure were also checked here to make sure that the simulated volume is still within the accuracy limits.

4.4.7 Uncertainties Analysis

Another issue with calibration of watershed models is that of uncertainty in the predictions. Watershed models suffer from large model uncertainties. These can be divided into: conceptual model uncertainty, input uncertainty, and parameter uncertainty. The conceptual model uncertainty (or structural uncertainty) could be of the following situations:

a) Model uncertainties due to simplifications in the conceptual model,
b) Model uncertainties due to processes occurring in the watershed but not included in the model,
c) Model uncertainties due to processes that are included in the model, but their occurrences in the watershed are unknown to the modeller, and

d) Model uncertainties due to processes unknown to the modeller and not included in the model either!

Input uncertainty is as a result of errors in input data such as rainfall, and more importantly, extension of point data to large areas in distributed models. Parameter uncertainty is usually caused as a result of inherent non-uniqueness of parameters in inverse modeling. Parameters represent processes. The fact that processes can compensate for each other gives rise to many sets of parameters that produce the same output signal. A short explanation of uncertainty issues is offered below.

Further errors could also exist in the very measurements we use to calibrate the model. These errors could be very large, for example, in sediment data and grab samples if used for calibration. Another uncertainty worth mentioning is that of "modeler uncertainty"! It has been shown before that the experience of modelers could make a big difference in model calibration. We hope that packages like SWAT-CUP can help decrease modeler uncertainty by removing some probable sources of modeling and calibration errors.

On a final note, it is highly desirable to separate quantitatively the effect of different uncertainties on model outputs, but this is very difficult to do. The combined effect, however, should always be quantified on model out puts.

4.4.7.1 Conceptual Basis of the SUFI-2 Uncertainty Analysis Routine

In SUFI-2, uncertainty of input parameters are depicted as uniform distributions, while model output uncertainty is quantified by the 95% prediction uncertainty (95PPU) calculated at the 2.5% and 97.5% levels of the cumulative distribution of output variables obtained through Latin hypercube sampling. SUFI-2 starts by assuming a large parameter uncertainty, so that the measured data initially falls within the 95PPU, then decrease this uncertainty in steps until two rules are satisfied:

(1) The 95PPU band brackets ''most of the observations'' and

(2) The average distance between the upper (at 97.5% level) and the lower (at 2.5% level) parts of the 95PPU is ''small''. Quantification of the two rules is somewhat problem dependent.

If measurements are of high quality, then 80–100% of the measured data should be bracketed by the 95PPU, while a low quality data may contain many outliers and it may be sufficient to account only for 50% of the data in the 95PPU. For the second rule we require that the average distance between the upper and the lower 95PPU be smaller than the standard deviation of the measured data. This is a practical measure based on our experience. A balance between the two rules ensures bracketing most of the data within the 95PPU, while seeking the smallest possible uncertainty band. We use the above two measures to quantify the strength of calibration and accounting of the combined parameter, model, and input uncertainties.

A short step-by-step description of SUFI-2 algorithm is as follows:

Step 1

In the first step an objective function is defined. The literature shows many different ways of formulating an objective function. Each formulation may lead to a different result; hence, the final parameter ranges are always conditioned on the form of the objective function. To overcome this problem, some studies combine different types of functions (e.g., based on root mean square error, absolute difference, logarithm of differences, R^2, Chi square, Nash-Sutcliffe, etc.) to yield a "multi-criteria" formulation. The use of a "multi-objective" formulation where different variables are included in the objective function is also important to reduce the non-uniqueness problem. The objective functions included in SUFI-2 are described later in the user manual of SWAT-CUP.

Step 2

The second step establishes physically meaningful absolute minimum and maximum ranges for the parameters being optimized. There is no theoretical basis for excluding any one particular distribution. However, because of the lack of information, we assume that all parameters are uniformly distributed within a region bounded by minimum and maximum values. Because the absolute parameter ranges play a constraining role, they should be as large as possible, yet physically meaningful:

Step 3

This step involves an optional, yet highly recommended "absolute sensitivity analysis" for all parameters in the early stages of calibration. We maintain that no automated

optimization routine can replace the insight from physical understanding and knowledge of the effects of parameters on the system response. The sensitivity analysis is carried out by keeping all parameters constant to realistic values, while varying each parameter within the range assigned in step one. Plotting results of these simulations along with the observations on the same graph gives insight into the effects of parameter changes on observed signals.

Step 4

Initial uncertainty ranges are next assigned to parameters for the first round of Latin hypercube sampling. In general, the ranges are smaller than the absolute ranges, are subjective, and depend upon experience. The sensitivity analysis in step 3 can provide a valuable guide for selecting appropriate ranges. Although important, these initial estimates are not crucial as they are updated and allowed to change within the absolute ranges.

Step 5

Latin Hypercube sampling is carried out next; leading to n parameter combinations, where n is the number of desired simulations. This number should be relatively large (approximately 500-1000). The simulation program is then run n times and the simulated output variable(s) of interest, corresponding to the measurements, are saved.

Step 6

As a first step in assessing the simulations, the objective function, g, is calculated.

Step 7

In this step a series of measures is calculated to evaluate each sampling round. First, the sensitivity matrix computed using: Next, equivalent of a Hessian matrix, $\mathbf{H}$, is calculated by following the Gauss-Newton method and neglecting the higher-order derivatives. Based on the Cramer-Rao theorem an estimate of the lower bound of the parameter covariance matrix is calculated.

The estimated standard deviation and 95% confidence interval of a parameter is calculated. Parameter correlations can then be assessed using the diagonal and off-diagonal terms of the covariance matrix as follows: Parameter sensitivities were

calculated by calculating the following multiple regression system, which regresses the Latin hypercube generated parameters against the objective function values.

A *t*-test is then used to identify the relative significance of each parameter. Furthermore, the relative sensitivities of different parameters, as indicated by the t-test, depend on the ranges of the parameters.

Step8

In this step measures assessing the uncertainties are calculated. Because SUFI-2 is a stochastic procedure, statistics such as percent error, R^2, and Nash-Sutcliffe, which compare two signals, are not applicable. Instead, we calculate the 95% prediction uncertainties (95PPU) for all the variable(s) in the objective function. As previously mentioned, this is calculated by the 2.5th (X_L) and 97.5th (X_U) percentiles of the cumulative distribution of every simulated point. The goodness of fit is, therefore, assessed by the uncertainty measures calculated from the percentage of measured data bracketed by the 95PPU band, and the average distance *d* between the upper and the lower 95PPU (or the degree of uncertainty) determined from:

$$dx = \frac{1}{k}\sum_{l=1}^{k}(X_u - X_L)_l$$ ---------- Eq. 4.9

Where, *k* is the number of observed data points.

The best outcome is that 100% of the measurements are bracketed by the 95PPU, and *d* is close to zero. However, because of measurement errors and model uncertainties, the ideal values will generally not be achieved.

A reasonable measure for *d,* based on our experience, is calculated by the *R-factor* expressed as:

$$R\text{-}factor = d_x/\sigma_x$$ ----------Eqn 4.1

Where, σ_X is the standard deviation of the measured variable *X*. A value of less than 1 is a desirable measure for the *R-factor*.

Step 9

Because parameter uncertainties are initially large, the value of *d* tends to be quite large during the first sampling round. Hence, further sampling rounds are needed with updated parameter ranges. While producing narrower parameter ranges for subsequent iterations, ensure that the updated parameter ranges are always centered

on the best estimates. The uncertainty in the sensitive parameters reduces faster than those of the insensitive parameters due to the inclusion of the confidence interval, which is larger for less sensitive parameters. Link between SWAT and SWAT-CUP is shown in flow chart below.

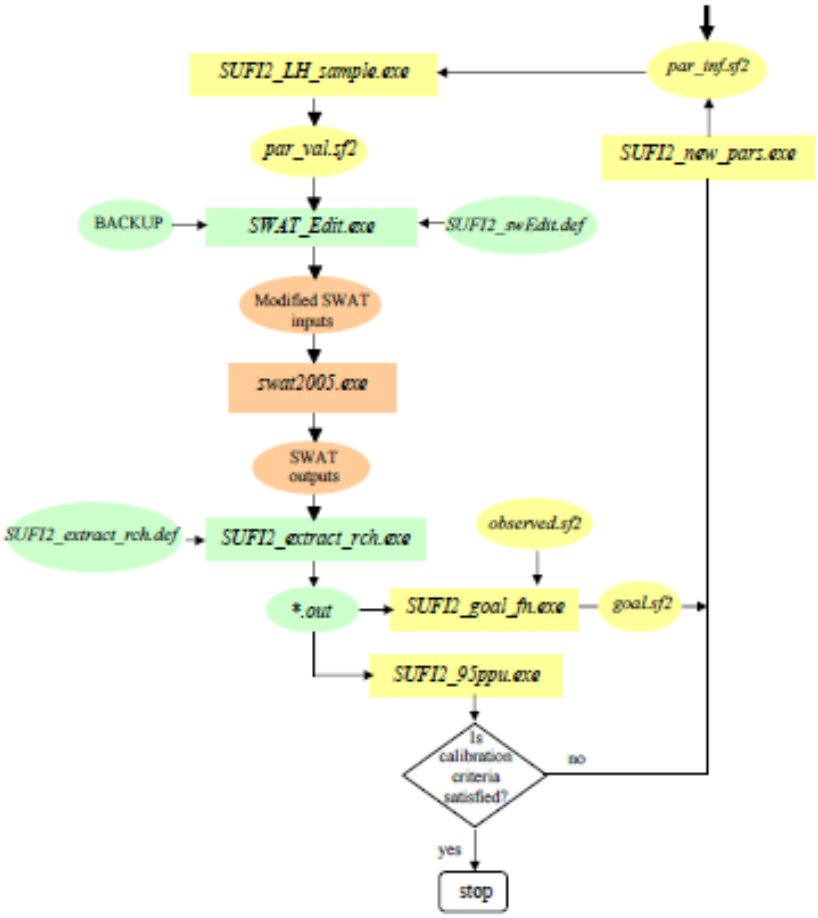

Figure 4-1: Link between SWAT (Orange), iSWAT (Green), and SUFI2 (Yellow) (Source: SWAT-CUP User Manual)

4.4.8 Determination of Impacted Flow

The areal value of daily temperature and precipitation found as output from the RegCM3 model were given as an input to the SWAT model. The remaining climatic and all other land use and soil hydrologic parameters used in model development under current climate conditions were assumed to be constant and remain valid under conditions of climate change.

5 DATA AVALIBILITY AND ANALYSIS

5.1 Data Availability and Description of Arc SWAT Model Input

The SWAT model requires the data on terrain, land use, soil and weather for impact assessment on Streamflow at desired locations of a drainage basin. These data for all the selected catchments of the basin (Birr, Koga, Muger, Guder and Didessa) have been used to generate the hydrological time series for the present/control (representing the period 1994–2003) and the future scenario (representing the period 2031–2100) simulated weather data. The selection of scale and resolutions for spatial data is based on the availability of the required terrain data and the processing effort required for its preprocessing using the GIS interface.

The following sections provide brief description of data elements used and preprocessing performed on them.

5.1.1 Topographic data

Generally the topography of the whole basin signifies two distinct features; the highlands in the center and eastern part of the basin and the lowlands in the western part of the basin. The altitude in the selected catchments ranges from 1275masl in low lands up to 3522masl in high lands.

Topography of the study areas are generally represented by Digital Elevation Model (DEM) having a resolution of 30m by 30m. It has been used in this study to provide the physical characteristics of the study area specifically to a raster or regular grid of spot heights that are required for hydrological modeling. It is the basic input of the Arc GIS integrated SWAT hydrologic model (ArcSWAT) to delineate watersheds and river networks.

5.1.2 Land use/Cover

Land use of the study areas are classified based on Abbay River Basin Master Plan study conducted by BCEOM, in 1996-1999 and Blue Nile River Basin Atlas prepared by

International Water Management Institute (IWMI) in 2009. SWAT has predefined land uses identified by four-letter codes and it uses these codes to link land use maps to SWAT land use databases in the GIS interfaces. Hence, while preparing the lookup-table, the land use types were made compatible with the input needs of the model. Detailed description of the land use types and areal coverage has been found in the table below and described graphically in Section 6.2 in Figure 6.1-5.

Table 5-1: Land use of the study area with their aerial coverage

No	Name of Catchments	Types of Land use/cover	Percentage covered
1	Birr	Intensively Cultivated --> IC	74.23
		Moderately Cultivated --> MC	20.78
		Bush Shurb Grassland --> BSG	4.99
2	Koga	Agricultural Land-Close-grown --> AGRC	67.26
		Range-Brush --> RNGB	27.47
		Agricultural Land-Row Crops --> AGRR	5.26
3	Muger	Intensively Cultivated --> IC	33.97
		Open Shrubland --> OS	18.58
		Open Grassland --> OG	37.06
		Euculaptus Woodland --> EW	10.39
		Urban or Built-Up Land --> UOB	0.01
4	Guder	Agricultural Land-Generic --> AGRL	80.76
		Distributed Highly Forest --> DHF	19.24
5	Didessa	Range-Grasses --> RNGE	24.63
		Agricultural Land-Generic --> AGRL	16.79
		Corn --> CORN	8.8
		Sugarcane --> SUGC	0.31
		Agricultural Land-Close-grown --> AGRC	19.61
		Distributed Highly Forest --> DHF	18.42
		Forest-Mixed --> FRST	11.46

5.1.3 Soil

Like land use the soil classification for the study area is also adopted from Abbay River Master Plan study in 1996-1999 conducted by BCEOM which was obtained from Ministry of Water and Energy (MoWE) and from Blue Nile River Basin Atlas.

The spatial distribution of different soil types is one of the very important factors affecting the overall hydrology of a watershed. SWAT model basically needs the soil

data in defining lumped land areas, HRUs. It also needs all physical and chemical properties of each soil types in the watershed. The soil types and their aerial coverage, and the soil map produced in a shape file format are shown in table 5.2 and figure 6.1-5 respectively.

Table 5-2: Soil of the study area with their aerial coverage

No	*Catchment's name*	*Soil types*	*Percentage coverage*	*Dominant soil*
1	Birr	Chromic Luvisols	82.31	Chromic Luvisols
		Chromic Vertisols	17.25	
		Eutric Nitosols	0.44	
2	Guder	Chromic Luvisols	41.25	Chromic Luvisols
		Orthic Luvisols	27.15	
		Chromic Vertisols	31.6	
3	Koga	Chromic Luvisols	64.15	Chromic Luvisols
		Chromic Vertisols	23.59	
		Eutric Nitosols	12.26	
4	Muger	Chromic Luvisols	19.7	Vertic Cambisols
		Eutric Nitosols	0.03	
		Vertic Cambisols	80.27	
5	Didessa	Dystric Cambisols	73.02	Dystric Cambisols
		Eutric Nitosols	1.57	
		Orthic Acrisols	12.2	
		Pellic Vertisols	13.2	

5.1.4. Meteorological Data

SWAT also needs long years of climate data for the simulation of hydrological processes. For this specific study, the necessary climate data were collected from the National Meteorological Services Agency (NMSA). Since there may be few meteorological stations which have relatively long period of record inside the catchment, data was also used from the station surrounding the basin. The types of

meteorological variables have been collected are like humidity, sunshine hours, and wind speed in addition to rainfall, maximum and minimum temperatures.

The number of meteorological variables collected varies from station to station depending on the class of the stations. Some stations contain only rainfall data. The other group includes maximum and minimum temperature in addition to rainfall data. There are also stations which contain variables like humidity, sunshine hours, and wind speed in addition to rainfall, maximum temperature and minimum temperature. The first class station which have all components of climatic variables mentioned above were used as weather generator station.

Data of precipitation, maximum and minimum temperatures, sunshine hours, relative humidity, and wind speed were collected for 21 meteorological stations within and around the watershed. The locations of the stations, distribution patterns and the details of the data collected are presented in Figure 6.1-5 and Table 5.3 below.

Table 5-3: List of station name, watershed area and metrological variables for all catchments

No	Sub Basin/Area, Km^2	Watershed/Area ,Km^2	Rainfall Stations	Temperature Stations	Weather Generator/PET Stations
1	South Gojjam/16,762	Birr/978	Dembecha, Tilili and Lay Birr	Dembecha and Lay Birr	Lay Birr
2	Tana/15,054	Koga/244	Bahir Dar, Adet, Zege and wetet Abay	Bahir Dar and Dangila	Dangila
3	Muger/8,188	Muger/489	Shola Gebeya and Sululta	Addis Ababa Obs.	Addis Ababa Obs.
4	Guder/7,011	Guder/524	Guder and Tikur Inchini	Ambo, Tikur Inchini and Guder	Ambo
5	Didessa/9,781	Didessa/9781	Arjo,Nakamte,Sekka,Limu, Jimma and Yafa	Arjo,Nekemte and Sekka	Arjo,Nekemte and Sekka

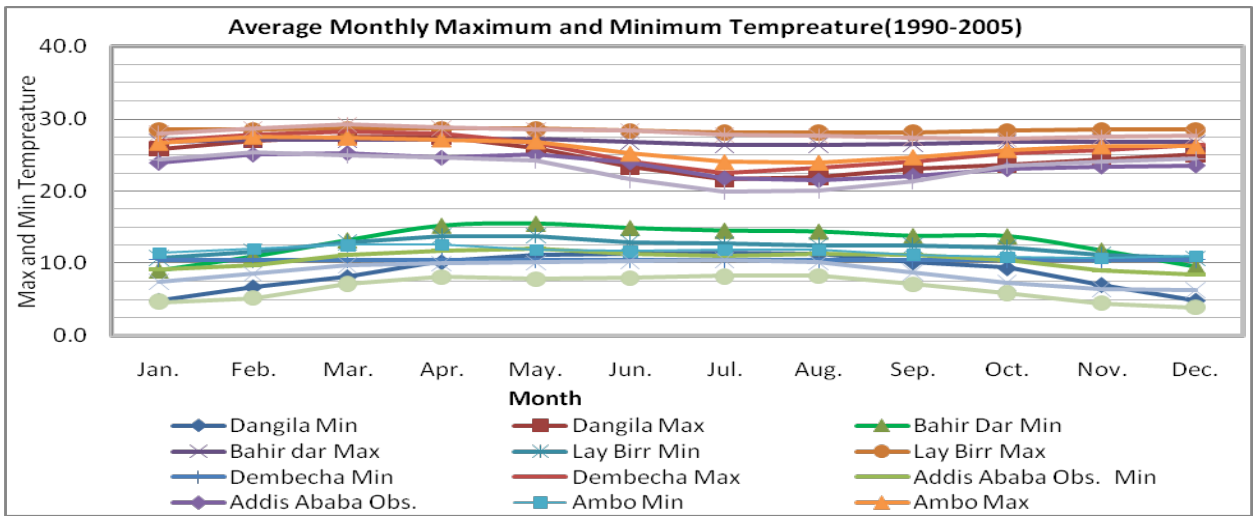

Figure 5-1: Average monthly min & max temperatures patterns of d/t stations (1990-2005)

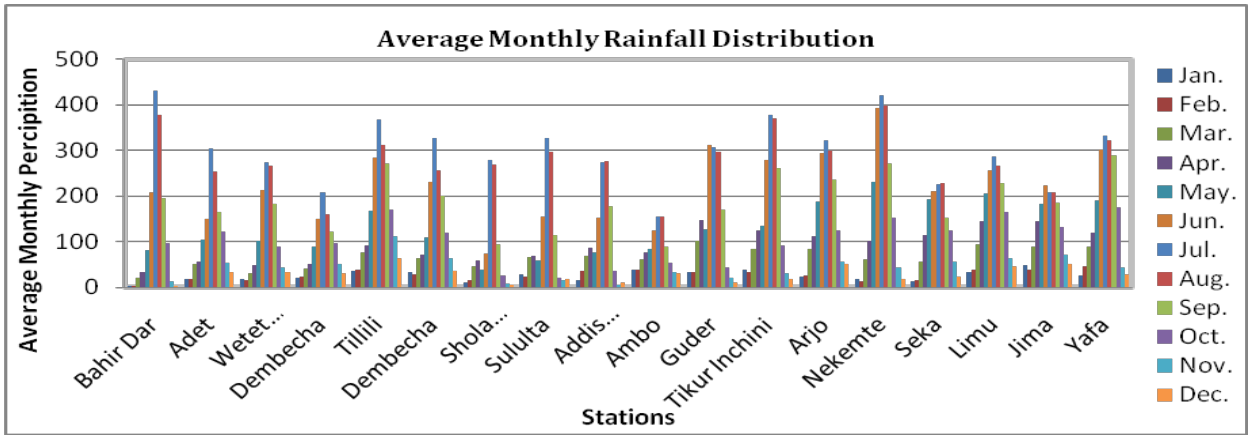

Figure 5-2: Average Monthly rainfall distributions for different stations (1990-2005)

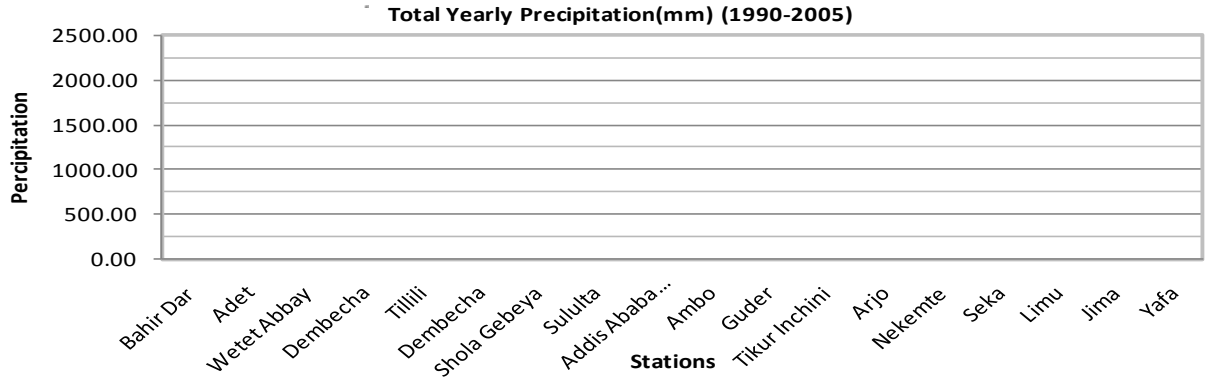

Figure 5-3: Total yearly rainfall distributions for d/t stations in study area (1990-2005)

5.1.5. Hydrological Data

All the rivers have continuous record for a relatively long period with some missed data and therefore daily streamflow data (1990-2006) for these stations were collected from the Hydrology Department of Ministry of Water and Energy (MoWE).

The measured streamflow of Birr, Koga, Muger, Guder and Didessa Rivers were required for calibrating and validating the model. The other gauged rivers near or inside the catchments have been used to fill the missed flow using linear regression techniques. Their details are presented in Table 5.4 as below.

Table 5-4: Details of stream flow data collected for 16 years from the MoWE

No	*River Name*	*UTM*		*Gauged Station name*	*Area SQKMs*	*Periods*
		X- Coordinate	*Y-Coordinate*			
1	Birr	323159	1177636	Jiga	978	1990-2006
2	Koga	287200	1257124	Merawi	244	1990-2006
3	Guder	362576	989468	Guder	524	1990-2006
4	Muger	470713	1027938	Chancho	489	1990-2006
5	Didessa	223228	952539	Arjo	9,981	1990-2001
			Total		**12,216**	

5.1.6. Climatic Scenario Data

The climatic scenario generated using Regional Climate Model version 3 (RegCM3) A1B emission scenario having a resolutions of 50km by 50km were used. The daily weather data on precipitation, temperature (maximum and minimum), solar radiation, wind speed and relative humidity at all the grid locations were availed.

The future climatic variables have been superimposed on the catchments. The centroid of each sub-basin is then taken as the location for the weather station to be used in the SWAT model. This procedure has been used for the present/control (representing series 1992–2003) and the future/scenario (representing series 2031–2100) climate data.

5.2 Data Analysis and Evaluation

As the result of any simulation depends of the quality of the available data, data-checking were made for their reliability. SWAT normally uses solar radiation values rather than daily-sunshine-hours data, and hence conversion of these variables was made using Cropwat 8. Statistical analysis of the daily data (monthly daily averages, standard deviations, probability of wet and dry days, skew coefficient) were carried out, which were latter used as an input for the data generator.

Finally, all the data were prepared in *.dbf* format as an input into the SWAT model. All the missing data were filled with a missing data identifier of -99. SWAT has a built-in weather generator that is used to fill these gaps. SWAT takes data of each climatic variable for every subbasin from the nearest weather station measured from the centroid of the subbasins. Data were checked for the unreliability and their monthly and yearly statistics were calculated for use in the calibration and validation of the simulated flows.

5.2.1. Checking Precipitation Data Quality/Consistency

To detect possible errors checking the station for data quality using appropriate method is crucial. Therefore, checking consistency of individual stations, the data qualities with regard to possible temporal variations or errors have been investigated by Double Mass Curve. As it is tried to show in Annex 4 the stations are consistence to each other.

5.2.2. Filling Missing Data

SWAT model requires daily weather data; however there are only few meteorological stations in the basin having long record of data. Furthermore, the quality of the data is not reliable and there are large amounts of missing data. Sharply and Williams, (1990) have developed their own weather generator (WXGEN) that uses monthly statistics to fill the missing data. But these monthly statistics must first be calculated based on the available daily data, hence, making WXGEN unusable for areas with no daily data.

SWAT, unless given read-in climate data, uses a random weather generator that uses information found in weather station WGN files. These WGN files contain the statistical data for the typical climatic activity at a certain station for different times of the year. In this study the weather generator algorithm in SWAT were used to fill in the missing data in monthly rainfall, minimum and maximum temperature.

Therefore, the missing data have been represented by –99 so that SWAT will fill in the gap. But missing data of flow data were filled by Regression Method from the other rivers as shown in Annex 1.1-3.

6 RESULT AND DISCUSION

6.1 SWAT Hydrological Model Results

6.1.1 Watershed Delineation

The Arc SWAT interface proposes the minimum, maximum, and suggested size of the sub basin area (in hectare) to define the minimum drainage area required to form the origin of a stream. Generally, the smaller the threshold area, the more detailed are the drainage networks, and the larger are the number of subbasins and HRUs. However, this needs more processing time and space.

As a result, an optimum size of a watershed that compromises both was selected. Dilnesaw (2006) did a sensitivity analysis of the threshold area on SWAT model performance and found that the optimum threshold area that can be used for the delineation procedure is $\pm 1/3$ of the suggested threshold area. Therefore, a threshold area of -1/3 of that suggested by the model was used.

In addition to those defined by the model itself, five watershed outlets were taken at the gauging stations, which were later used as a point of calibration and validation of the simulated flows. As a result, five watersheds mentioned in Table 6.1 were delineated.

6.1.2 Determination of Hydrologic Response Units (HRUs)

The catchment delineation was followed by the determination of HRUs, which are unique soil and land use combinations within subbasins modeled regardless of their spatial positioning. This describes better the hydrologic water balance and increases the accuracy of flow predictions (Luzio et al. 2002 cited Githui, 2006). SWAT predicts the land phases of the hydrologic cycle separately for each HRU and routes to obtain the total flow of the subbasins.

The HRUs were determined by assigning one HRU for each subbasin considering the dominant soil/land use combinations, which makes the automatic calibration easy.

Table 6-1: Delineated catchments with their hru's and area coverage

No	Name	Elevation Ranges			Delineated areas and number of sub basin and HRU's		
		Max	Min	Mean	Area, KM²	Number of Sub basin's	Number of Hru's
1	Koga	3124	1928	2120	244	11	11
2	Birr	3522	1755	2280	978	17	17
3	Muger	3378	2536	2686	489	11	11
4	Guder	3222	2009	2507	524	11	11
5	Didessa	3155	1288	1816	9981	29	29

After mapping the basins for terrain, land use and soil, each of the basins has been simulated for the given hydrologic response units and subbasins in the table above. Detail descriptions of the soil, land use/cover and slope combinations used in catchment delineations are listed in Table 6.2 below.

Table 6-2: Detail descriptions of all catchments soil, land use and slope

No	Name of Catchments	Types of Land use/cover	Soil types	Slope
1	Birr	Intensively Cultivated --> IC Moderately Cultivated --> MC Bush Shurb Grassland --> BSG	Chromic Luvisols Chromic Vertisols Eutric Nitosols	0-5% 5% - 10% 10% - 15% 15% - 20% >20%
2	Koga	Agricultural Land-Close-grown --> AGRC Range-Brush --> RNGB Agricultural Land-Row Crops --> AGRR	Chromic Luvisols Chromic Vertisols Eutric Nitosols	0-5% 5% - 10% 10% - 15% 15% - 20% >20%
3	Muger	Intensively Cultivated --> IC Open Shrubland --> OS Open Grassland --> OG Euculaptus Woodland --> EW Urban or Built-Up Land --> UOB	Chromic Luvisols Eutric Nitosols Vertic Cambisols	0-5% 5% - 10% 10% - 15% 15% - 20% >20%
4	Guder	Agricultural Land-Generic --> AGRL Distributed Highly Forest --> DHF	Chromic Luvisols Orthic Luvisols Chromic Vertisols	0-5% 5% - 10% 10% - 15% 15% - 20% >20%
5	Didessa	Range-Grasses --> RNGE Agricultural Land-Generic --> AGRL Corn --> CORN Sugarcane --> SUGC Agricultural Land-Close-grown --> AGRC Distributed Highly Forest --> DHF Forest-Mixed --> FRST	Dystric Cambisols Eutric Nitosols Orthic Acrisols Pellic Vertisols	0-5% 5% - 10% 10% - 15% 15% - 20% >20%

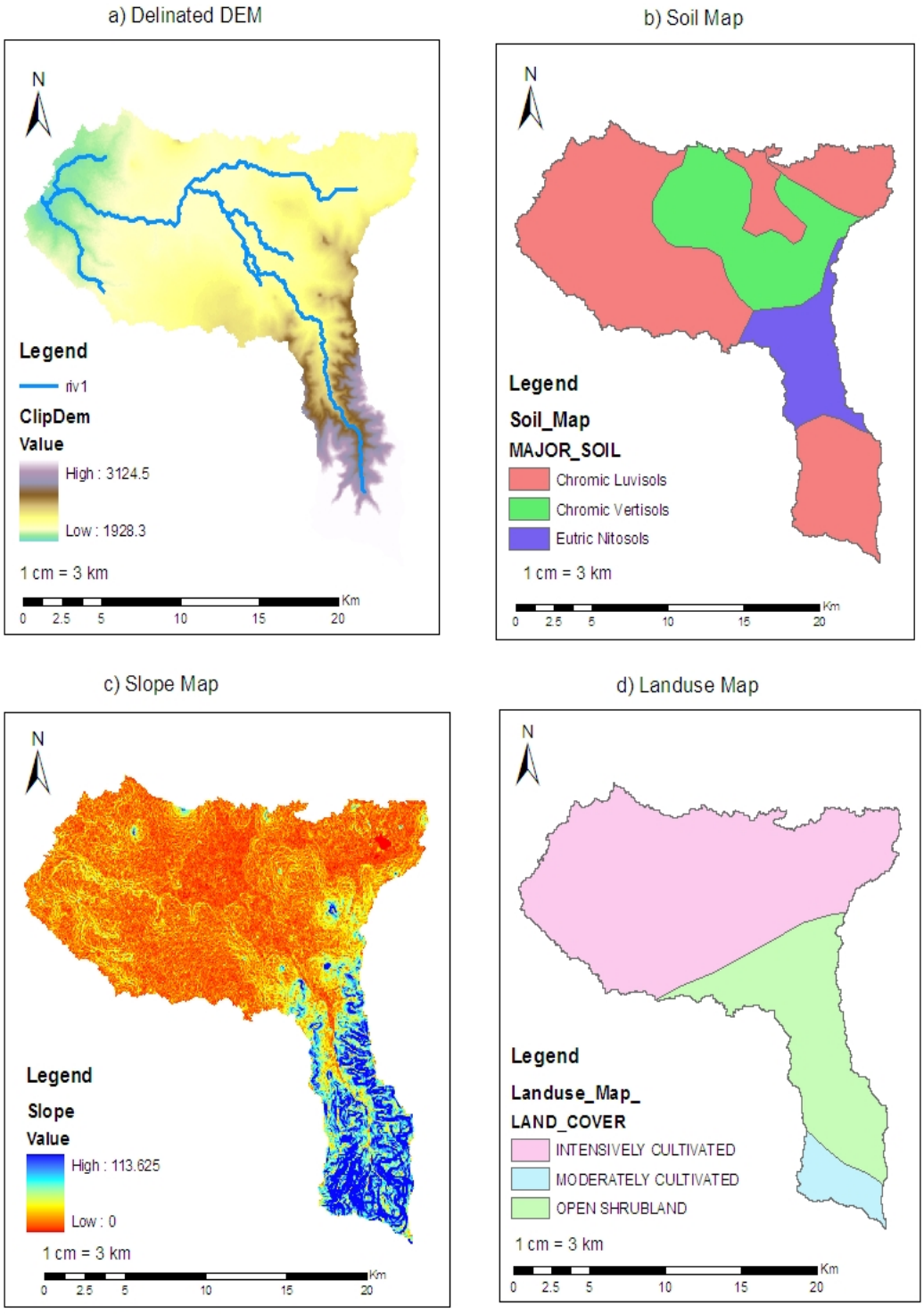

Figure 6-1: The delineated subbasins, land use, slope and soil map of the Koga Catchment

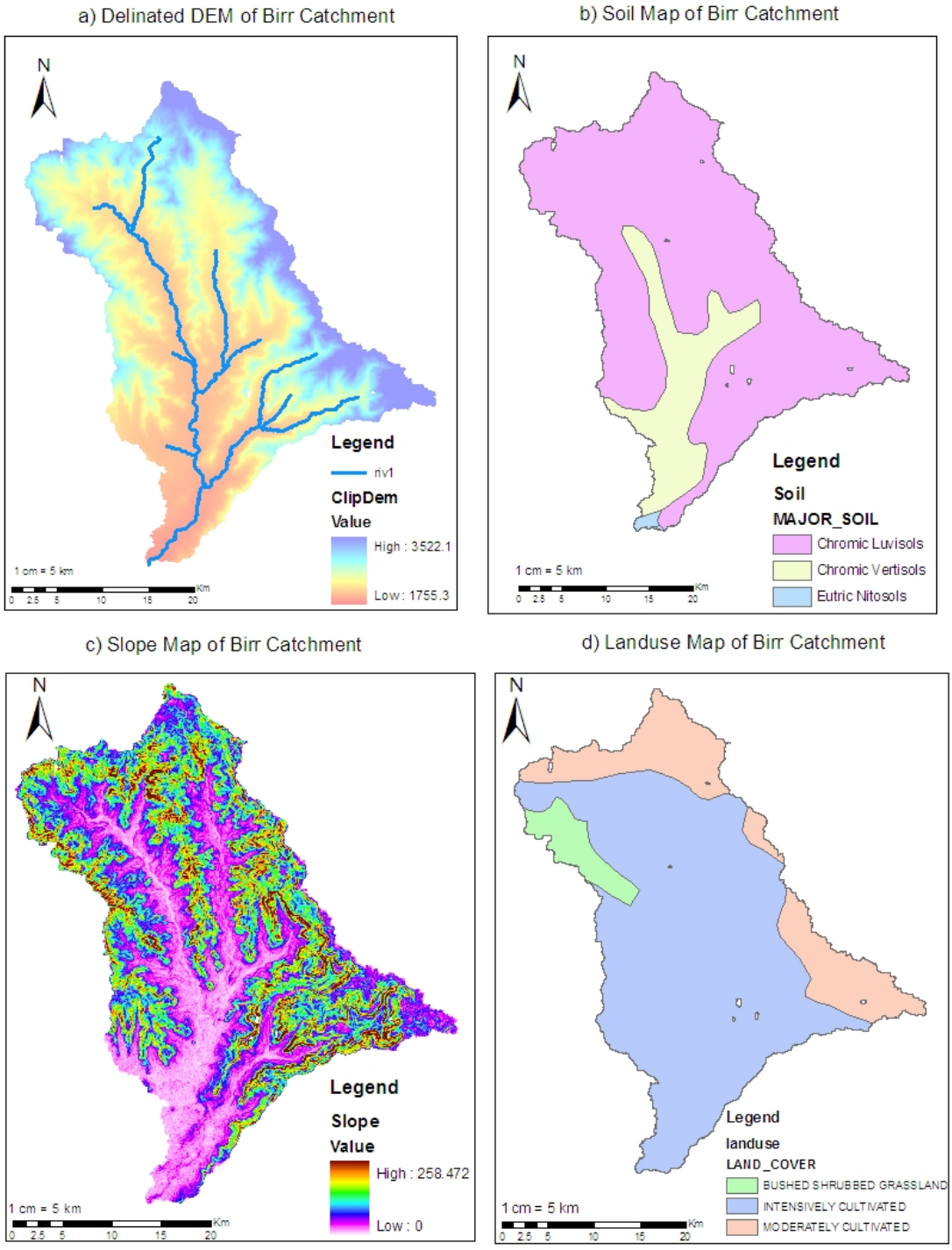

Figure 6-2: The delineated subbasins, land use, slope and soil map of the Birr Catchment

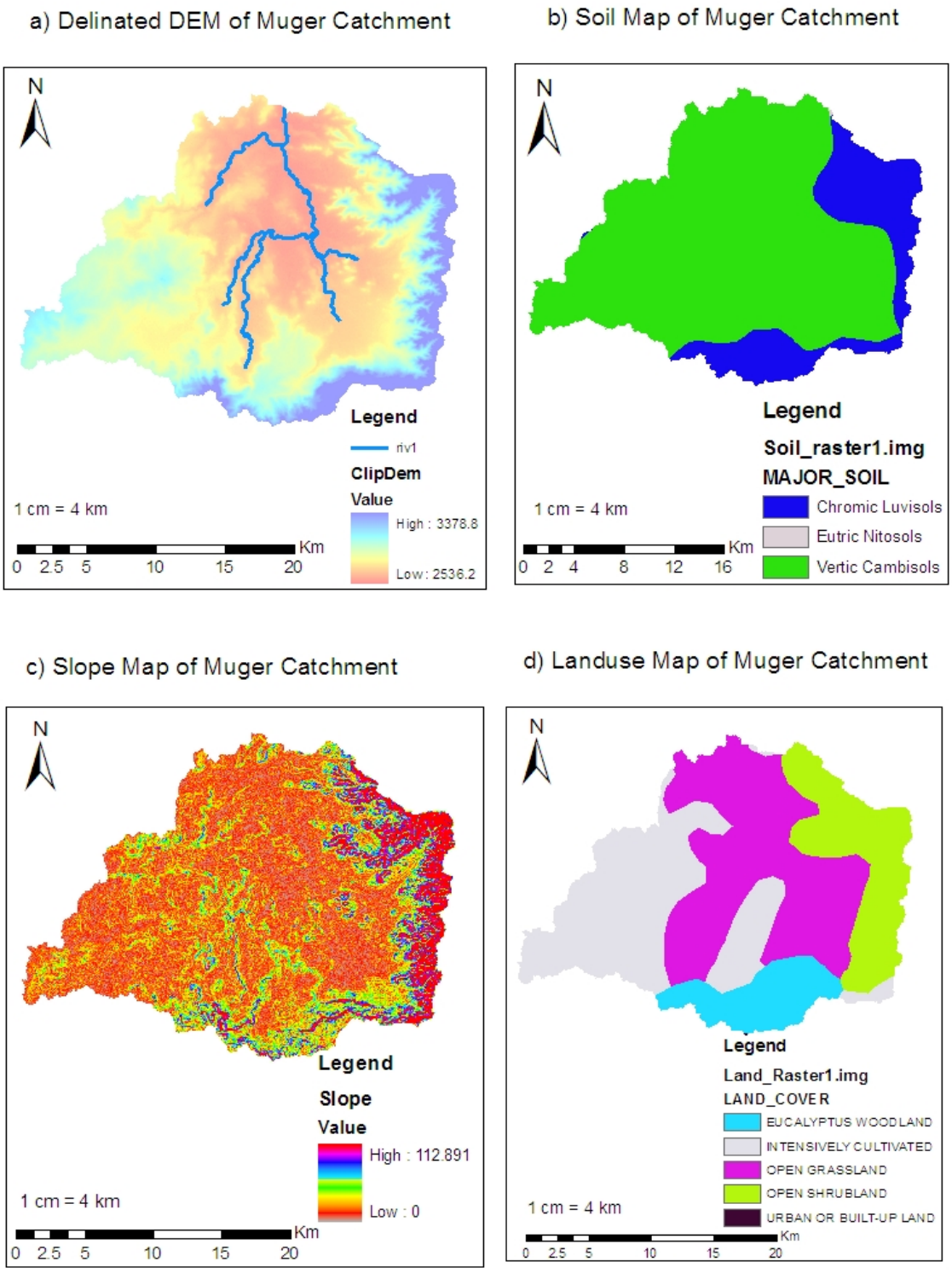

Figure 6-3: The delineated sub basins, land use, slope and soil map of the Muger catchment

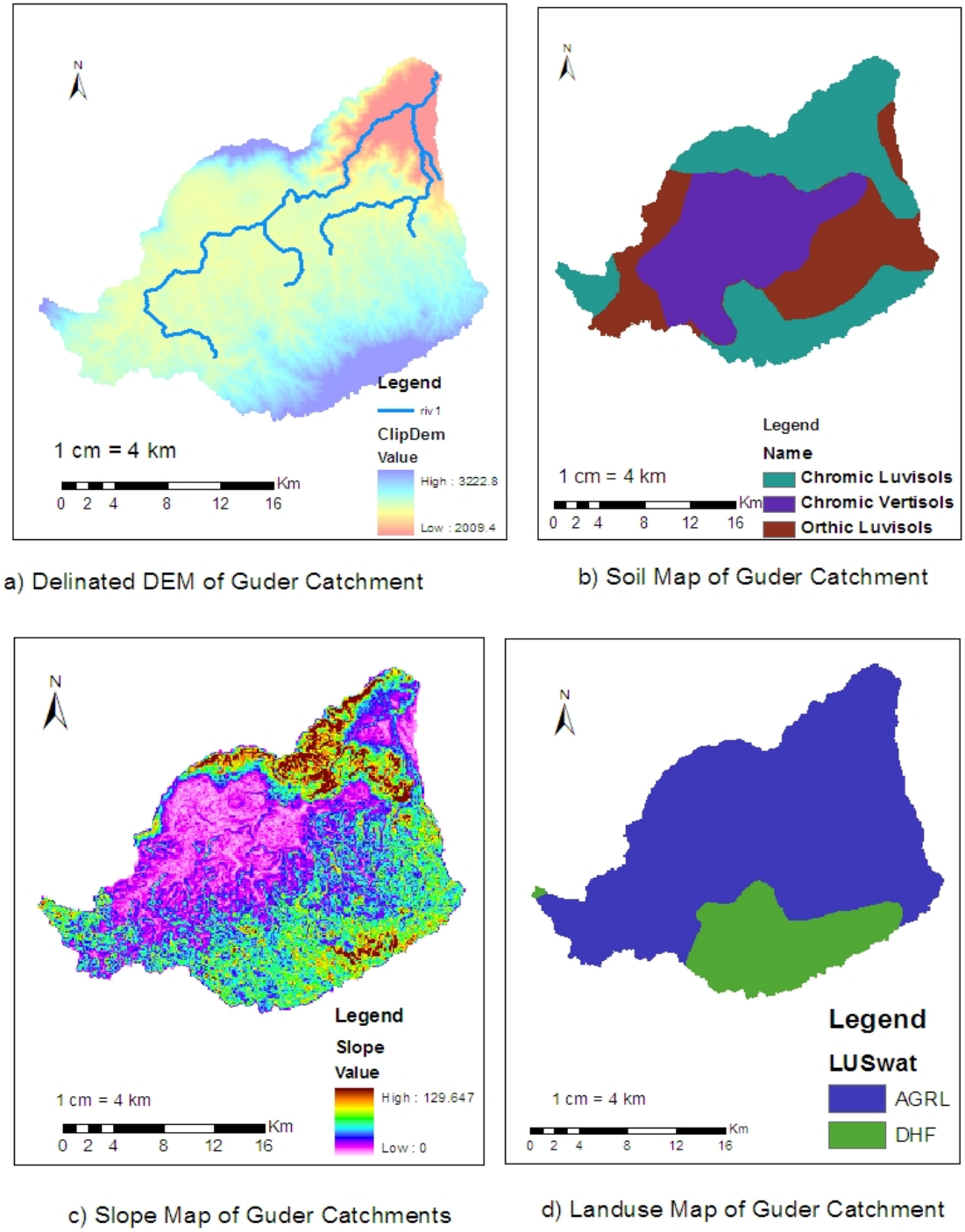

Figure 6-4: The delineated subbasins, land use, slope and soil map of the Guder Catchment

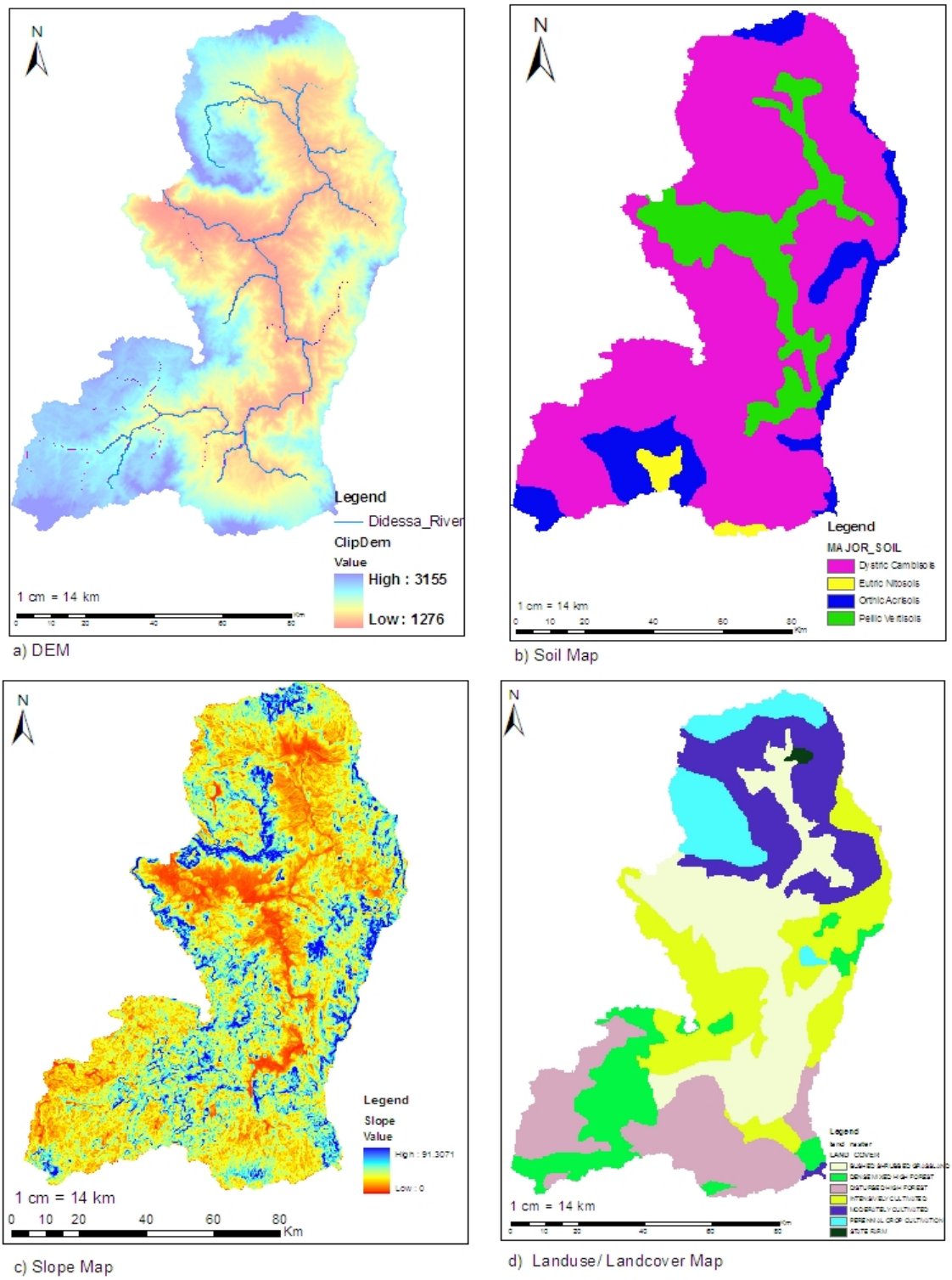

Figure 6-5: The delineated subbasins, land use, slope and soil map of the Didessa Catchment

6.1.3 Performance Evaluation of the Hydrologic Model

6.1.3.1 Sensitivity Analysis

The sensitivity analysis were carried out for a period of 14 years, which included both the calibration period (from January 1st, 1994 to December 31st, 2005) and the warm up period (from January 1st, 1992 to December 31st, 1993) except for Koga river, which is calibrated from January 1st, 1996 to December 31st, 2001 due to flow inconsistency for 1994-1995. Even though 26 parameters with ten intervals of Latin Hypercube (LH) sampling (totally 270 iterations) were used for the sensitivity analysis against the observed streamflow, only 7-9 of them revealed meaningful effect on the daily flow simulation of the period 1992-2005 as it is shown in Annex 2.2.

It is demonstrated by the Mean Relative Sensitivity value (MRS) for which small to negligible ($0 \leq MRS < 0.05$), medium ($0.05 \leq MRS < 0.2$), high ($0.20 \leq MRS < 1.0$), and very high ($MRS \geq 1.0$) Lenhart et al. (2002).

Accordingly, the parameters having Mean Relative Sensitivity value (MRS) greater than 0.05 are meaningfully in defining sensitivities.
As it is indicated in table in Annex 2.2, the four parameters relatively high sensitive are CN2, ALPHA_Bf, ESCO and Bali, being the curve number (CN2) is the most sensitive of all. The other parameters are in medium range. The most sensitive parameters controlling the surface runoff in the catchments are the curve number (CN2), the soil available water capacity (SOL_AWC) and the soil evaporation compensation factor (ESCO). With respect to the base flow, the threshold water depth in the shallow aquifer flow (GWQMN) and the ground water recession factor (ALPHA_Bf) have the highest influence in controlling the base flow for all catchments.

In general the sensitivity analysis result reveals that CN_2 is the most sensitive parameter for Koga, Muger and Didessa catchments, while ALPHA_Bf is for Birr and Guder Catchments. Blai and Esco are relatively sensitive in medium range for Birr and Guder while they are the most sensitive for Koga catchments. But Canmx, Gwqmn and

Sol_Z are medium for all catchments, except Gwgmn is less sensitive for birr. List of the sensitive parameters for each catchments are shown in Annex 2.1 and 2.

6.1.3.2 Calibration and Verification

After the sensitive parameters identification calibration followed by verification were executed for the significant parameters.

The calibration of the model was executed to evaluate the performance of the model simulation using automatic calibration tools embedded in SWAT in addition to manual calibration technique for all catchments.

For the study period between 1994-1995 year records, observed hydrographs shape have no consistent flow pattern for Koga river watershed. That causes the calibration and the validation period short and even it was difficult to select which time period for calibration and validation from the given 1992-2005 period.

Generally for others except Koga and Didessa flow calibrations were performed for a period of eight years from January 1st, 1994 to December 31st, 2001 using the sensitive parameters identified. However, flow was simulated for ten years from January 1st, 1992 to December 31st, 2001, within which the first two years were considered as a warm up period.

Validation is also proves the performance of the model for simulated flows in periods different than the calibration periods, but without any further adjustment in the calibrated parameters. Consequently, validation was performed for three to four years period from January 1st, 2002 to December 31st, 2005 for all rivers except for Didessa River which is from January 1st, 1998 to December 31st, 2001.

As discussed previously in the methodology section, the flows were calibrated manually followed by automatic calibration tools using the observed flow gauged at the outlet of the each watershed. First of all, both the surface runoff and base flow components of the gauged flow were balanced with that of the simulated flow. Afterwards the adjusted flow was further calibrated temporally by making fine adjustments to ensure best fitting of the simulated flow curves with the gauged flow curves. Manipulation of the

parameter values were carried out within the allowable ranges recommended by SWAT developers.

The performance of the model is demonstrated by the correlation coefficient (R^2) and the Nash-Sutcliffe (1970) simulation efficiency (ENS) values.

For this study, in addition to the criteria stated in methodology section, the criteria of $E_{NS} > 0.4$ and $R^2 > 0.5$ were chosen to assess how well the model performed (Green et al., 2006) with results greater than 0.4 and 0.5 for E_{NS} and R^2, respectively, meaning that the model performed satisfactorily and results below those numbers intending that the model did not perform well.

Finally adjusted parameter values are shown in Table 6.4. The calibration and validation result in Table 6.3 shows that there is a good agreement between the simulated and gauged flows in month for all Rivers except Didessa River.

As a result, all catchments except Didessa fulfilled the requirements suggested by Santhi et al. (2001) for $R^2 > 0.6$ and $E_{NS} > 0.5$ for months. While Didessa catchment's according to requirement proposed by Green et al., 2006 the model perform unsatisfactory during calibration and poor for validation.

Table 6-3: Average daily calibration and validation in months

	Calibration			Validation		
River	**Period**	**R^2**	**E_{NS}**	**Period**	**R^2**	**E_{NS}**
Muger	1994-2001	0.76	0.71	2002-2004	0.85	0.83
Koga	1996-2002	0.88	0.78	2003-2005	0.71	0.53
Birr	1994-2001	0.61	0.58	2003-2005	0.76	0.67
Guder	1994-2001	0.80	0.71	2002-2005	0.74	0.54
Didessa	1992-1997	0.51	0.26	1998-2001	0.29	0.17

The above table shows the calibration and validation results of the catchments. The very high correlation coefficient (R^2=0.88) and the Nash-Sutcliffe simulation efficiency (E_{NS}=0.78) values show the very good agreement between the simulated and gauged monthly flows for the Koga River during calibration. These values satisfied the

recommendation made by Santhi et al. (2001), where R^2 and E_{NS} are expected to have values more than 0.6 and 0.5, respectively.

The optimized parameters through the auto calibration for all catchments are summarized in table below.

Table 6-4: Final adjusted parameter values of the flow calibration at the outlet of the catchments

Muger		Birr		Koga		Guder		Didessa	
Calibrated Values		Calibrated Value		Calibrated Value		Calibrated Value		Calibrated Value	
Cn2	-0.25	Alpha_Bf	0	Cn_2	0.246	Alpha_Bf	0.17	Alpha_Bf	0.03
Alpha_Bf	0	Esco	0.05	Esco	0.6	Blai	1	GW_Delay	5.7
Sol_Awc	-0.13	Canmx	9.6	Gwqmn	339.7	Canmx	10	Ch_K2	95
Gwqmn	990	Sol_Z	0.212	Sol_Z	-0.249	Ch_K2	150	Sol_Awc	0.17
Revapmn	44	Cn_2	0.249	Alpha_Bf	0	Esco	0	Sol_Z	0.03
Canmx	1.8	Sol_Awc	-0.24	Sol_Awc	-0.25	Gwqmn	-315.2	Canmx	9.67
Blai	0.99	Blai	0.15			Slope	-0.249	Esco	0.03
Sol_Z	0.24					Sol_Awc	0.25	Gwqmn	0
						Sol_K	-0.248	Revapmn	16.7
						Sol_Z	0.25		0.03

Table 6-5: Calibration statistics of the average daily simulated and gauged flows in months at the outlet of each catchment

River	Period	Average Flow(m^3/s)		% Error	R^2	E_{NS}
		Observed	Simulated			
Muger	1994-2001	6.87	8.86	29.01	0.76	0.71
Koga	1996-2001	5.83	5.36	-8.18	0.88	0.78
Birr	1994-2001	17.86	21.90	22.62	0.61	0.58
Guder	1994-2001	11.94	13.11	9.76	0.80	0.71
Didessa	1992-1997	88.25	98.18	11.25	0.51	0.26

Table 6-6: Validation statistics of the average daily simulated and gauged flows in months at the outlet of each catchment

River	Period	Average Flow(m^3/s)		% Error	R^2	E_{NS}
		Observed	Simulated			
Muger	2002-2004	8	7	12	0.85	0.83
Koga	2003-2005	5	4.9	0.4	0.71	0.53
Birr	2003-2005	15	19	-27	0.76	0.67
Guder	2002-2005	10	15	-42	0.74	0.54
Didessa	1998-2002	76	352	66	0.29	0.17

As shown in Annex 3.1-5, except the slight underestimation during the 1999, 2000 and 1994 flow, the model was able to reproduce a flow curve almost similar to that of the gauged flow for Koga, Birr and Muger respectively and overestimation during 1996 for Muger and Guder. Besides, as described in Table 6.6 above, the calibration statistics, the percentage error of the simulated flow are well within the acceptable range of $\pm 15\%$ of the gauged flow except for Muger and Birr Rivers. Hence, SWAT proved to perform well in simulating the flows of all catchments except for Didessa and Guder Rivers.

The Annex 3.1-5 shows the validation results of the catchments. The very high correlation coefficient (R^2=0.85) and the Nash-Sutcliffe simulation efficiency (E_{NS}=0.83) values show the very good agreement between the simulated and gauged monthly flows of the catchments. These values satisfied the recommendation made by Santhi et al. (2001), where R^2 and E_{NS} are expected to have values more than 0.6 and 0.5, respectively.

Generally, the values of the performance criteria show that during the calibration period overall performance of SWAT model is better compared to the validation period for Koga and Guder and reverse for Birr and Muger Catchments. For the detail observation of the model performance (E_{NS} and R^2) value for each catchments are presented in the Table 6.3.

As it is shown in Annex 3.1-5, peak values are slightly underestimated during 2003 for Koga and Birr and for Muger for all period, and overestimated during 2002-2004 for Guder. This may be due to unreliable precipitation data given as an input to the model or gauged flow used for the calibration. However, the overall flow trend is well simulated by the model except Didessa River.

Thus, the model performed well in simulating flows for periods outside of the calibration based on parameters adjusted during the calibration period. Therefore, these adjusted parameters can be considered to be fairly explaining the hydrologic characteristic of the catchments. As a result, further simulations can be carried out by using these parameters for any extra period of time for all except Didessa River.

6.1.4 Parameter Uncertainty Analysis

SWAT was calibrated based on the daily measured flow, at the outlets for each catchment using the automatic calibration method embedded in Arc Swat. A split sample procedure 60 and 40 percent was used for calibration and validation respectively. For most of the selected catchments data from the period of 1994–2001 were used for calibration, and data from 2002–2005 were used to validate the model. List of the SWAT's parameters that were fitted and their final calibrated values with their list of period used during calibration and validation process are show in table 6.2 in above section.

It should be noted that a watershed model can never be fully calibrated and validated. Calibration of models at a watershed scale is a challenging task because of the possible uncertainties that may exist as discussed in section 3 and 4 in detailed. Sources of uncertainties in distributed models are due to inputs such as rainfall and temperature. Rainfall and temperature data are measured at local stations and regionalization of these data may introduce large errors. In SWAT, climate data for every subbasin is furnished by the station nearest to the centroid of the subbasin. Direct accounting of rainfall or temperature distribution error is quite difficult as information from many stations would be required.

Therefore, carrying out uncertainty analysis for the prediction of the hydrological model is crucial to decide the calibrated parameters to transfer to other homogenous catchments and also using for further predictions. In SUFI-2, parameter uncertainty accounts for all sources of uncertainty, e.g., input uncertainty, conceptual model uncertainty, and parameter uncertainty, because disaggregation of the error into its source components is difficult, particularly in cases common to hydrology where the model is nonlinear and different sources of error may interact to produce the measured deviation (Gupta et al., 2005 cited SWAT-CUP User Manual).

The calibration process initially includes parameters which are calibrated in SWAT as input in the SUFI-2 algorithm. In each iteration1000 model calls were performed, for a total of 5000 simulations, at testing the efficiency of SUFI 2. An ‘‘absolute sensitivity analysis’’ (changing the parameters one at a time while keeping other parameters constant) was performed for all parameters after the second iteration.

These simulations are based on a calibration that used average daily discharge in months in the objective function. The calibrated parameter ranges by SWAT model were used. The calibration and validation statistics are also given in the figures for ease of referencing. The shaded region (95PPU), which is the simulation result, quantifies all uncertainties because it brackets a large amount of the measured data, which contains all uncertainties.

6.1.4.1 Uncertainty Analysis Results for Koga River

The simulated flow using SWAT was initially calibrated based on the observed streamflow at the watershed outlet at Merawi. This calibrated model produced good results of variable for calibration and validation periods. The results are graphically shown in Annex 3.1 above for daily averaged streamflow in months. The parameter ranges were selected based on the calibrated parameter ranges of SWAT model.

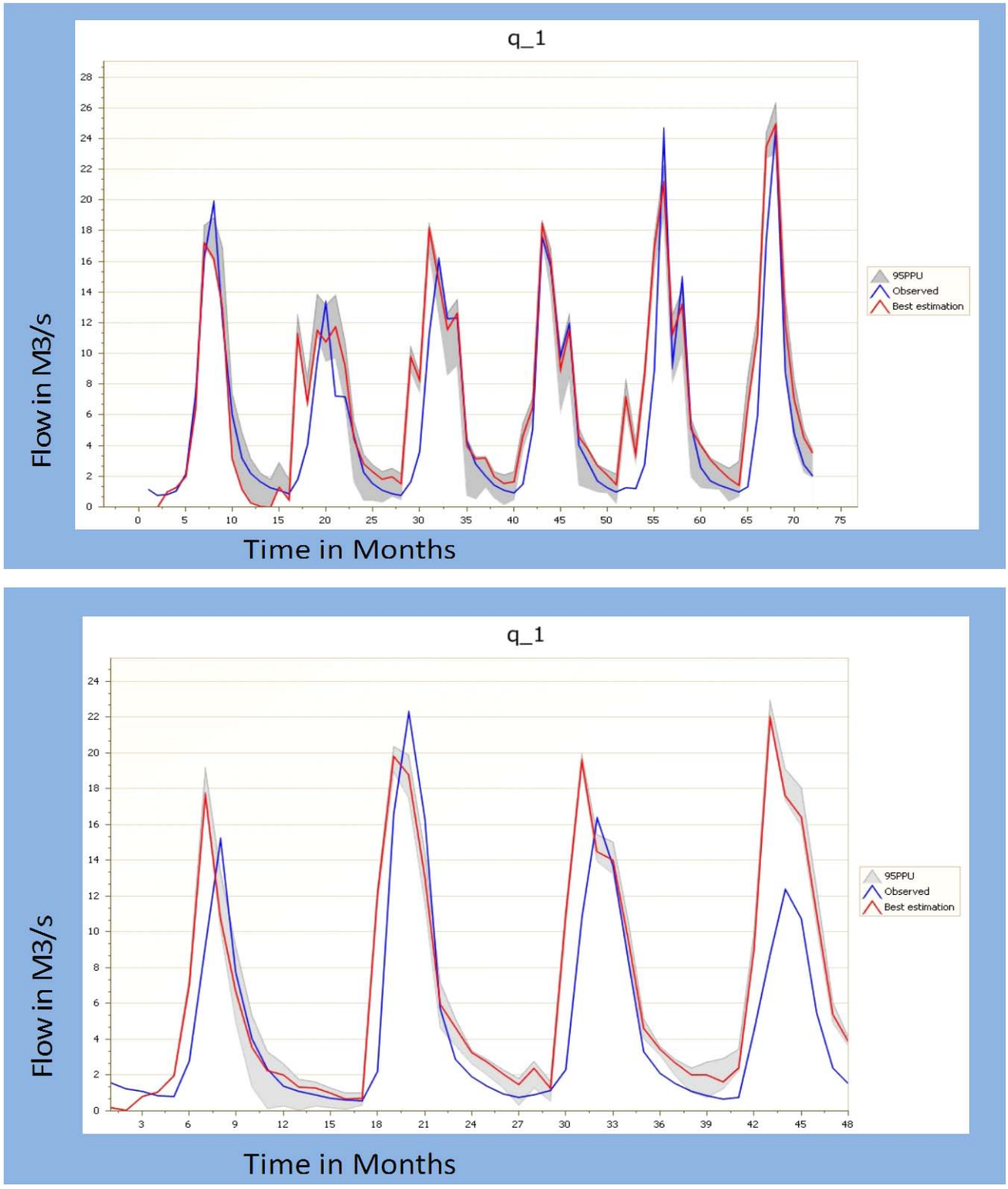

Figure 6-6: The 95% prediction uncertainty (95PPU) for Koga River at Merawi. Top, flow calibration (1996–2001); and bottom, validation (2002–2005)

Table 6-7: Uncertainty analysis results using SUFI2 for Koga River

Koga River-Calibration Period of 1996-2001				
Variable	P_factor	R-factor	R^2	NS
q_1(flow in M^3/s)	0.71	0.39	0.88	0.78
Verification Period of 2002-2005				
q_1(flow in M^3/s)	0.45	0.26	0.71	0.53

Accordingly, the result for flow calibration shows that 71% of the observed data is bracketed by the 95PPU (p-factor) and r-factor had a value of 0.39, which are good results. The smaller the r-factor, which quantifies the thickness of the 95PPU, the smaller the uncertainties and the better calibration work. A value close to 1 is highly desirable for r-factor with a p-factor also close to 1. For the Streamflow validation, 45% of the measured data were bracketed by the 95PPU while the r-factor had value of 0.26. Unlike the calibration, the flow simulation during verification is satisfactory with relatively large uncertainties, r-factor = 0.26, while bracketing only 45% of the data.

On behalf of the above possible errors, calibration and validation results of the watershed could be qualified as ‘‘good’’ in this study. This indicates a fair quality of the input data as well as small conceptual model errors in the dominant processes in the watershed.

6.1.4.2 Uncertainty Analysis Results for Birr River

Like Koga River, the simulated flow using SWAT for this was also initially calibrated based on the observed streamflow at the watershed outlet near Jiga. This calibrated model produced good result during calibration and fair result during validation periods. The results are graphically shown in Annex 3.2 for daily averaged streamflow in months. The parameter ranges were selected based on the calibrated parameter ranges of SWAT model.

Table 6-8: Uncertainty analysis results using SUFI2 for Birr River

Birr River- Calibration Period of 1994-2001				
Variable	**P_factor**	**R-factor**	**R^2**	**E_{NS}**
q_1(flow in M^3/s)	0.55	0.60	0.61	0.58
Verification Period of 2002-2005				
q_1(flow in M^3/s)	0.70	0.61	0.76	0.67

Figure 6-9: The 95% Prediction Uncertainty (95PPU) for Birr River near Jiga. Top, flow calibration (1994–2001); and bottom, validation (2002–2005)

Accordingly, the result for flow calibration shows that 55% of the observed data is bracketed by the 95PPU (p-factor) and r-factor had a value of 0.60. For the validation, 70% of the measured data were bracketed by the 95PPU while the r-factor had value of 0.61. Like the calibration, the flow simulation during verification is quite good with relatively small uncertainties, r-factor=0.61, while bracketing 70% of the data for validation.

Given the above possible errors, calibration and validation results of the watershed could be qualified as ‘‘very good’’ in this study. This indicates a fair quality of the input data as well as relatively small conceptual model errors in the dominant processes in the watershed.

6.1.4.3 Uncertainty Analysis Results for Muger River

For the Streamflow calibration, 44% of the measured data were bracketed by the 95PPU while the r-factor had a desired value of 0.54. The validation results were also quite fair with 31% of the data bracketed with r-factor equal to 0.25.

Table 6-9: Uncertainty analysis results using SUFI2 for Muger River

Muger River-Calibration Period of 1994-2001				
Variable	**P_factor**	**R-factor**	**R^2**	**NS**
q_1(flow in M^3/s)	0.44	0.54	0.76	0.71
Verification Period of 2002-2004				
q_1(flow in M^3/s)	0.31	0.25	0.85	0.83

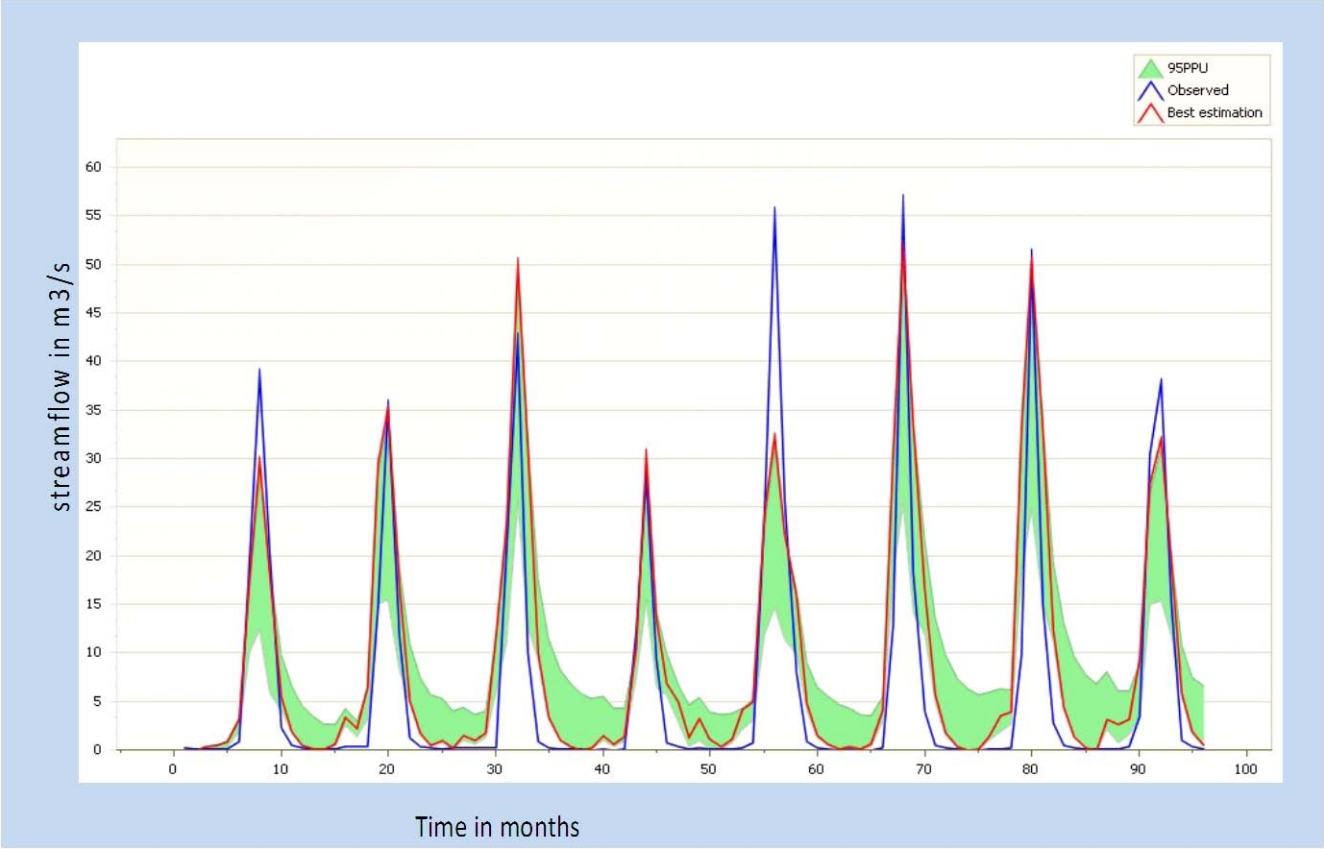

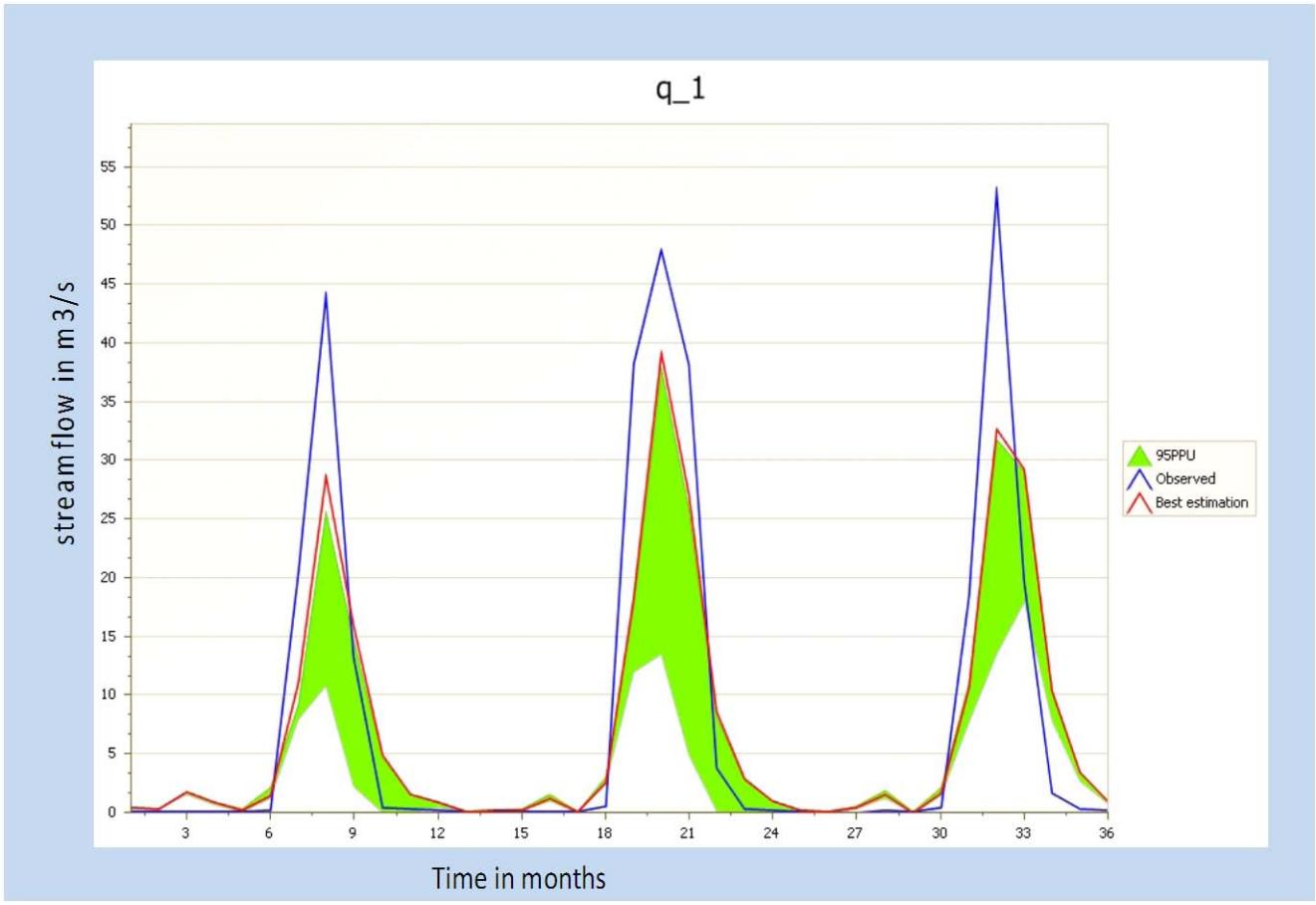

Figure 6-11: The 95% Prediction Uncertainty (95PPU) for Muger River near Chancho. Top, flow calibration (1994–2001); and bottom, validation (2002–2004)

Having the above possible errors, calibration and validation results of the watershed could be qualified as ‘‘satisfactory’’ in this study. As a result further using of the calibrated parameters leads to relatively large uncertainty. This indicates a relatively fair quality of the input data as well as conceptual model errors.

6.1.4.4 Uncertainty Analysis Results for Guder River

The flow calibration of this river accounts, 20% of the measured data were bracketed by the 95PPU while the r-factor had a desired value of 0.05. The validation results were small with 17% of the data bracketed with r-factor equal to 0.07.

Table 6-10: Uncertainty analysis results using SUFI2 for Guder River

Guder River- Calibration Period of 1994-2000				
Variable	**P_factor**	**R-factor**	**R^2**	**NS**
q_1(flow in M^3/s)	0.20	0.05	0.80	0.71
Verification Period of 2001-2005				
q_1(flow in M^3/s)	0.17	0.07	0.74	0.54

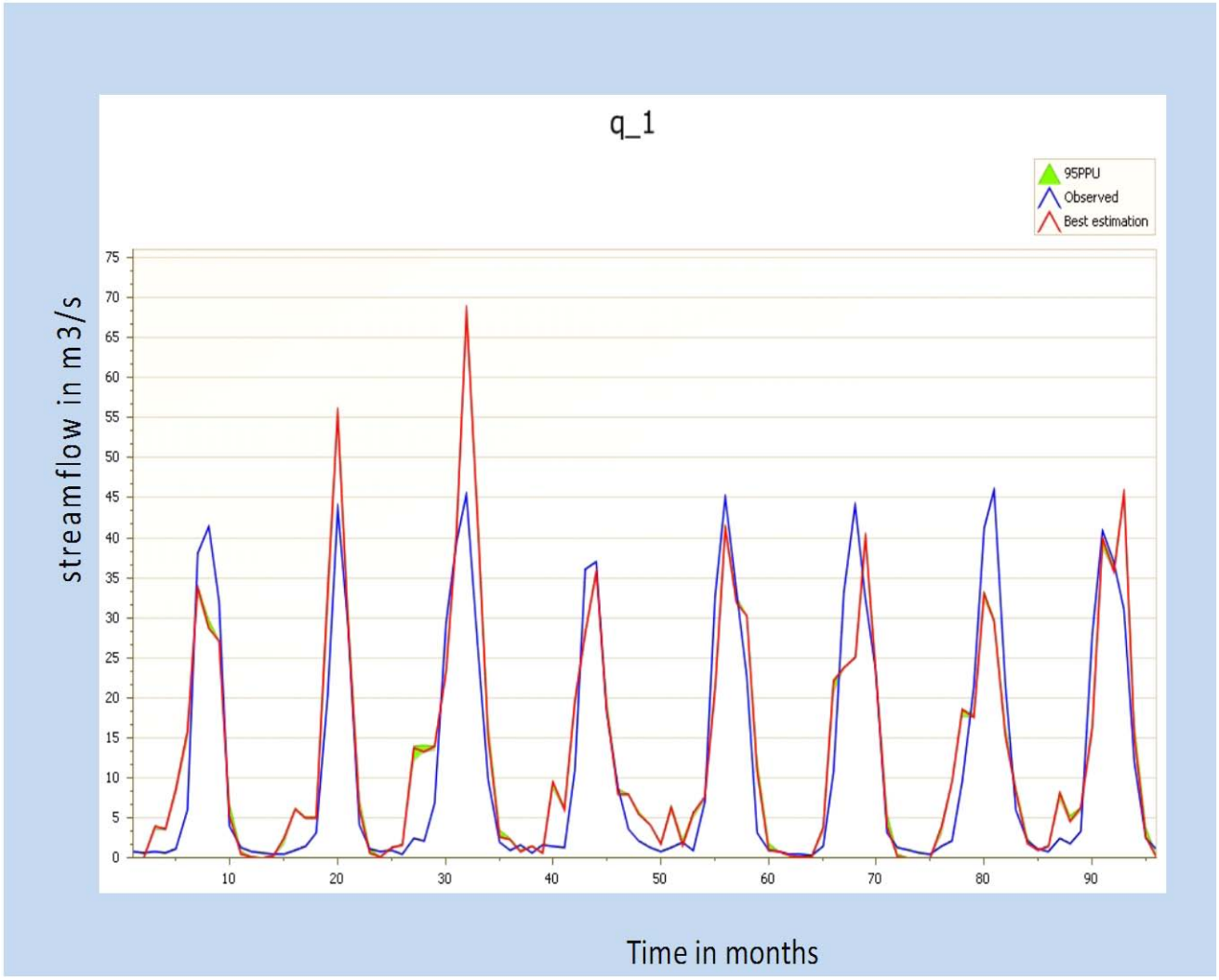

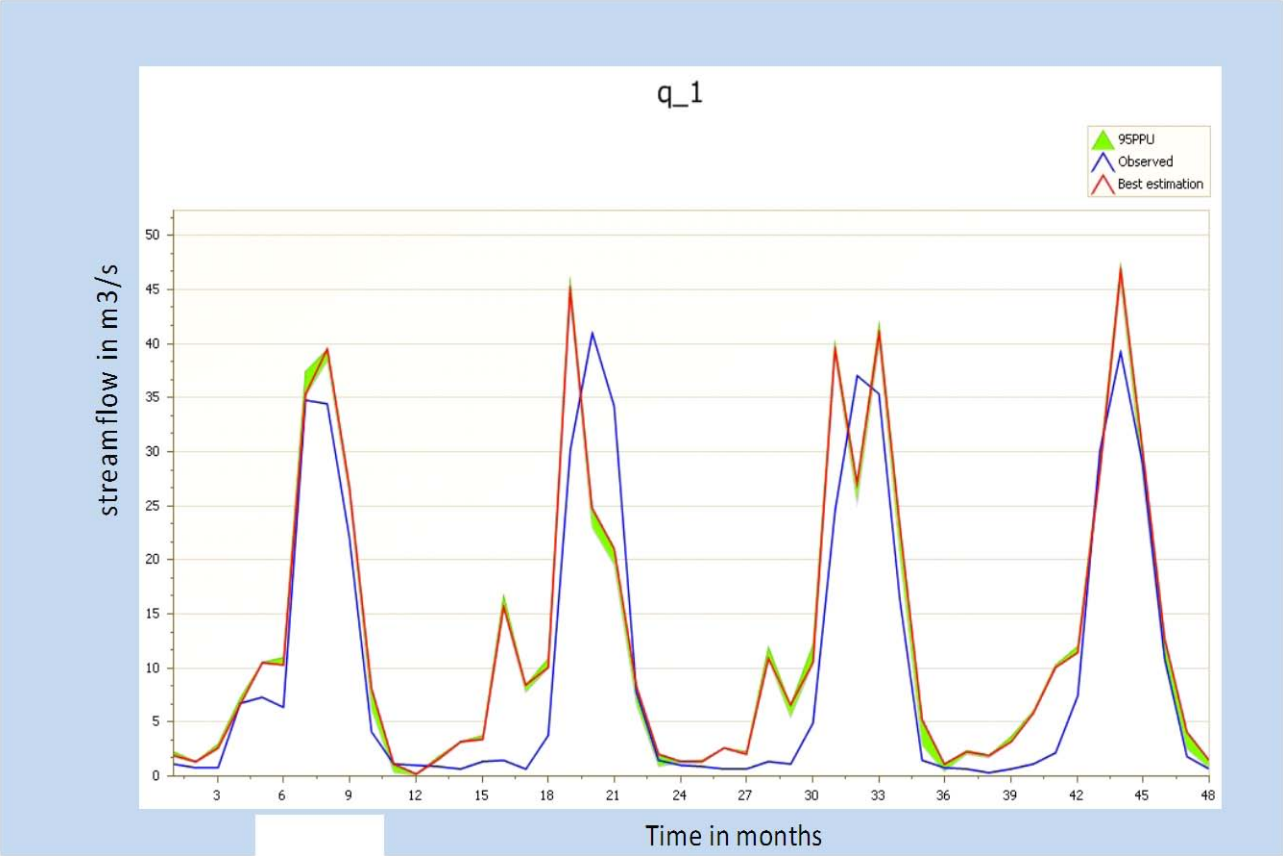

Figure 6-7: The 95% prediction uncertainty (95PPU) for Guder River at Guder. Top, flow calibration (1994–2001); and bottom, validation (2002–2005)

Hence, having the above possible errors, calibration and validation results of the watershed could be qualified as ‘‘poor’’ in this study. As a result further using of the calibrated parameters leads to relatively significant uncertainty. This indicates a poor quality of the input data as well as large conceptual model errors in the watershed model.

6.1.4.5 Uncertainty Analysis Results for Didessa River

The flow calibration of Didessa River accounts, 24% of the measured data were bracketed by the 95PPU while the r-factor had a value of 0.98. The validation results were very poor with only 8% of the data bracketed with r-factor equal to 0.06.

Table 6-11: Uncertainty analysis results using SUFI2 for Didessa River

Didessa River- Calibration Period of 1992-1997				
Variable	**P_factor**	**R-factor**	**R^2**	**NS**
q_1(flow in M^3/s)	0.24	0.98	0.51	0.26
Verification Period of 1998-2001				
q_1(flow in M^3/s)	0.08	0.06	0.29	0.17

Figure 6-8: The 95% prediction uncertainty (95PPU) for Didessa River at Arjo Top, flow calibration (1992–1997); and bottom, validation (1998–2001)

Hence, having the above possible errors, calibration and validation results of the watershed could be qualified as ‘‘very poor’’ in this study. As a result further using of the calibrated parameters leads to relatively significant uncertainty. This indicates that it may be due to poor quality of the input data as well as large conceptual model errors in the watershed model.

Table 6-12: Summary of uncertainty analysis results using SUFI2

Catchments	Periods	P_factor	R-factor	R2	ENS
			Calibration		
Koga	1996-2001	0.71	0.39	0.88	0.78
Birr	1994-2001	0.55	0.6	0.61	0.58
Muger	1994-2001	0.44	0.54	0.76	0.71
Guder	1994-2000	0.2	0.05	0.8	0.71
Didesssa	1992-1997	0.24	0.98	0.51	0.26
			Validation		
Koga	2002-2005	0.45	0.26	0.71	0.53
Birr	2002-2005	0.7	0.61	0.76	0.67
Muger	2002-2004	0.31	0.25	0.85	0.83
Guder	2001-2005	0.17	0.07	0.74	0.54
Didesssa	1998-2001	0.08	0.06	0.29	0.17

6.2 Climate Scenarios Used

The baseline climate scenario represents current climate conditions. As in most of the previous climate change studies in this region, the baseline scenario is described using monthly precipitation and temperature for the period from 1994 to 2003. The generated data for the period 2031-2100 were used for the future climate forcing. The generated scenario was divided in to two 10 years of data ranges based on the availability of the data as 2030s, being 2030's in the middle and 2090s, being 2090's in the middle. The future scenarios were developed by dividing the future time series into two periods of 10 years: 2031-2040, and 2091-2100. The period from 1994-2003 (or here called as "base period") was taken a base period with which the comparison was made.

6.2.1 Scenarios Developed for the Future (2031-2100)

6.2.1.1 Scenarios Developed of the Future (2031-2100) for Koga Catchment

The generated future scenarios for the three climate variables (precipitation, maximum temperature, and minimum temperature) are graphically plotted in order to observe the trend. Therefore, the general trend exhibits rising for temperature and decreasing for total annual precipitation (Figure 6-11 and 12).

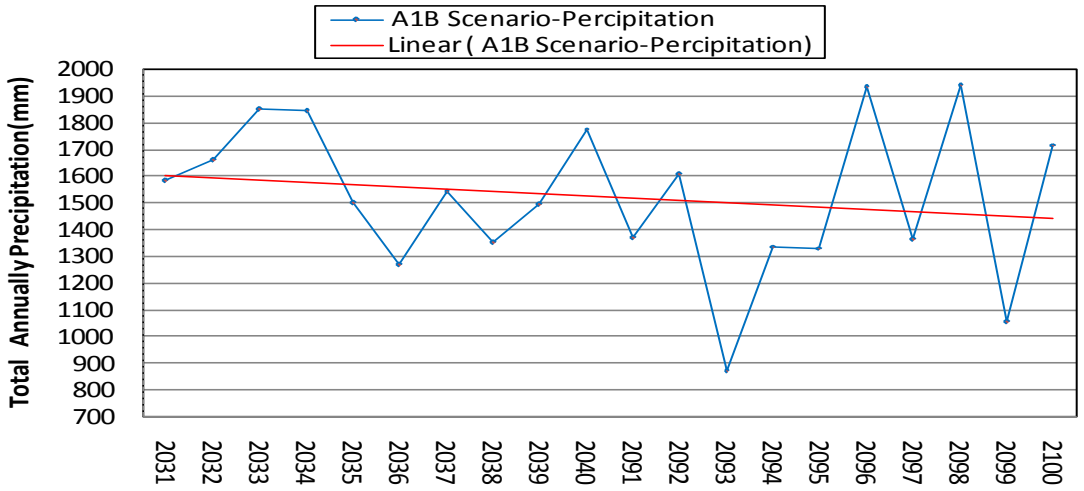

Figure 6-9: Future pattern of total annual precipitation (2031-2100)

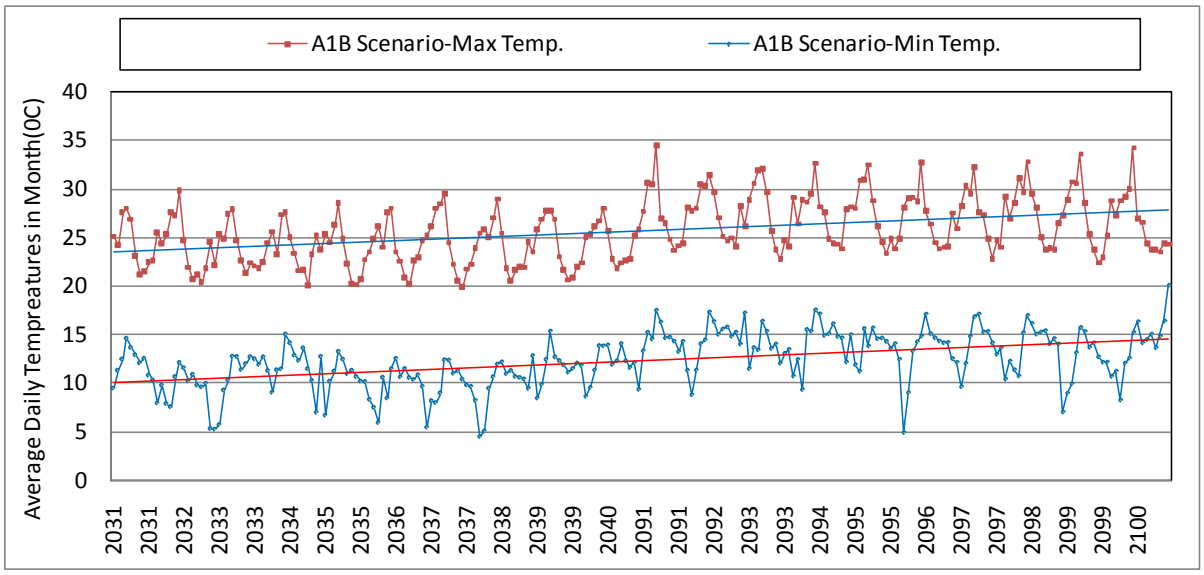

Figure 6-10: Future pattern of average daily max & min temperatures in months (2031-2100)

6.2.1.2 Scenarios Developed of the Future (2031-2100) for Muger Catchment

The general trends for the generated future scenarios used for Muger catchment of the three climate variables (precipitation, maximum temperature, and minimum temperature) generally exhibit an increasing trend as shown in (Figure 6-13 and 14) below.

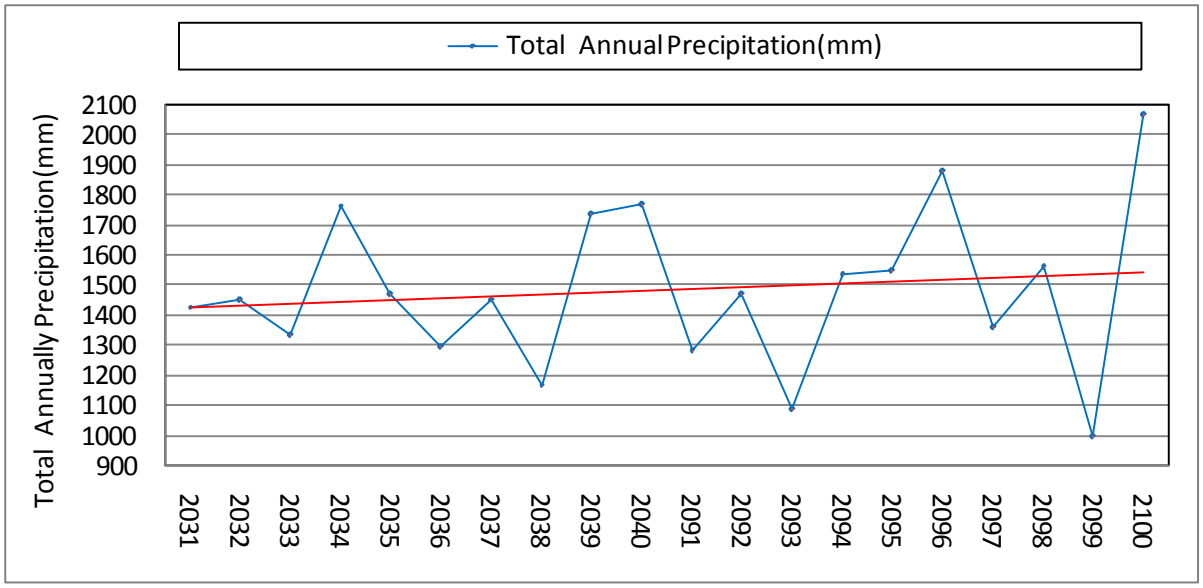

Figure 6-13: Future pattern of total annual precipitation (2031-2100)

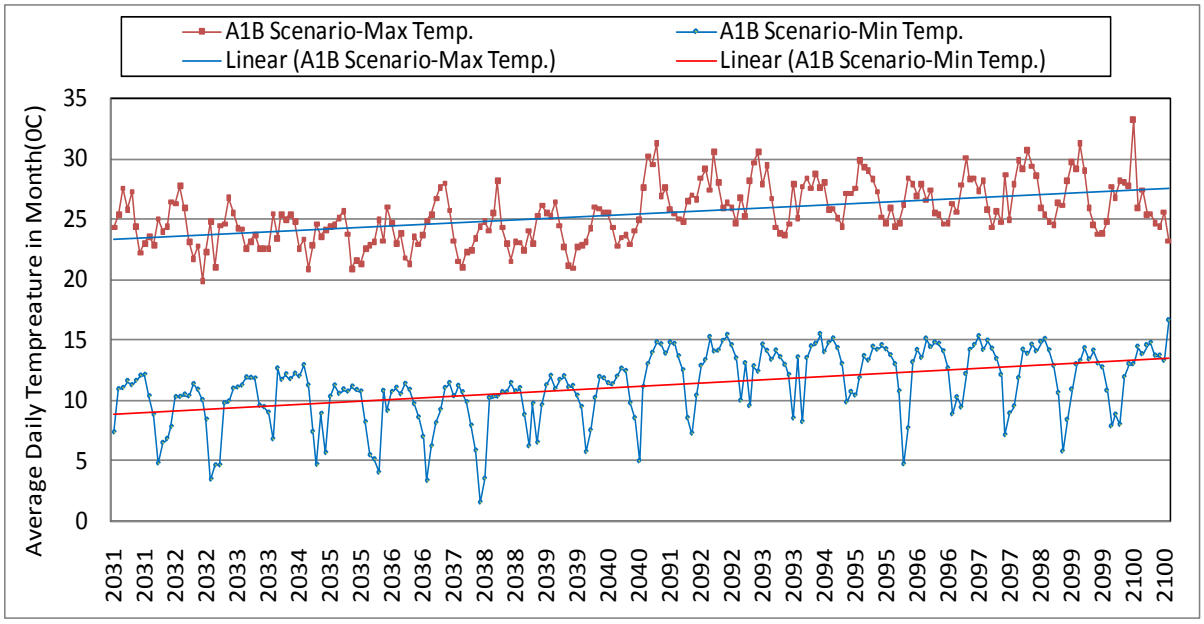

Figure 6-14: Future pattern of average daily max & min temperatures in month (2031-2100)

Like Koga catchment, the respective average daily in month and annual climatic variables for Muger were also plotted graphically for total annual precipitation in mm and maximum and minimum temperatures in degree centigrade. The trends show an increasing for all climatic variables in both periods as discussed shown in graphs above.

6.2.1.3 Scenarios Developed for the Future (2031-2100) for Birr Catchment

The generated future scenarios for maximum and minimum temperatures are generally shows an increasing trend and decreasing for total annual precipitation (Figure 6-15 and 16).

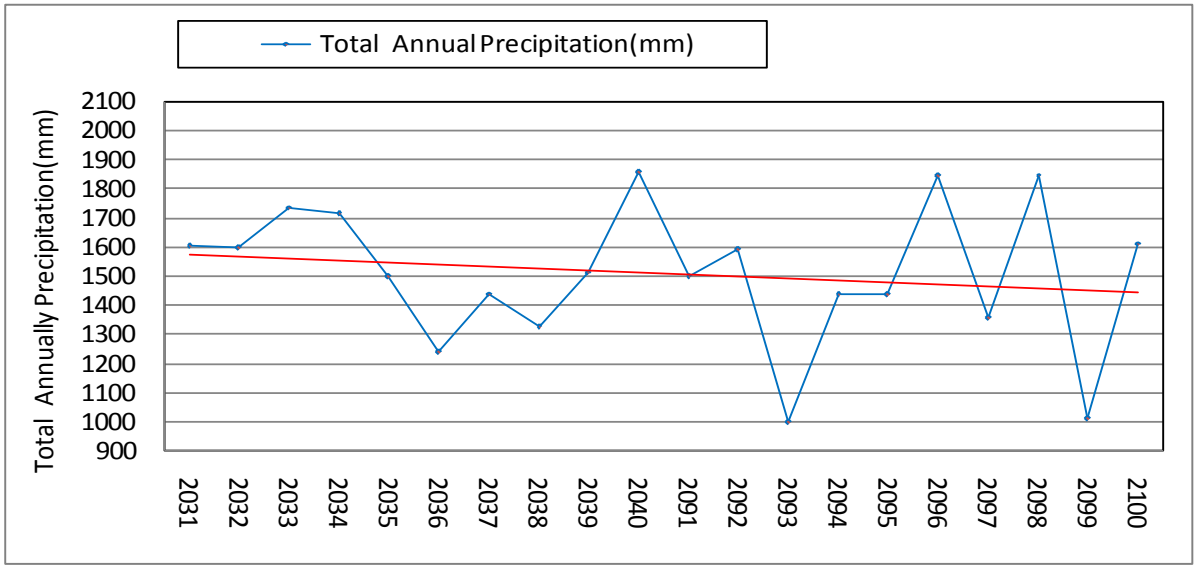

Figure 6-15: Future pattern of total annual precipitation (2031-2100)

The respective average daily in month and annual climatic variables for the generated scenario were plotted graphical to observe the trends for total annual precipitation in mm and maximum and minimum temperatures in degree centigrade. As a result, the generated future scenarios are generally shows an increasing trend for temperature and decreasing trend for total annual precipitation.

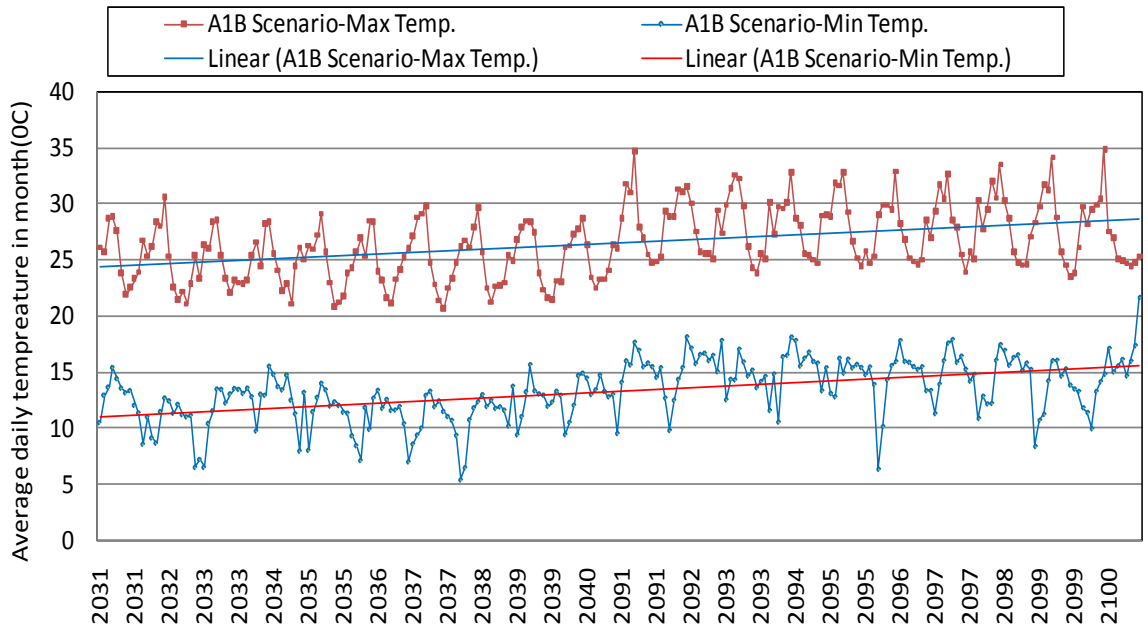

Figure 6-16: Future pattern of average daily max & min temperature in month (2031-2100)

6.2.1.4 Scenarios Developed for the Future (2031-2100) for Guder Catchment

The generated future scenarios for the three climate variables (precipitation, maximum temperature, and minimum temperature) generally show an increasing trend for temperature and a decreasing trend for precipitation in both periods as shown in (figure 6-17 and 18).

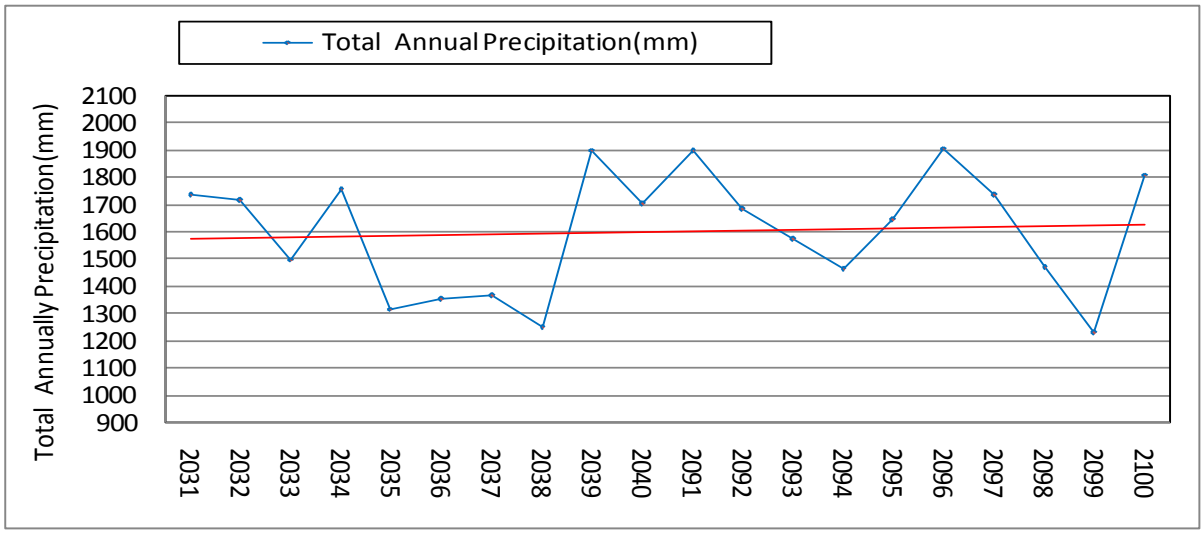

Figure 6-17: Future pattern of total annual precipitation (2031-2100)

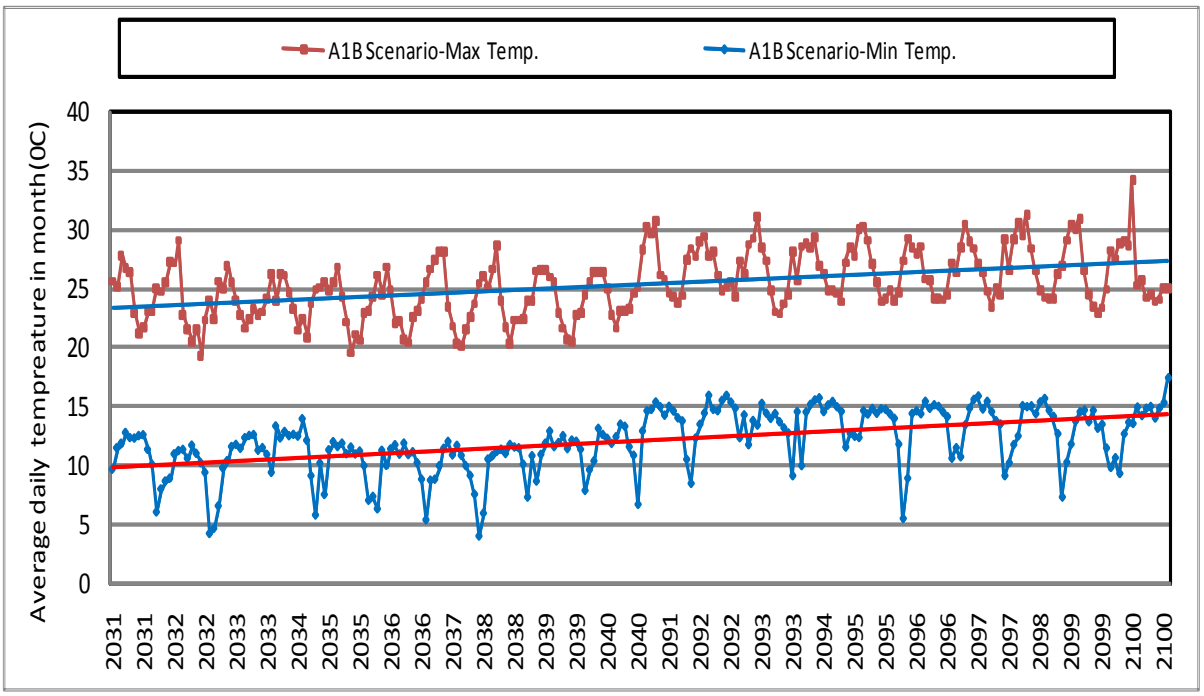

Figure 6-18: Future pattern of average daily max & min temperature in month (2031-2100)

6.2.1.5 *Scenarios Developed for the Future for Didessa Catchment*

The generated future scenarios for the three climate variables (precipitation, maximum temperature, and minimum temperature) generally show an increasing trend in both periods (Figure 6-19 and 20).

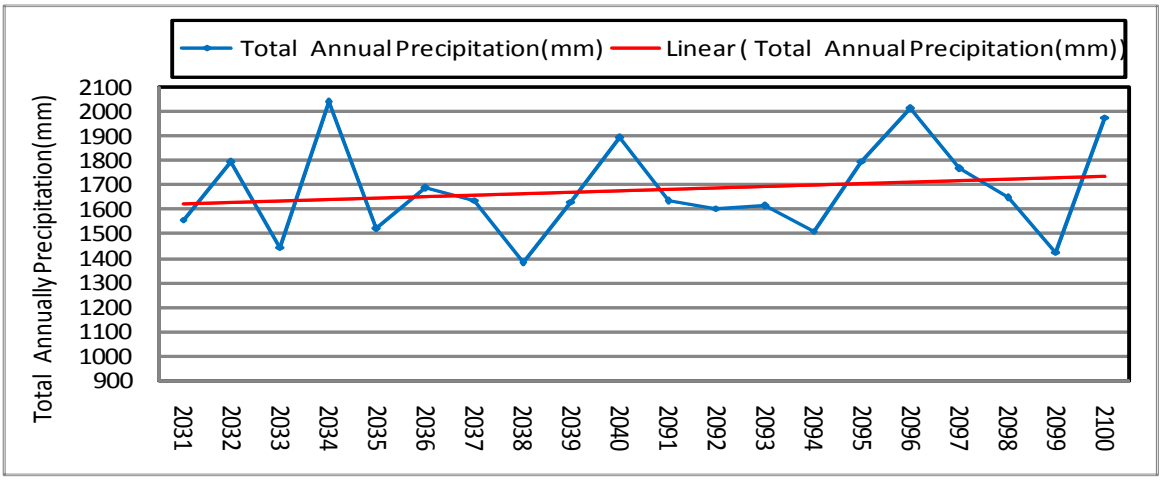

Figure 6-19: Future pattern of total annual precipitation (2031-2100)

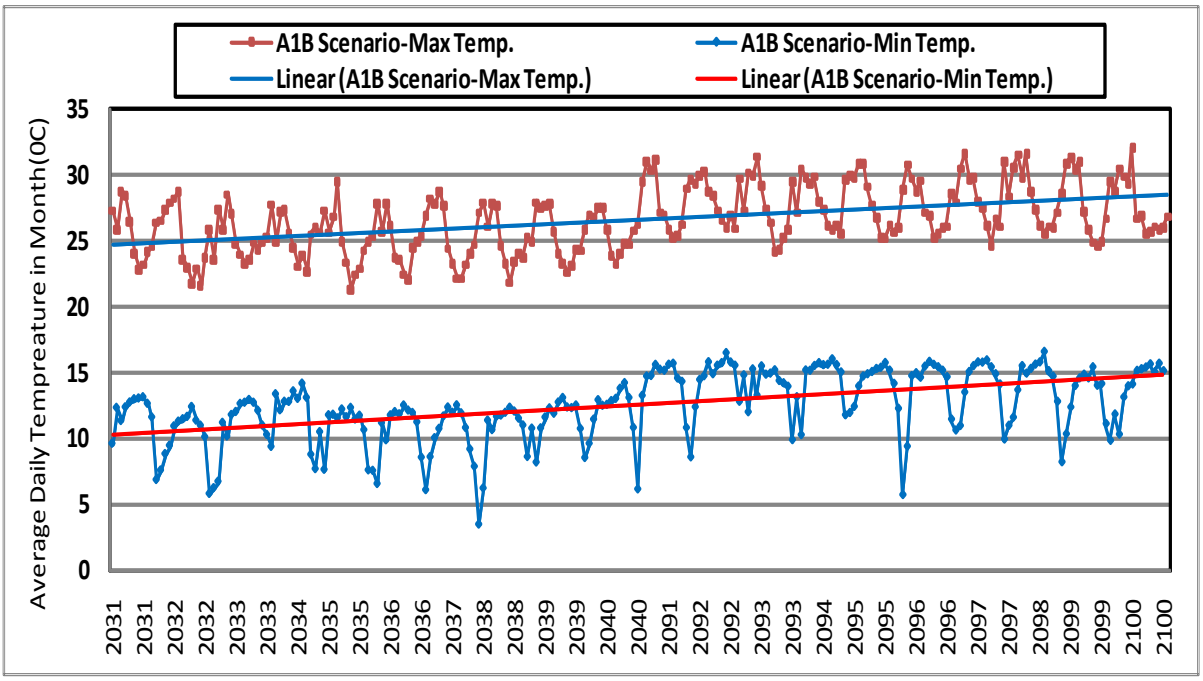

Figure 6-20: Future pattern of average daily maximum & minimum temperature in month (2031-2100)

6.3 Climate Change Impact on Future Flow Volume

Streamflow is mainly dependent on the amount of precipitation falling on its watershed area and the actual evapotranspiration amount released into the atmosphere. Hence, changes in precipitation and temperature can significantly influence river flow patterns. The effect of climate change on streamflow was analyzed on a monthly, seasonal and annual basis. The results for the analysis were discussed in the following sections and the summarized results for all selected Rivers are enclosed in Figures 6.21-30.

The impact of climate change was analyzed taking the 1994-2003 simulated river flow as the baseline flow against which the future flows for the 2030s and 2090s compared. The daily precipitation, minimum and maximum temperature were used as input in to SWAT on a monthly basis using the scenarios for the future two periods of 10 years: 2031-2040 and 2091-2100. The historical or base period was then re-run with the future climate inputs. Other climate variables as wind speed, solar radiation, and relative humidity were assumed to be constant throughout the future simulation

periods. Even though it is definite that in the future land use changes will also take place, this was also assumed to be constant as the objective of this study is only to get indicative results with respect to the change in the climate variables keeping all other factors constant.

6.3.1 Impact on Monthly, Seasonal and Annual Flow Volume

A) Koga River

The impact of climate change was analyzed taking the 1994-2003 simulated river flow as the baseline flow against which the future flows for the 2030s and 2090s compared. The monthly percentage change in flow volume for the period 2030s and 2090s are presented in Figure 6.21 below. In both periods, the flow volume may show a decreasing trend for all the months except for months from April to September for a period of 2030s and in August and October for 2090s. In these periods maximum decrease up to 99.28% and an increase up to 58% in monthly flow volume may be expected. The overall trend shows that the monthly future flow volume in the Koga River exhibits a decreasing trend which may reach 32% in 2030s and 43% in 2090s. In general the result of this study reveals that the overall future flow volume of the river may decrease by 38% in the coming 70 years (2031-2100).

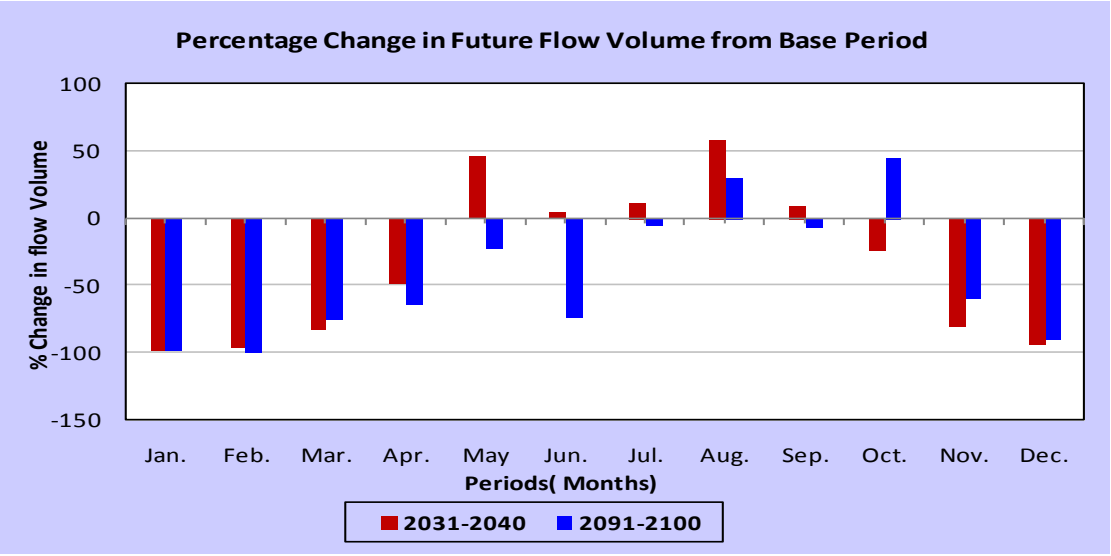

Figure 6-11: Monthly % change in flow volume against the baseline flow volume of Koga River

The impacts of climate change on the seasonal and annual flow volume were also presented so as to foresee its consequence on the socio-economic condition of the area. As discussed earlier there are three seasons in the study area: Kiremt (rainy and cropping season), Belg (small rain season) and Bega (dry season). Figure 6.22 below reveal the implication of climate change on the river flow in these seasons.

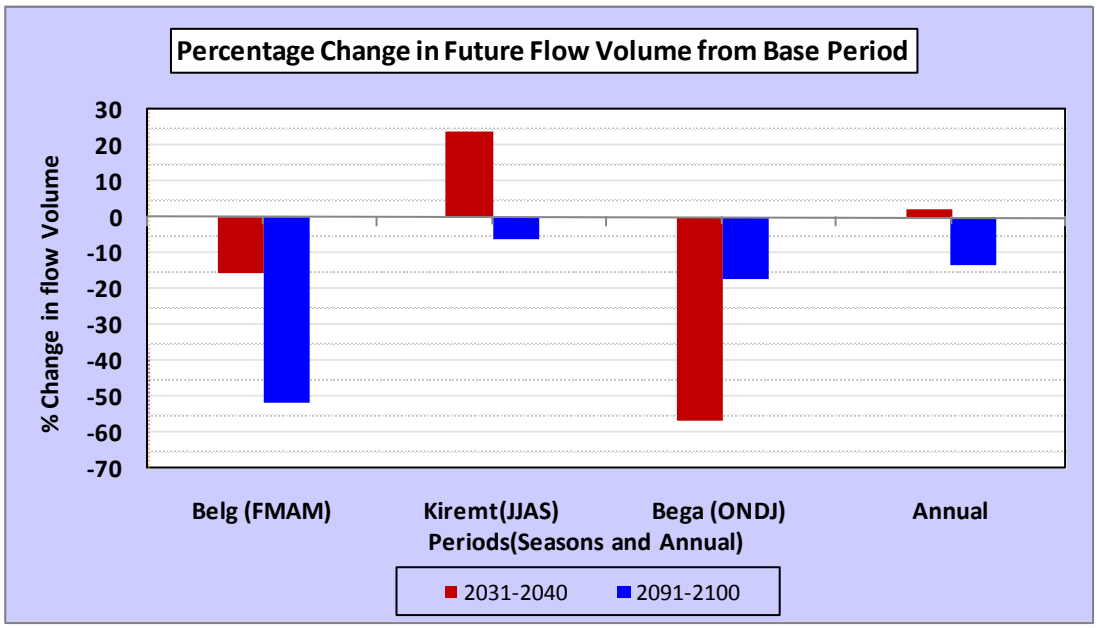

Figure 6-12: Percentage change in seasonal and annual flow volume in respect to baseline

As can be seen from Figure above, there may be an annual increase in flow volume by 2.3% in 2030s and annual decrease by 13.6% in 2090s. Kiremt season is expected to show the larger share in increased flow volume by 24% for the period of 2030s. While Bega and Belg seasons are expected to show the larger share in decreased flow volume in 2030s and 2090s respectively.

The estimation of the annual average flow volume changes in the future in 2030s and 2090s periods shows, the flow volume might increase by 2.3% and decrease 13.6%, respectively.

Overall, according to the scenario, since the year 2031 there might be a significant reduction in total average annual flow up to 5.6%. Here is interesting to note that the decreasing trend of the average annual flow volume is mainly because of the decrease

in the Belg flow volume by about 43%. Therefore, the Belg season is likely to contribute the biggest portion of the annual flow loss in the future.

B) Muger River

The impact was analyzed taking the 1994-2003 simulated river flow as the baseline flow against which the future flows for the 2030s and 2090s compared. The monthly percentage change in flow volume for the period 2030s and 2090s are presented in Figure 6.23. In the 2030s for the generated scenario, the flow volume may show an increase for all the months except for months August to January and in the 2090 also may show an increase in flow volume for all months except for months August to January. In these periods a maximum of an increase up to 745% in monthly flow volume may be expected, this is exaggerated.

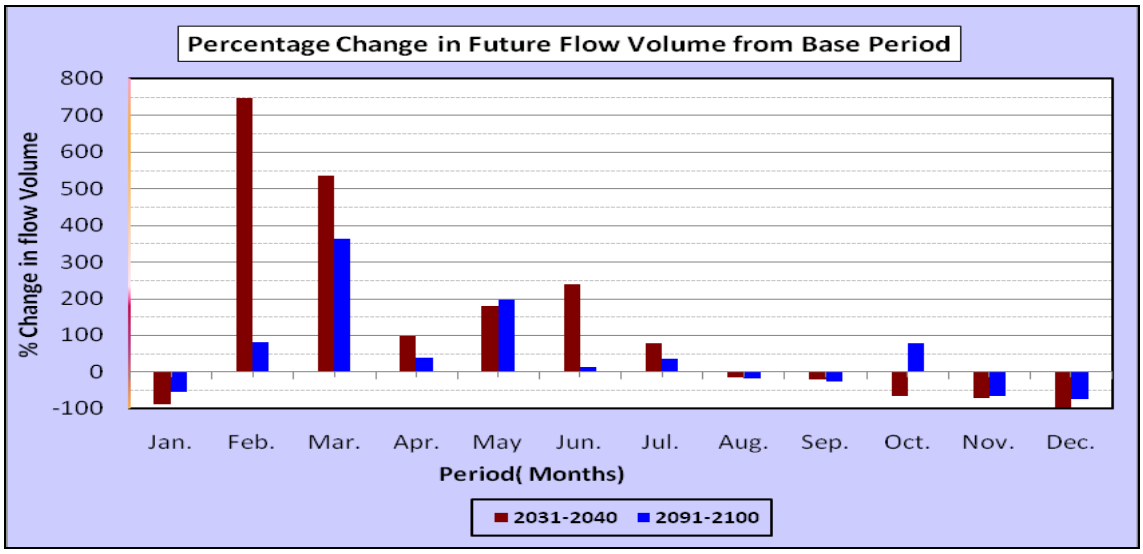

Figure 6-13: Monthly % change flow volume against the baseline flow

The impacts of climate change on the seasonal and annual flow volume are also presented so as to predict its consequence on the socio-economic condition of the area. As discussed earlier, there are three seasons in the study area: Kiremt (rainy and cropping season), Belg (small rain season) and Bega (dry season). Figure 6.24 below reveal the implication of climate change on the river flow in these seasons.

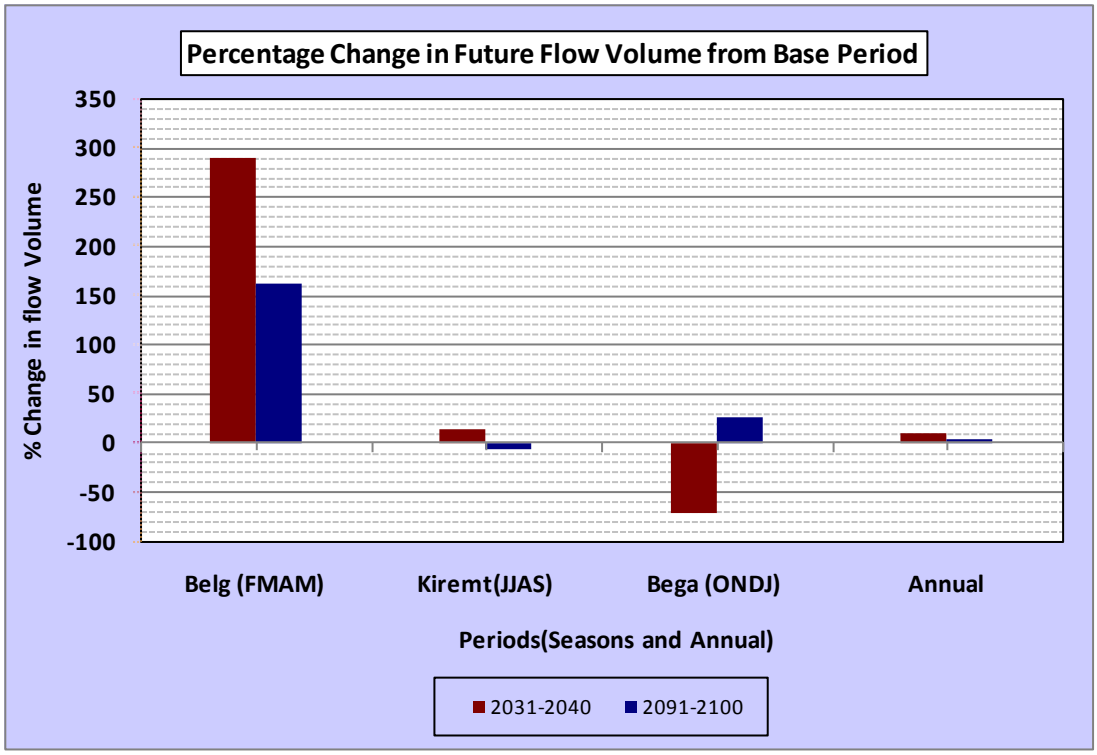

Figure 6-14*: Percentage change in seasonal and annual flow volume in respect to baseline climate*

As it was shown in Figure 6.24 above, there may be an annual average increase in flow volume for the next 70 years by 6.7%. Belg season in both periods is expected to show the larger share in increased flow volume. The average increase may reach up to 225% in both periods.

C) Birr River

The impact of climate change was analyzed taking the 1994-2003 simulated river flow as the baseline flow against which the future flows for the 2030s and 2090s compared. The monthly percentage change in flow volume for the period of 2030s and 2090s are presented in Figure 6.25. In 2030s period for the generated scenario, the flow volume may show an increase for all the months except in November to March. While in 2090s for the generated scenario, the flow volume may show an increase for all the months

except in January to April and Jun. In these months a maximum decrease of up to 92% and an increase up to 136% in monthly flow volume may be expected.

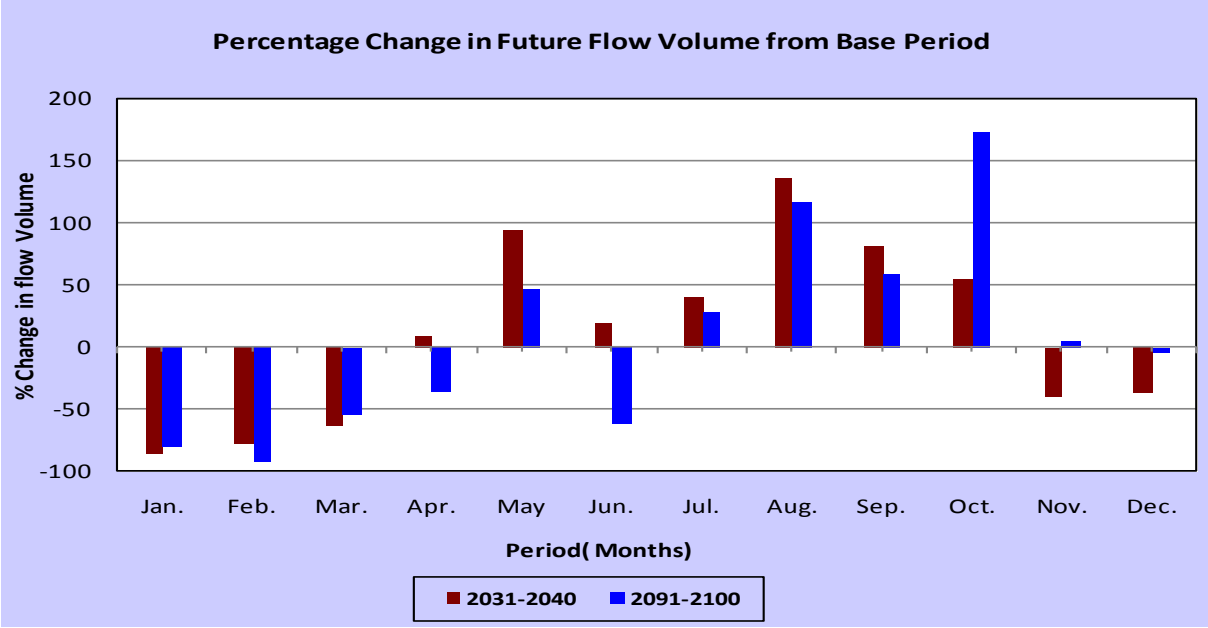

Figure 6-15: Monthly percentage change in flow volume against the baseline flow

Like the other river catchments seen above, the impacts of climate change on the seasonal and annual flow volume are also presented so as to predict its consequence on the socio-economic condition of the area. Figure 6.26 below reveal the implication of climate change on the river flow in seasonally and annually. As a result in both periods the future flow volume may exhibits an increasing trend for all seasons and annual except in Belg for 2090.

As it can be seen in figure below, there may be an average annual increase in flow volume for the next 90 years by 53% in 2030s and 42% in 2090s. Kiremt season is expected to show the larger share in increased flow volume in both periods. The average increase may reach up to 54%. Bega season also shows an increase in flow volume by 87% in 2090s.

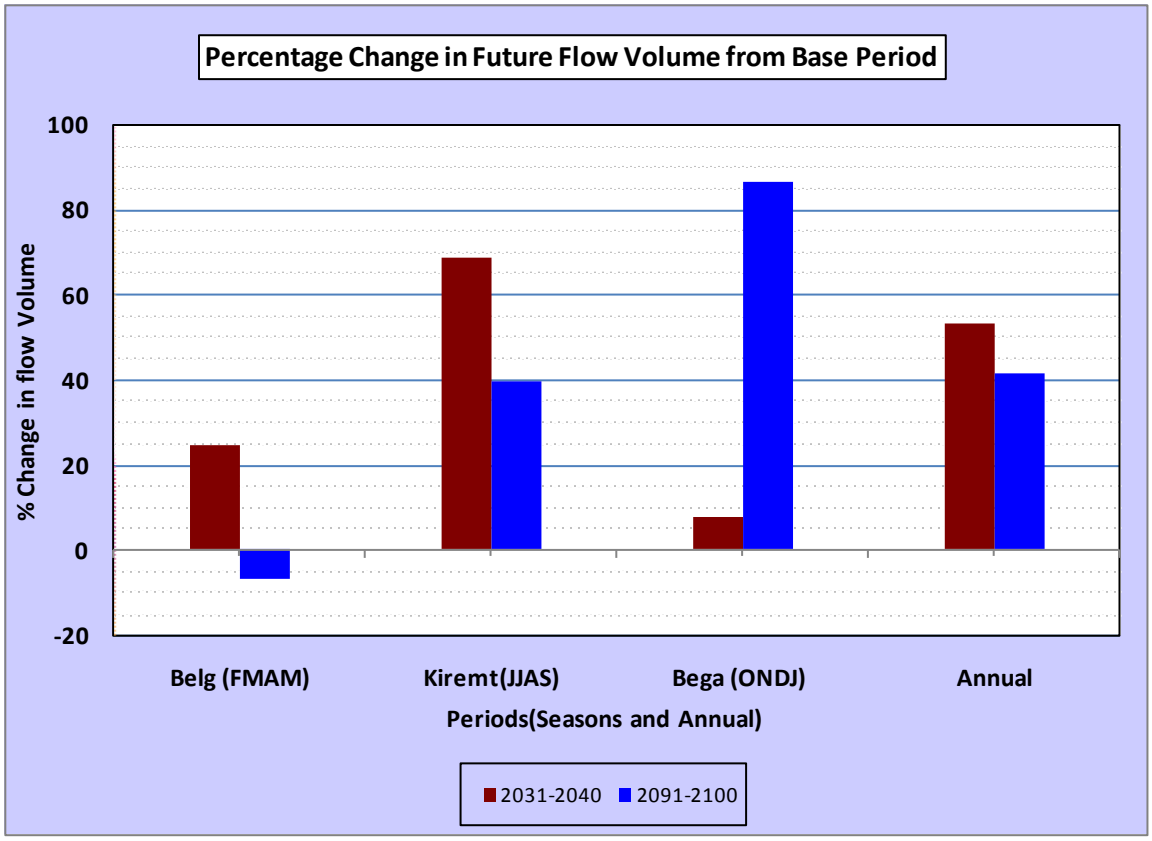

Figure 6-16: Percentage change in seasonal and annual flow volume in respect to baseline

The expected annual average flow volume changes in the future in 2030s and 2090s periods shows, the total flow volume might increase by 53% and 42%, respectively. Overall, according to the scenario, since the year 2031 there might be a significant increment in total average annual flow up to 48%.

D) Guder River

The impact was analyzed taking the 1994-2003 simulated flow as the baseline flow against which the future flows for the 2030s and 2090s compared. The monthly percentage change in flow volume for the period 2030s and 2090s are presented in Figure 6.27. In 2090s period for the generated scenario, the flow volume may show an increase for all the months and in 2030 period for the generated scenario, the flow volume may show an increase for all the months except in January to April and Nov. In these periods maximum decrease up to 68% in monthly flow volume may be expected.

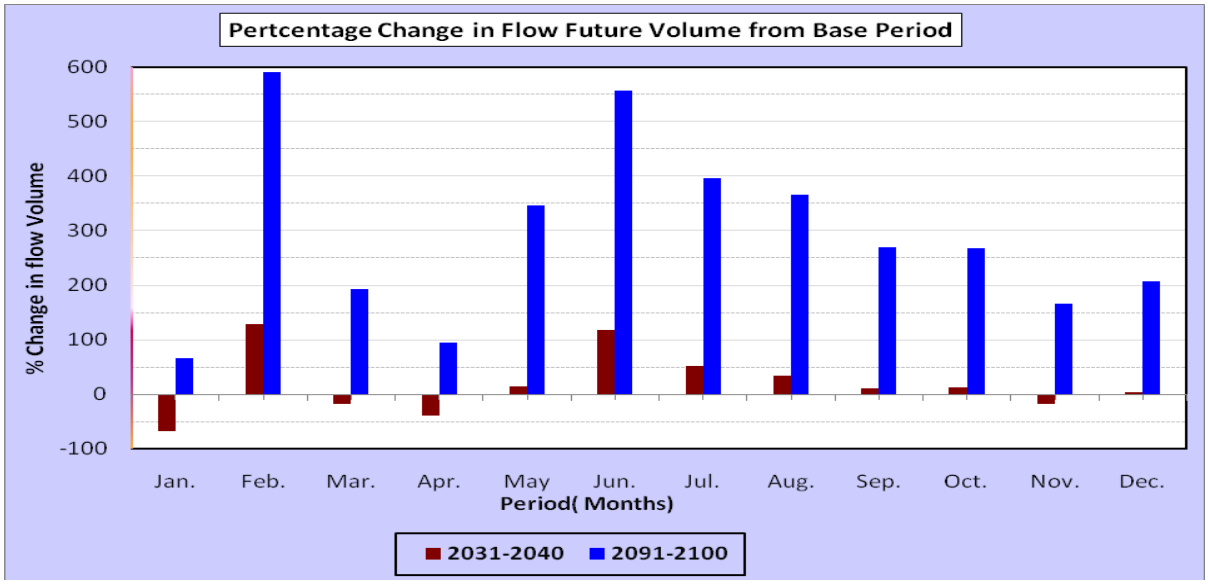

Figure 6-17: Monthly percentage change in flow volume against the baseline flow volume

The impacts of climate change on the seasonal and annual flow volume are also presented. As discussed earlier there are also three seasons in the study area: Kiremt (rainy and cropping season), Belg (small rain season) and Bega (dry season). Figure below reveal the implication of climate change on the river flow in these seasons.

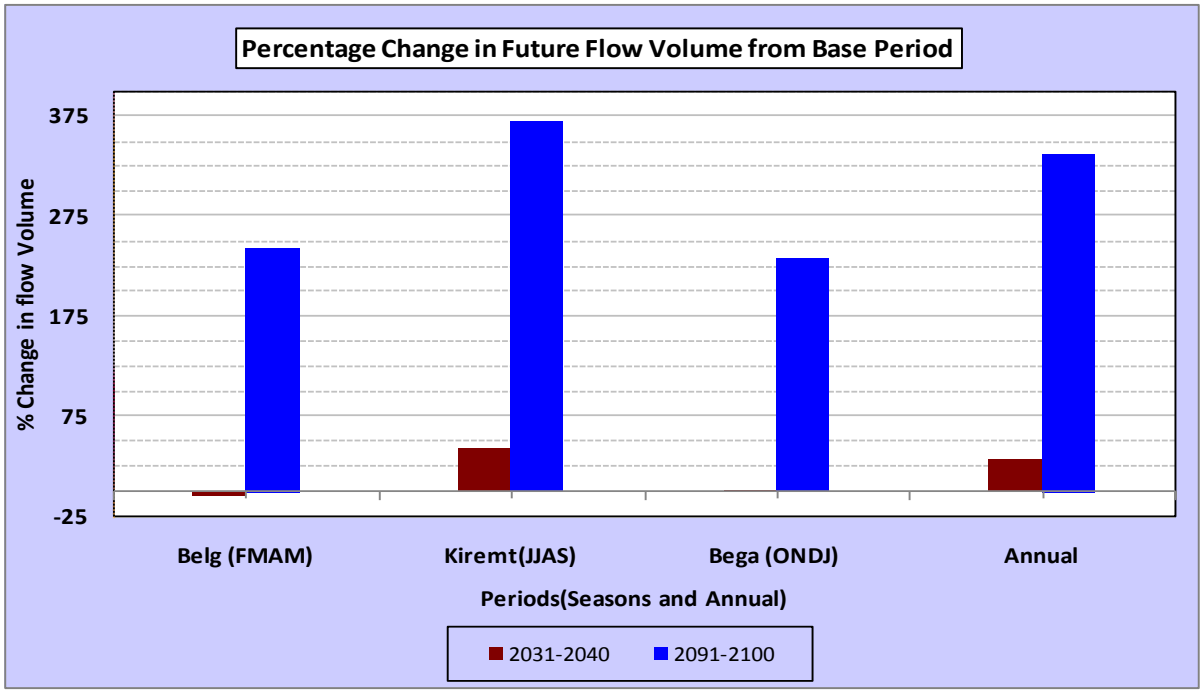

Figure 6-18: Percentage change in seasonal and annual flow volume in respect to baseline

As it is tried to show in above figure, there may be an annual increase in flow volume for the next 90 years by 32% in 2030s and 337% in 2090s. Kiremt season is expected to show the larger share in an increased flow volume. The increment may reach up to 42% in 2030s and 370% in 2090s. However, in 2030s show that there might be a large decrease in flow volume in 2030 and an increase in 2090 of Belg season by values of 4% and 243%, respectively.

The estimation of the annual average flow volume changes in the future in 2030s and 2090s periods shows, the total flow volume might averagely increase by 185%. The general increase in precipitation is reflected in an increase flow volume and a decrease in precipitation is reflected in a decreased flow volume.

E) Didessa River

It was analyzed taking the 1992-2001 simulated flow as the baseline flow against which the future flows for the 2030s and 2090s compared. The monthly average flow volume for the period 2030s and 2090s are presented in figure below. In the periods 2030s and 2090s for the generated scenario, the flow volume may show a decrease for all the months except Jan, Feb and Oct. In these periods a maximum of a decrease up to 50% and an increase up to 180% for 2030s and a maximum decrease up to 40% and a maximum increase up to 30% in monthly flow volume may be expected.

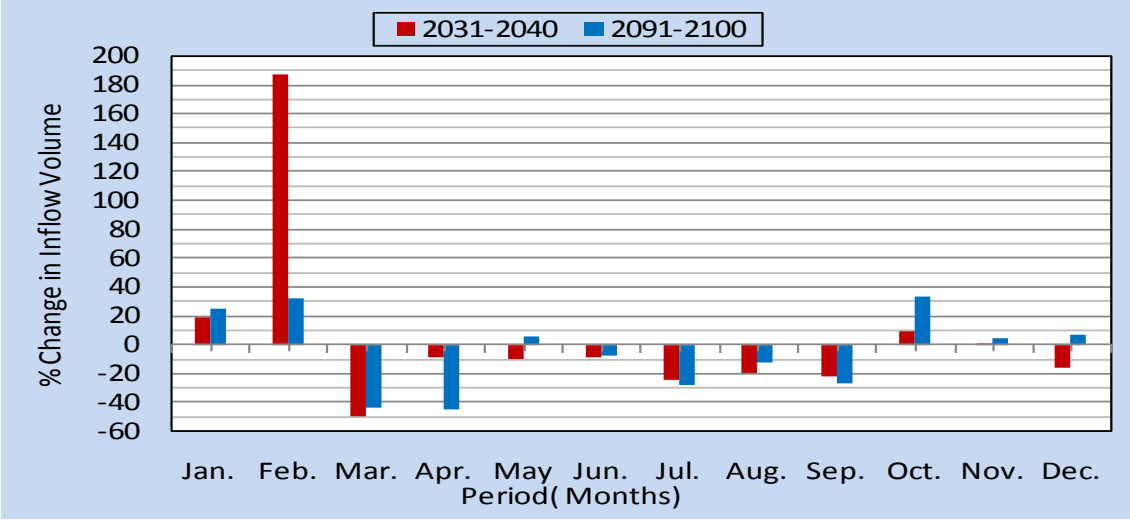

Figure 6-19: Monthly percentage change in flow volume against the baseline flow volume

Like the above stated catchments, the impacts on the seasonal and annual flow volume are also presented so as to foresee its consequence on the socio-economic condition of the area in Figure below.

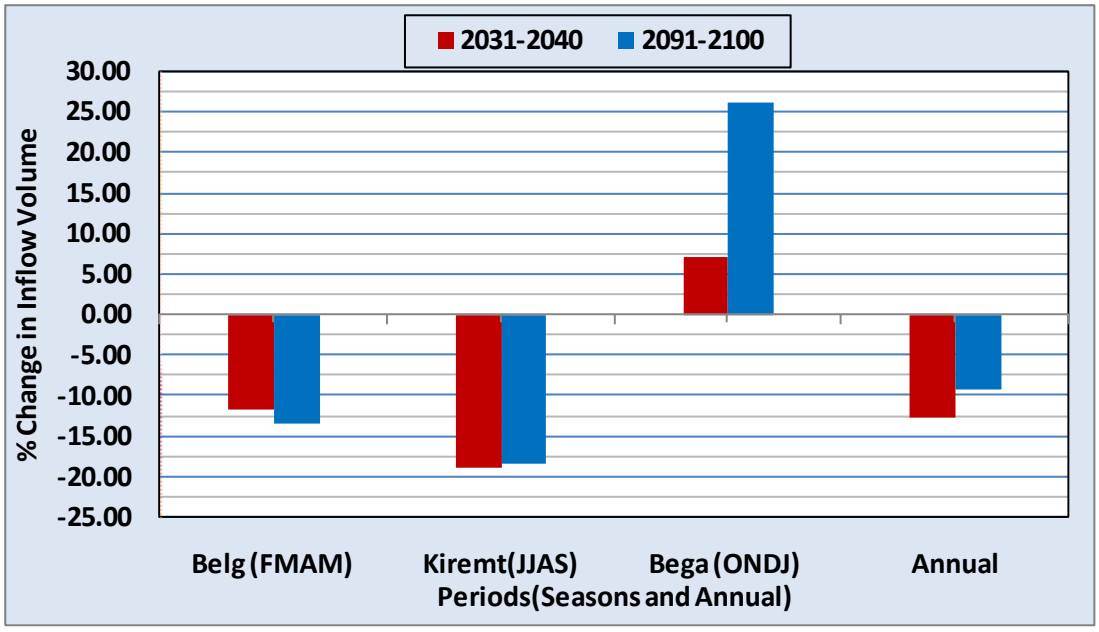

Figure 6-20: Percentage change in seasonal and annual flow volume in respect to baseline climate

As it can be seen from figure above, there may be an annual decrease in flow volume for the next 70 years by 12.7% in 2030s and 9.3% in 2090s. Kiremt season is expected to show the larger share in decreased flow volume. *Belg* season also shows a descent decrease in flow volume by ranges from 11.6% in 2030s to 13.3% in 2090s. However, in 2030 and 2090 show that there might be an increase in flow volume in *Bega* season. The increments would reach up to 7% in 2030 and 26% in 2090. It is interesting to note that the decreasing trend of the average annual flow volume is mainly because of the decrease in the *Kiremt* flow volume by about 18.8%. Similarly, the *Belg* season flow might also decrease by 16% between 2030s and 2090s. Therefore, the *Kiremt* season is likely to contribute the biggest portion of the annual flow loss in the future.

6.3.2 Sensitivity of Streamflow to Climate Change

Most climate change impact studies involve the use of a hydrological model, the modeling approach generally provides a reliable estimate of the hydrologic sensitivity to climate when a suitable model is used and calibrated properly (Ashenafi, 2009).
An alternative to the modeling approach is to estimate the sensitivity of streamflow to climate directly from the historical climate data, particularly when only estimates of changes in mean annual stream flow are required. An example of this approach is the robust nonparametric estimator of the rainfall elasticity of streamflow (schaake, 1990; Sankarasubramaniam et al., 2001; Chiew, 2006 cited in Ashenafi, 2009),

$$\text{Ep} = median\left[\frac{Qt - QP}{Pt - QT}\right] - - - - - - - - - - - - - - - - - Eqn - 6.1$$

Where: P and Q are the mean annual rainfall and streamflow respectively.

Pt and Qt in the annual time series, and

$\boldsymbol{\varepsilon}_{\text{P}}$ is the nonparametric estimator of the rainfall elasticity of streamflow.

The rainfall elasticity of stream flow, $\boldsymbol{\varepsilon}_{\text{P}}$, is defined as the proportional change in mean annual streamflow divided by the proportional change in mean annual rainfall, that is the elasticity of 2 indicates that the 1% change in rainfall a 2% change in streamflow.

Rainfall is the key driver of streamflow, and comparative studies indicate that simulations using different hydrological models as well as the data driven approach generally give similar estimates of the sensitivity of streamflow to rainfall (Chiew et al, 2005; Jones et al., 2006; Chiew, 2006 cited in Ashenafi, 2009). However, estimates of the sensitivity of streamflow to temperature from different models can be different because of the different methods used by different models to simulate actual evapotranspiration.

The changes in mean annual streamflow for a given change in mean annual rainfall and mean temperature can be expressed as,

$$\delta Q = \varepsilon P * \delta P - \varepsilon T * \delta T \ldots\ldots\ldots\ldots\ldots\ldots \text{Eqn-6-2}$$

Where: δQ is change in mean annual runoff, δP is change in mean annual rainfall and

δT is change in mean annual temperature, and

εP and εT are the rainfall and temperature elasticity's of streamflow.

Using Eqn 6-1 and Eqn 6-2 the change in mean annual runoff for a given change in mean annual rainfall and temperature for each 5 (five) catchments of Upper Blue Nile Basin the following relations are developed:-

Table 6-13 *Relations developed for the catchments*

S No.	Catchments	Developed Equations
1	Koga	$\delta Q = 1.17\,\delta P - 1.11\,\delta T$
2	Muger	$\delta Q = 1.12\,\delta P - 1.07\,\delta T$
3	Guder	$\delta Q = 1.06\,\delta P - 0.95\,\delta T$
4	Birr	$\delta Q = 1.03\,\delta P - 0.98\,\delta T$
5	Didessa	$\delta Q = 0.78\,\delta P - 0.95\,\delta T$

The relations developed above may be used to estimate the change in mean annual streamflow for a given change in mean annual rainfall and temperature for each 5(five) catchments in Upper Blue Nile Basin at any time in the future without using hydrological model. The elasticity's εP and εT shows how much sensitive the flow is for a 1% change in annual precipitation for constant temperature and constant precipitation. Accordingly, catchments like Guder, Koga, Birr and Muger are more sensitive to rainfall change relative to the other catchments, and Didessa is more sensitive to temperature, and this output is similar with other studies (Muluneh B. (2008) using hypothetical scenarios).

Table 6-14*: Summary of streamflow sensitivity to climatic change*

Rivers	Average Monthly % Change			Seasonal & Annual % change				Climatic Variables	
(1994-2003)	2030s	2090s	2031-2100	Kiremt	Belg	Bega	Annual	PCP	Mean Temp
Koga	-32	-43	-38	9	-22	-41.3	-5.6	**Sensitive**	Less sensitive
Birr	10.8	8.5	9.6	54	19	38	47.5	**Sensitive**	Less sensitive
Muger	126	47	86.8	0.5	199	-10.5	6.7	**Sensitive**	Less sensitive
Guder	19.2	293	156	206	104	128	185	**Sensitive**	Less sensitive
Didesssa	4.9	-4.3	0.33	-18.7	-15	17.3	-11.7	Less sensitive	**Sensitive**

The sensitivity analysis results of the climatic variable change on streamflow shows Guder, Muger, Birr and Koga catchments, which are contributing the flow in to Abbay River, are seems likely to be seriously dominated by the impact of the precipitation changes than temperature changes. While Didessa catchment seems likely to be seriously dominated by the impact of the temperature change than the precipitation change. The change is largely covered by the temperature change because of direct relation with the fact that it is due to a simple hydrological relationship between temperature and evapotranspiration: the increased temperature increased evapotranspiration and reduced the flow like a decreased precipitation decreasing the flow.

6.3.3 Significance of Climate Change Impact on Future Flow Volume

This study on the impact of climate change on water availability involved a series of models and model outputs, which are based on simplified assumptions.

Hence, it is unquestionable that the uncertainties presented in each of the models and model outputs kept on cumulating while progressing towards the final output.

The types of uncertainties existing throughout the whole process can be associated with the data quality, the GCMs and SRES scenarios selected, the downscaling method used, and the hydrologic modeling applied. Besides, the knowledge gap related to the atmospheric chemistry of the local climatic processes can also be one source of uncertainty. Data scarcity and reliability is also one of the challenges in the execution of this study. Big gaps in the time series data and unusually very high or very low values were common. Even though appropriate data checking and missing data filling by using weather generators were carried out before analysis, there was a difficulty in the

calibration and validation of hydrologic model. It is, therefore, certain that some level of insecurity could be involved at this stage, and hence becoming the first source of uncertainty in the modeling process.

GCM outputs have also a lot of uncertainties even if using RCM output reduces uncertainties. Although uncertainties can be minimized by using outputs of different GCMs, this study made use of only one model outputs, which is RCM. Besides, GCMs use the future forcing scenarios to produce ranges of climate change. These scenarios represent a set of assumptions about population growth, economic and technological development, and socio-political globalization, where all of these variables contain a high degree of uncertainty. The IPCC report on emission scenarios, SRES, (IPCC 2001) clustered these scenarios into six groups. Despite their equal probability, model results based on these scenarios may vary noticeably. Hence, choosing among the scenarios adds to the uncertainty.

The resolutions levels of GCM model output also need narrowing the temporal and spatial resolution disparity; the techniques involved are still another source of uncertainty.

The assumptions involved in the hydrologic model simulations are also a portion of the uncertainty. As described in section 6.2.5 above, the determination of the impacted flow was only based on the precipitation and temperature changes in the future. The other climatic variables as wind speed, solar radiation, and relative humidity were assumed to be constant throughout the future simulation periods. Even though it is definite that in the future land use changes will also take place, this is also assumed to be constant. Hence, these assumptions can definitely lead to a certain level of additional uncertainty.

As a result, it is clear that all types of uncertainties discussed above are propagated on the future predicted flow volume. Especially uncertainties observed during hydrologic model simulation in baseline periods with observed data influencing the future prediction strength of the model.

Accordingly, as it is showed in figure 6.21(a) below that, the future flow of Koga River significantly impacted by climatic change in months of June, July, August and October. It is also shown in figure 6.21(b) below, the future flow predicted in Annual and Belg

season are within the uncertainty bands which showed that the future flow observed will be dominated by the uncertainties than the climatic change impact. Therefore, it might be possible to conclude that the climatic change impact will be significant in Bega and Kiremt in the period of 2030 than in Belg and Annual for both periods. The cumulative uncertainty observed is the worst in propagation on the predicted future flow volume in Annual and Belg.

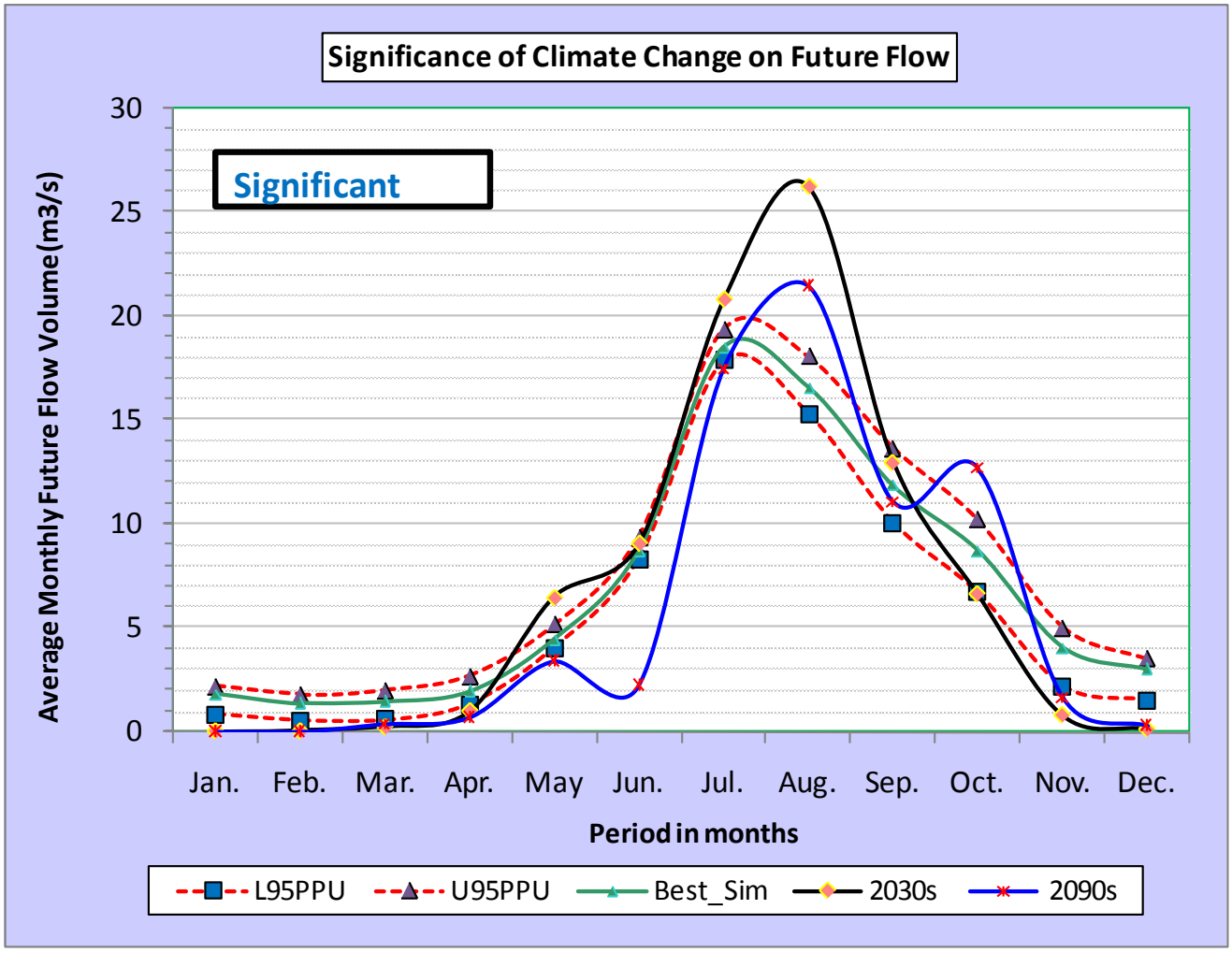

a. Monthly

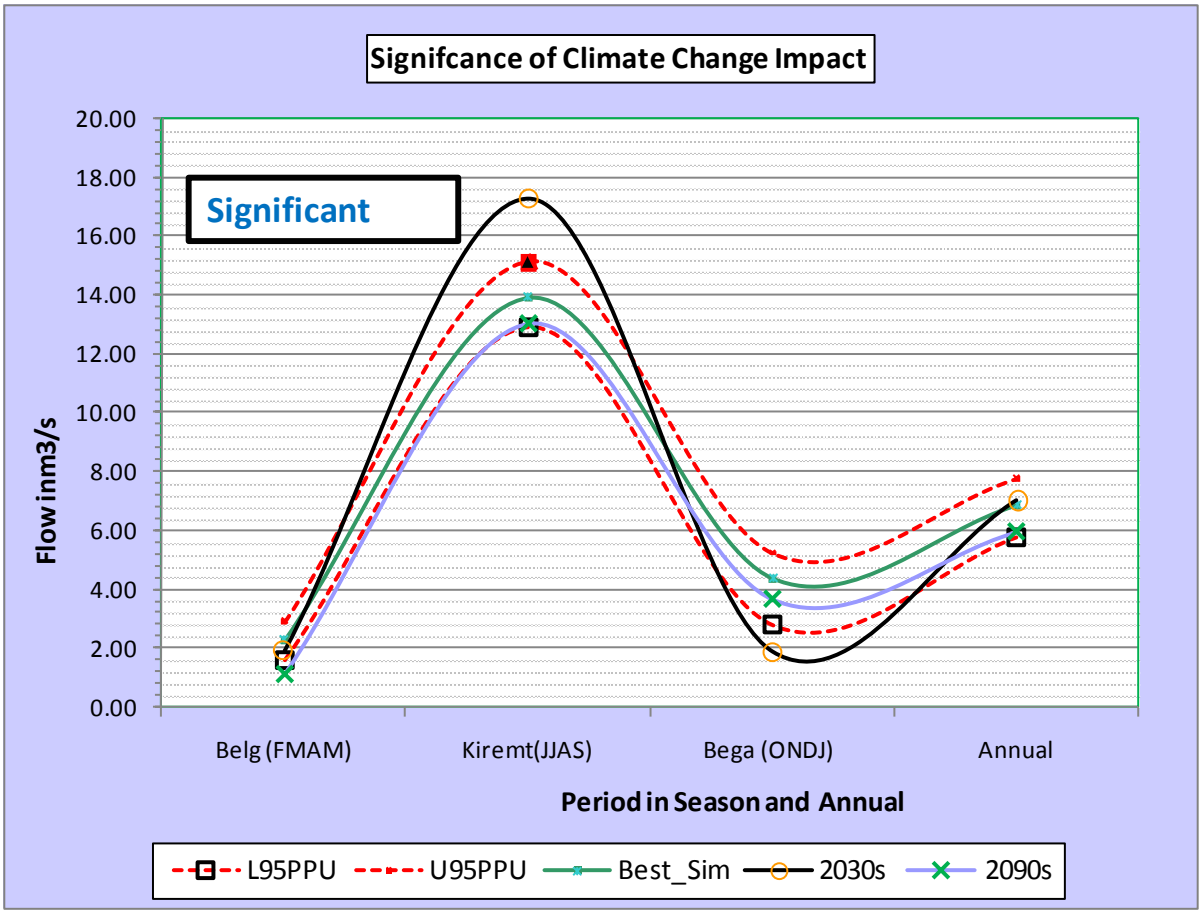

b.Seasonal

Figure 6-21: Significance of future impacted flow and uncertainty bands of Koga River

Thus, considering the assumptions and methods used in this study, the result shows that impacted future flow volume of Koga River will be significantly affected by the climate change impacts.

As it is shown in figure 6.22(a) below the future flow in 2030s and 2090s for most months are in the range of uncertainty limits and this showed that the climatic change impact may be insignificant. Rather the propagated uncertainty will be significantly affecting the future predicted flows. Figure 6.22(b) shows the future flow predicted in all Seasons and Annual are within the uncertainty bands which shows the future flow observed are dominated by the uncertainties than the climatic change impact.

Therefore, it might be possible to conclude that the observed climatic change impact is insignificant in all Seasons and Annual in both periods.

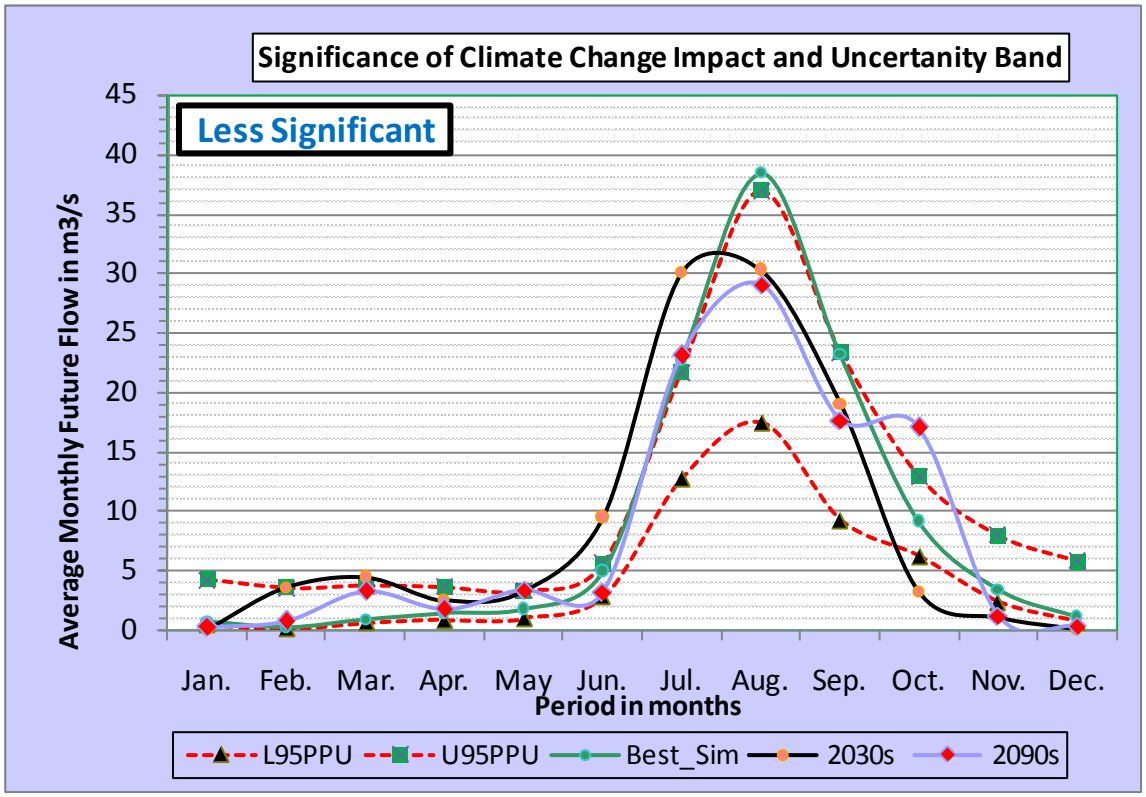

a. Monthly

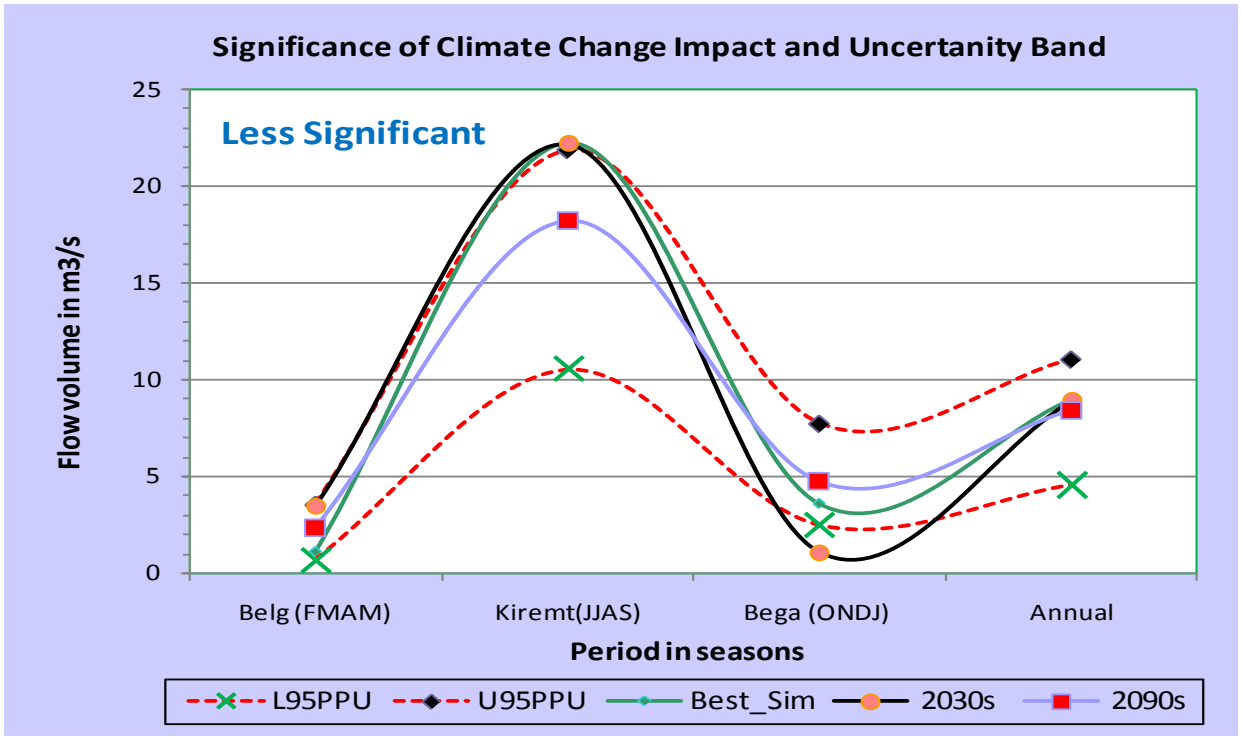

b. Seasonal

Figure 6-22: Significance of future impacted flow and uncertainty bands of Muger River

Thus, considering the assumptions and methods used in this study, the result shows that impacted future flow volume of Muger River is less significantly affected by the climate change impact annually and seasonally in both periods.

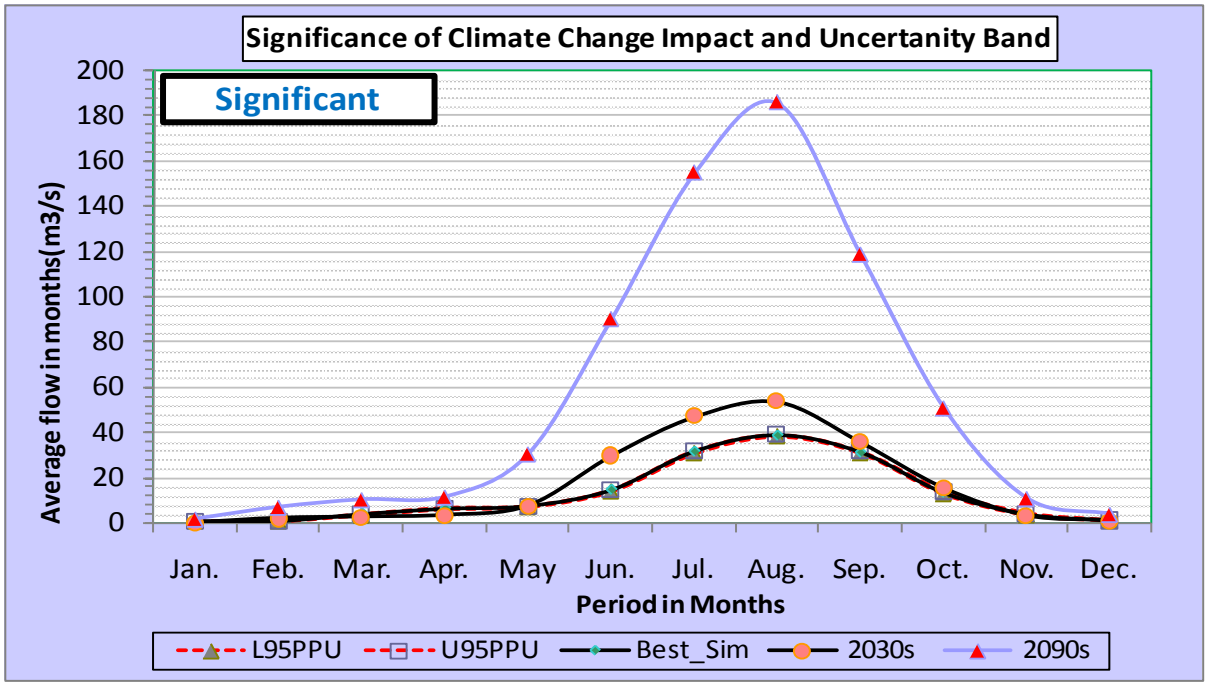

a. Monthly

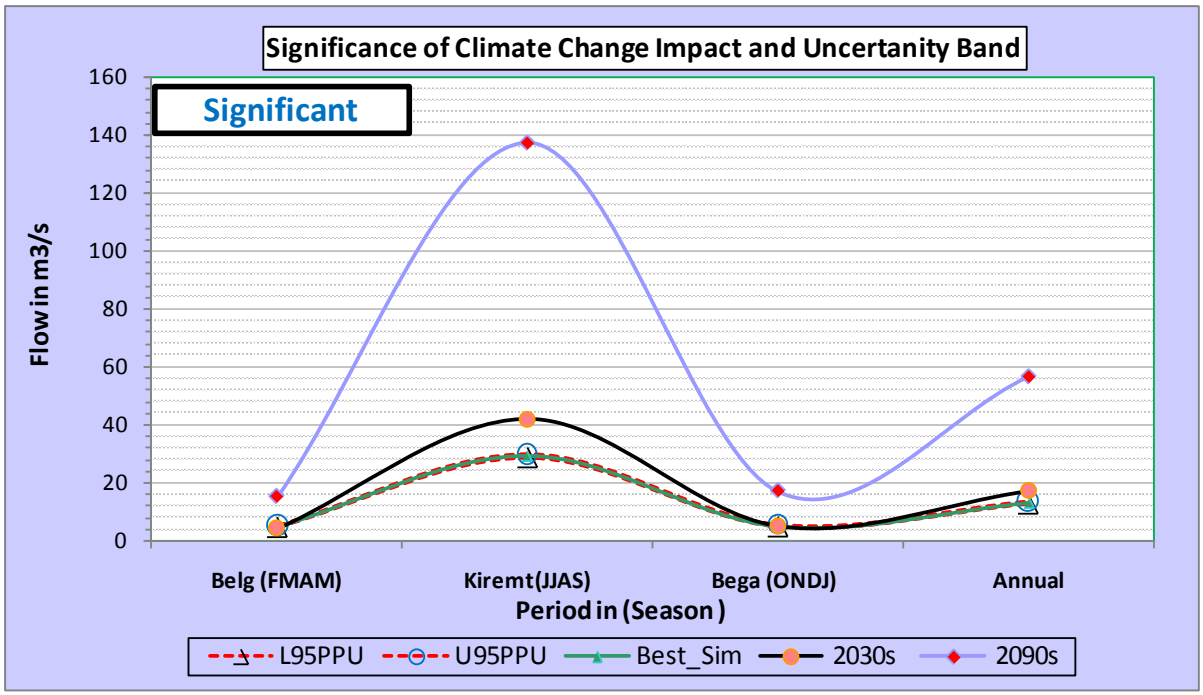

b. Seasonally

Figure 6-23: Significance of future impacted flow and uncertainty bands of Guder River

Here for Guder River as it is shown in figure 6.23(a) above the future flow in 2030s and 2090s for all months are out of the uncertainty limits except for some months such as Jan, Feb, Mar, Nov and Dec, these showed that the climatic change impact may be significant in most months. And seasonally as it is shown in figure 6.23(b) above the future flow of the river is significantly influenced by the climatic change impacts seasonally and annually in both periods except in Belg for both periods and Bega in 2030. The propagated uncertainty will be insignificant in affecting the future predicted flows in most months, annual and seasons.

Thus, considering the assumptions and methods used in this study, the result shows that impacted future flow volume of Guder River is significantly affected by the climate change impact annually and seasonally in both periods.

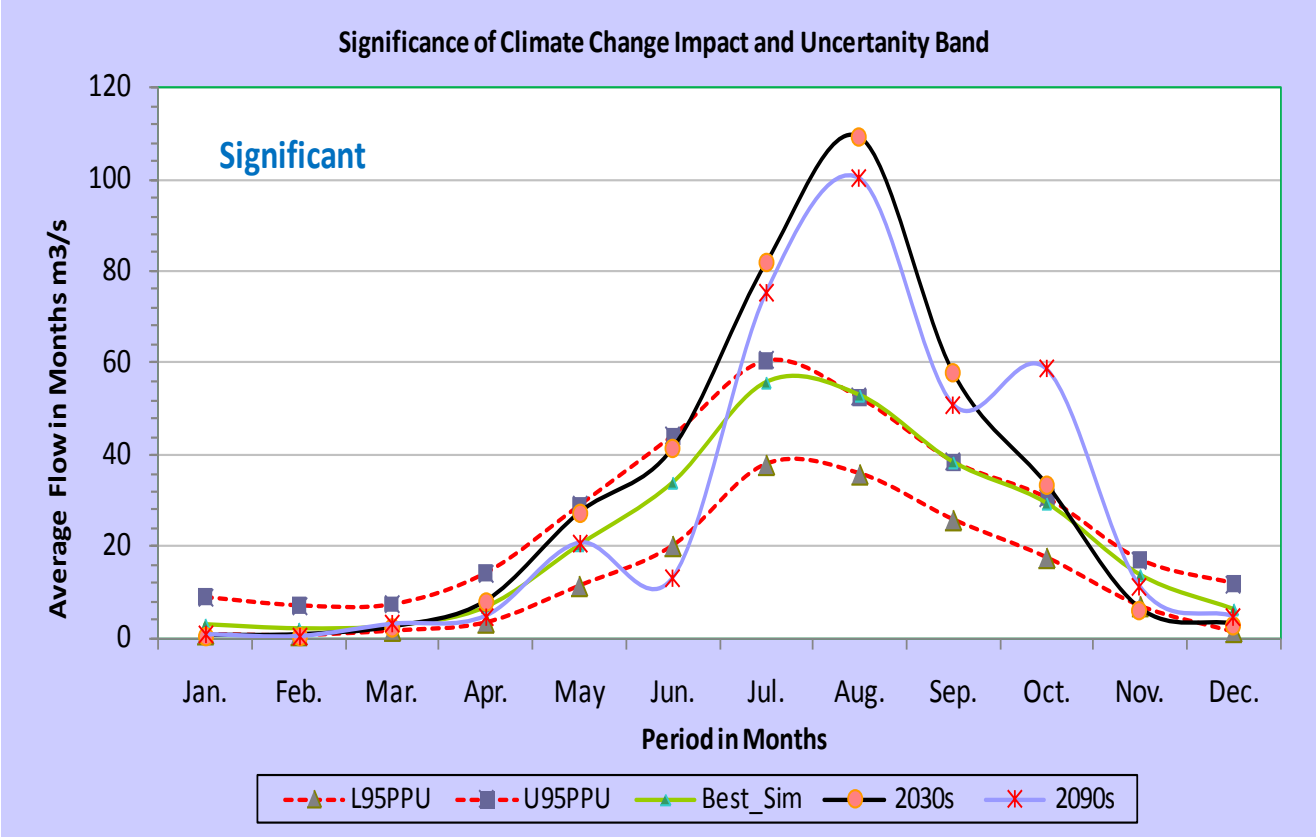

a. Monthly

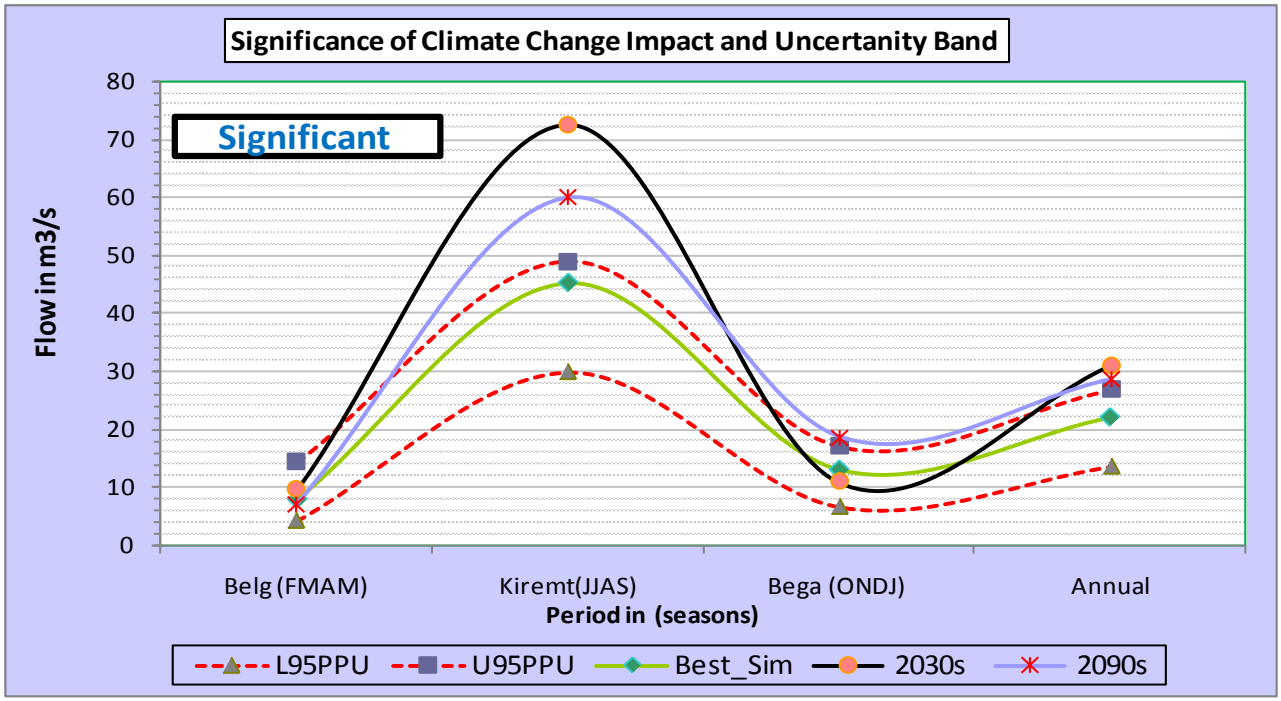

b. Seasonally and Annually

Figure 6-24: Significance of future impacted flow and uncertainty bands of Birr River

As it is shown in figure 6.24(b) above the future flow of the river is significantly influenced by the climatic change impacts seasonally and annually in both periods. The propagated uncertainty will be insignificant in affecting the future predicted flows.

Thus, considering the assumptions and methods used in this study, the result shows that impacted future flow volume of Birr River is significantly affected by the climate change impact annually and seasonally in both periods.

Unlike other, Birr catchment due to reasons which is difficult to justify the streamflow is increasing while the precipitation is decreasing and temperature is increasing.

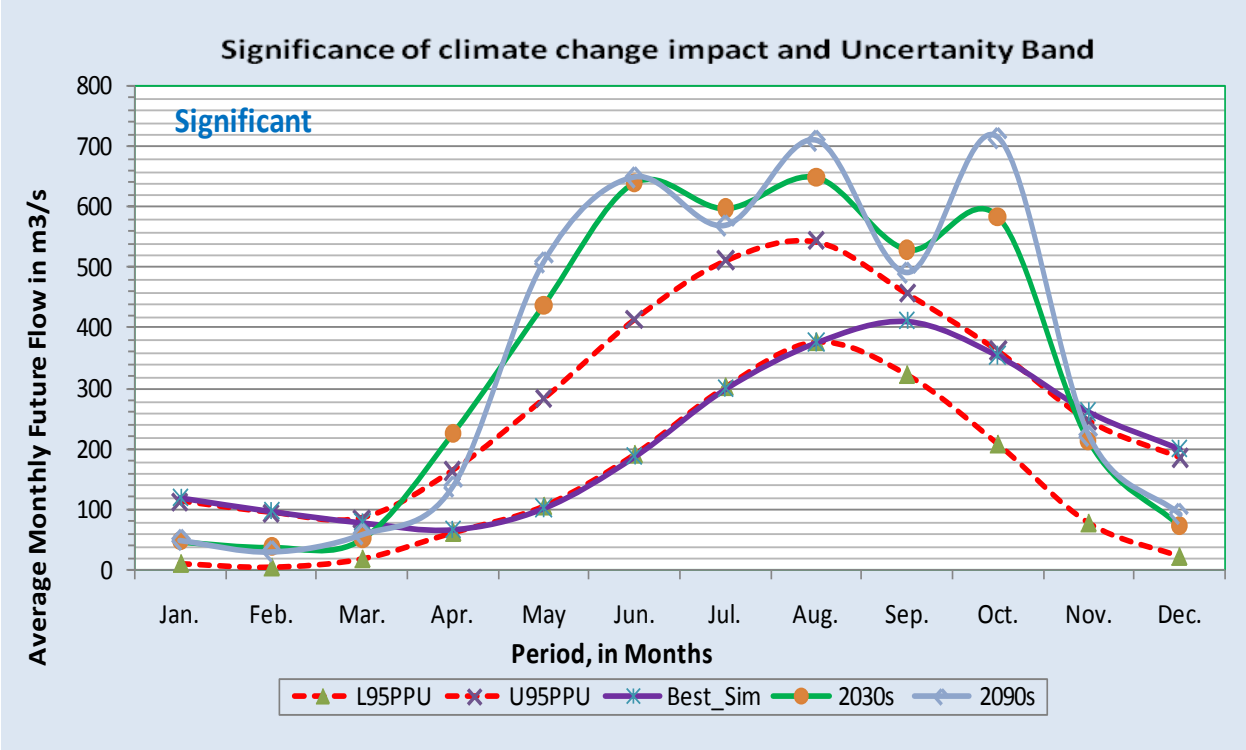

a. Monthly

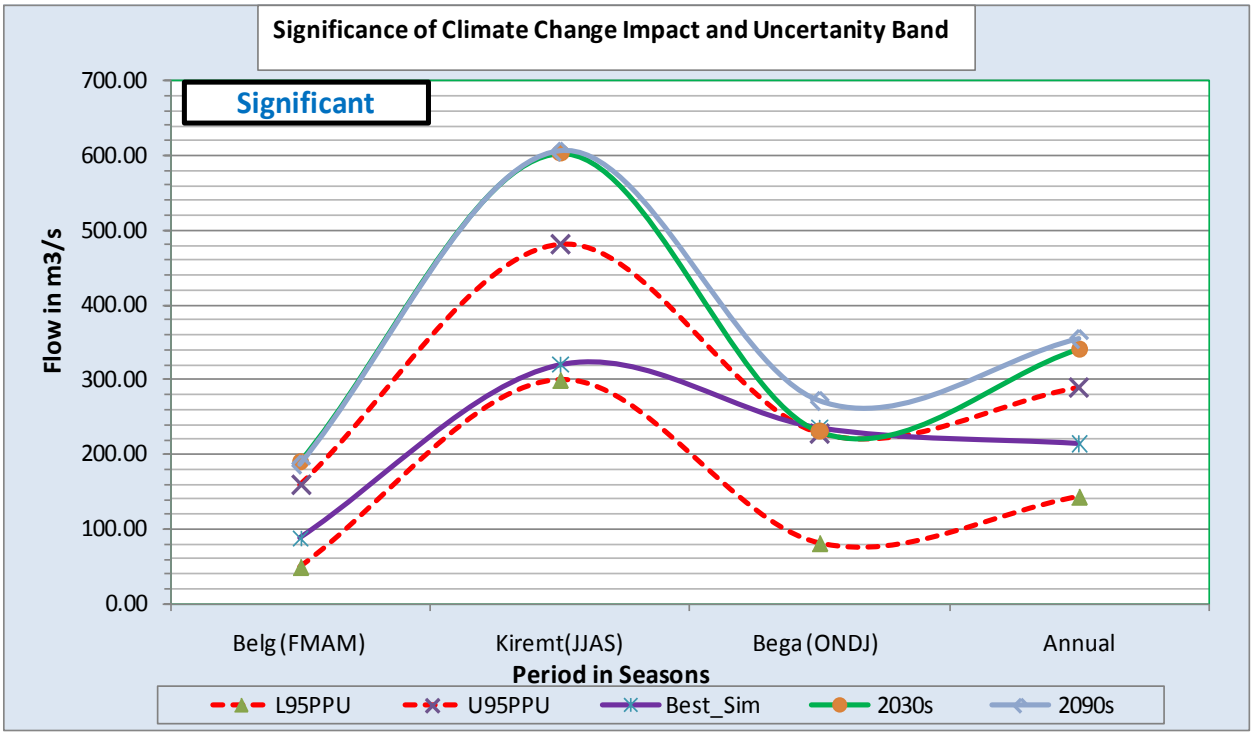

b. Seasonally and Annually

Figure 6-25: Significance of future impacted flow and uncertainty bands of Didessa River

As it is shown in figure 6.25(a) that, the future flow is insignificantly impacted by climatic change in months of Jan, Feb, March, April, Nov and December. It is also shown in figure 6.25(b); the future flow predicted in Bega seasons is within the uncertainty bands which showed that the future flow observed is dominated by the uncertainties than the climatic change impact. Therefore, it might be possible to conclude that the climatic change impact is significant in seasons such as Belg and Kiremt and annually.

The significance of the cumulated uncertainty propagated on the future Didessa River flow is strong in Bega and fair for Annual.

Thus, considering the assumptions and methods used in this study, the result shows that impacted future flow volume of Didessa River is significantly affected by the climatic change impact in Kiremt, Belg and fairly in Annual.

Generally for Guder and Didessa due to the catchments are performing unsatisfactory in uncertainty, it is difficult to conclude about the significance of climate change impact for both catchments rather the results are described for the sake of comparison.

7 CONCULUSION AND RECOMMENDATIONS

7.1. Conclusions

Studies like this, which focus on likely future climate change scenario and their impact on water resource availability of the basin at catchment scale, are essential because of the fact that most water resources developments are carried out at local scale. As understanding the problem is part of the solution, grasping the level of impact is a prerequisite to propose adaptation measures that can reduce the damage and consider the problems for future developments implemented in the area. Hence, the impact of climate change on selected Watershed of Upper Blue Nile Basin on water availability using SWAT was carried out to address the problem and help to propose the adaptation measures.

As a result, SWAT has proved to be good to simulate the hydrological process of the catchments except for Didessa which is unsatisfactory. The regression coefficient and the Nash-Sutcliffe (1970) simulation efficiency values obtained proved this fact. Hence, it can be concluded that SWAT is able to fairly explain the hydrological characteristic of the catchments except for Didessa where simulation efficiency is found to be poor.

Model uncertainty was also done to establish the uncertainty bounds of the model, which is also important boundary limit to evaluate the significance of the impact of climate change. The uncertainty analysis was done by using SUFI2 in SWAT-CUP. Overall the calibration and validation of the model were satisfactory except for Guder and Didessa. It was also shown from the model uncertainties analysis that the percentage of the simulated data within the uncertainty bound is only 20%. But for other 4 catchments the percentage of simulated flow within the uncertainty limit is more than 40%.

The study used a Regional Climatic Model Version 3(RegCM3) climate change scenario to assess the impacts of these changes on the water resource and determining the significance of impacts for the selected catchments. The climate change scenarios of

precipitation and temperature developed for the years 2031-2100 using the outputs of RegCM3 showed that both temperature and precipitation are likely to show an increasing trend in Guder, Muger and Didessa catchments. On the contrary, in Koga and Birr catchments, total annual precipitation show a decreasing trend while average monthly temperature shows an increasing trend. These climate variables were applied to SWAT hydrological model to simulate future flows.

In general in all catchments; except in Didessa and Koga, the impact of climate change may cause an increase in monthly and annually flow volume in both periods. The estimation of the annual average flow volume changes in the future in both periods shows, the total flow volume might increase within a range 48% to 185% and decrease within the range of 0.33% to 6.7%.

The changes in the climate variables are likely to have significant impacts on the flow volume into the rivers. As per the sensitivity analysis result precipitation is the most sensitive variable for all catchments except for Didessa. Despite the change of both climatic variables in the future, the change in monthly average temperature seems to be obscured by change in monthly average precipitation for all except for Didessa catchment. It is important to understand that these outcomes have been the result of a very elaborate computation of continuous water balance with daily time through the distributed hydrological modeling framework. This has enabled the simulation of the natural processes in a realistic manner so as to represent the complex spatio-temporal variability inherent in the natural systems.

The increase in Belg season flow will have a paramount importance for small scale irrigation activities practiced by local farmers. It is observed that there may be a net annual decrease in flow volume in Koga and Didessa rivers due to climate change. Koga River is the tributary river feeding into Lake Tana, any effect on this river is reflected in the Lake water level. The decrease in flow will directly affect the ongoing water resource developments planned on the Abbay, Didessa and Lake Tana. However, it may also aggravate the recurrent flooding problems in the surrounding areas of the other rivers.

According to the uncertainty analysis carried out, the significance of the climatic change impact for all catchments was analyzed. As a result it might be possible to conclude that in all rivers except Muger and Koga rivers the climate change impact were significant in main rainy season (Kiremt) and in Annual.

Therefore, it can be deduced that climate change impact is the most sensitive than the propagated uncertainty for all catchments except on Muger and Koga rivers during rainy season (Kiremt) and in Annual.

7.2. Recommendations

This study involved a number of models and model outputs where each possessed a certain level of uncertainty. Even though, uncertainty analysis of the hydrologic model prediction was done considering the base period, the uncertainty due the model used to generate and downscale future climatic variables and the limited emission scenario are still with uncertainties. Hence, the results of this study should be taken with care and be considered more indicative than accurate predictions. Meanwhile, this study should be extended by considering changes in landuse, soil and other climate variables in addition to the changes in precipitation and temperature. The impacts of climate change on the water utilizing socio-economic sectors should also be considered.

Continuing studies; however, should consider the wide range of uncertainties associated with models and try to reduce these uncertainties by the use of different GCM outputs, downscaling techniques, and emission scenarios. Use of a number of RCMs can help to generate a more “reliable” ensemble mean. Further downscaling techniques, which especially improve precipitation-downscaling, should be given a due attention. Besides, with regard to the emission scenarios, as all SRES scenarios have equal probability of occurrence, future studies should also consider the entire range of reasonable possible future scenarios.

The physically based, spatially distributed, and public domain Soil and Water Assessment Tool (SWAT) is found to be a very appropriate tool to simulate both

historical as well as impacted hydrological processes in the watershed. Therefore, SWAT can be utilized very well for hydrological simulations in all catchments except in Didessa which have to be used with care. Besides, the model should be further tested for its suitability in other catchments of Upper Blue Nile Basin. In addition this study especially for Didessa catchment indicate that SWAT has fell to model the hydrologic characteristics due to problem of the model structure in capturing the hydrologic swamp in the catchment.

It is believed that the results of this study give a clue and increase awareness on the possible future risks of climate change. Hence, such studies should continue on different Ethiopian Basins for better preparedness in the future. This will contribute partly to the sustainability if impacts of climate change are considered at all levels (from planning to execution and management) of water resource development projects.

The challenge of having adequate, reliable and good quality data may be a far away dream in the developing countries. Input data should, therefore, be checked for missing and unrealistic values in order to come up with good results. It was quite a discouraging task to collect data and when it was made available, the quality was always questionable. As such, other types/sources of data such as remotely sensed data (e.g. for rainfall) could be explored to provide a wider coverage of rainfall distribution and complement the already existing records.

REFERENCES

1. **Abbaspour, 2007.** SWAT-CUP2: SWAT Calibration and Uncertainty Programs - A User Manual. Department of Systems Analysis, Integrated Assessment and Modeling (SIAM), Eawag, Swiss Federal Institute of Aquatic Science and Technology, Duebendorf, Switzerland, 95pp.
2. **ABMP-Main Report, 1999.** Abbay Basin Master Plan, Ministry of Water Resources (MoWR),Addis Ababa, Ethiopia
3. **Arnold, etal. 1995.** Automated base flow separation and recession analysis techniques. Ground Water Vol 33(6): 1010-1018pp
4. **Ashenafi S.A. (2009).** Evaluation of Impacts of Climate Change on Hydrology and Water Resource Availability of Upper Blue Nile Basin, Ethiopia, M.Sc. Thesis degree at the Arba Minch University, Ethiopia.
5. **Bceom, 1999**. Abbay River Basin Integrated Development Master Plan Project: phase 2 data collection-site Investigation Survey and Analysis.
6. **Beven, K. and J. Freer. (2001).** Equifinality, data assimilation, and uncertainty estimation in mechanistic modeling of complex environmental systems using the GLUE methodology, Journal of Hydrology. 249: 11-29.
7. **Blue Nile Basin Atlas. (2009).** Characterization and Atlas of the Blue Nile Basin and its Sub basins. Aster Denekew Yilma and Seleshi Bekele Awulachew. International Water Management Institute. January, 2009
8. **Chow, V.T. (1988).** Applied Hydrology, McGraw HILL INTERNATIONAL EDITIONS. New York.
9. **Conway D, and M. Hulme (1993)**. Recent fluctuations in precipitation and runoff over the Nile subbasins and their impact on main Nile discharge. Climatic Change 25:127 151.
10. **Conway. D (1999).** A water balance model of the Upper Blue Nile in Ethiopia Hydrological Sciences Journal des Sciences Hydrologiques, 42(2)

11. **Conway & Hulme. (1996).** The impact of climate Variability and Climate Change in the Nile Basin on Water resource in Egypt: water resource Development, Vo l, 12, No.3, pp 277-296
12. **Conway. D (2000)**. The Climate and Hydrology of the Upper Blue Nile River, School of Development Studies, University of East Anglia, Norwich NR4 7U,The Geographical Journal, Vol. 166, No. 1, March 2000, pp. 49-62.
13. **Conway, D. (2005).** From headwater tributaries to international river: Observing and adapting to climate variability and change in the Nile basin.
14. **Dilnesaw A. (2006).** Modeling of Hydrology and Soil Erosion of Upper Awash River Basin. PhD Thesis, University of Bonn: 233pp.
15. **Eckhardt K. and J. G. Arnold**, **2001**. "Automatic calibration of a distributed catchment model", Journal of Hydrology, vol. 251, no. 1/2, 2001, pp. 103-109.
16. **Gassman, etal. 2005.** Climate Change Sensitivity Assessment on Upper Mississippi River Basin Streamflows Using Swat. Journal of the American Water Resources Association. 42(4): 997-1015.
17. **Green C.H. etal, 2006.** Auto-calibration in Hydrological Modeling: Using SWAT 2005 in small-scale watersheds. Science Direct, Environmental Modeling & Software (2004), 422-434, available at: *www.sciencedirect.com* [Accessed 07 December 2010]
18. **Guithi, 2006**. Use of soil and water assessment tool (SWAT) and historical data to estimate the streamflow in ungauged catchment: A case study from Naivasha basin – Kenya.
19. **Gleick, etal. 2002.** Regional Hydrologic Consequences of Increases in Atmospheric CO2 and Other Trace Gases. Climate Change 10: 137-161.
20. **IPCC, 2001**. Climate Change 2001. The Scientific Basis. Contribution of Working Group I to the Third Assessment Report of the Intergovernmental Panel on Climate Change [Houghton, J.T.,Y. Ding, D.J. Griggs, M. Noguer, P.J. van der Linden, X. Dai, K. Maskell and C.A. Johnson]. Cambridge University Press, Cambridge, United Kingdom and New York, NY, USA, 881pp.
21. **IPCC, 2007**. Technical Summary 2007: The Scientific Basis. Technical Summary of the Working Group I Report [Houghton, J.T., Y. Ding, D.J. Griggs, M. Noguer, P.J. van der

Linden, X. Dai, K. Maskell, and C.A. Johnson]. Cambridge University Press, Cambridge, United Kingdom and New York, NY, USA, 94pp.

22. **Kedir A., 2008.** Assessment of Climate Change impacts on the Hydrology of Gilgel Abbay Catchment in the Tana Sub Basin, Ethiopia, M.Sc. Thesis degree at the UNESCO-IHE Institute for Water Education, Delft, the Netherlands.
23. **Muluneh B. (2008).** Evaluation of Impact of Climate Change on Water Resource Availability in the Catchments of Blue Nile Basin, MSC Thesis degree at Arba Minch University, Arba Minch, Ethiopia.
24. **Katz, R.W. and B.G. Brown. 1992.** Extreme Events in a Changing Climate: Variability is More Important than Averages. Climate Change 21:289-302.
25. **Mearns**, **etal, (2003):** Guidelines for use of climate scenarios developed from Regional Climate Model experiments. Data Distribution Centre of the International Panel of Climate Change, 38 pp. Available for download from: *http://ipcc-ddc.cru.uea.ac.uk*
26. **NMSA, 2001.** Convention on Climate Change (UNFCCC), National Meteorological Services Agency, Addis Ababa, Ethiopia
27. **Nash J.E.**, **Sutcliff, J.V., 1970**. River Flow Forecasting through Conceptual Models Part I- A discussion of Principles. Journal of Hydrology, 10:282-290.
28. **Neitsch S.L., etal, 2005**. Soil and Water Assessment Tool (SWAT) Theoretical Documentation, Version 2005, Grassland Soil and Water Research Laboratory, Agricultural Research Service, Blackland Research Center, Texas Agricultural Experiment Station.
29. **Santhi, etal**, **(2001 a,b).** Validation of SWAT model on a large river basin with point and nonpoint sources. Journal of the American Water Resources Association 37:1169-1188.
30. **Strom, G., etal, 1997**. Development and test of the distributed hydrological model, Journal of Hydrology
31. **Tarekegn D. and Tadege A. (2006**). Assessing the impact of climate change on the water resource of Lake Tana sub–basin using WAtBAL model.
32. **Thorpe A.J., 2005,** Climate Change Prediction: A challenging scientific problem. Institute of physics,., available at:*http://www.iop.org/activity/policy/Publications/file_4147.pdf* [accessed 14 Sep 2010]

33. **Wilby, R.L. 1995.** Simulation of precipitation by weather pattern and frontal analysis. Journal of Hydrology. 173: 91–109.

34. **Yehun D. (2009).** Hydrological Modeling to Assess Climate Change Impact at Gilgel Abbay River, Lake Tana Basin, MSC Thesis degree at Lund University, Sweden.

35. **Zeray, L., 2006**. Climate Change Impact on Lake Ziway Watershed Water Availability, Ethiopia. MSc. Cologne: University of Applied Sciences Cologne, Institute for Technology in the tropics.

Websites used for software downloads

SWAT (ARCSWAT) website *http://www.brc.tamus.edu/swat/avswat.html* [Accessed June 2010]

Baseflow-program for the automated base flow separation and recession analysis technique *http://www.brc.tamus.edu/swat/soft_baseflow.html* [Accessed 22 July 2010]

Weather parameter calculator WXPARM (Williams, 1991) and dew point temperature calculator DEW02 programs *http://www.brc.tamus.edu/swat/soft_links.html* [Accessed 5 July 2010]

ANNEXES

Annex 1: Summary of stream flow regression for a period of 1992-2005 for rivers considered in the modeling work

Linear Fit: y=a+bx	
Coefficient Data:	
a =	1.200834
b =	0.085721

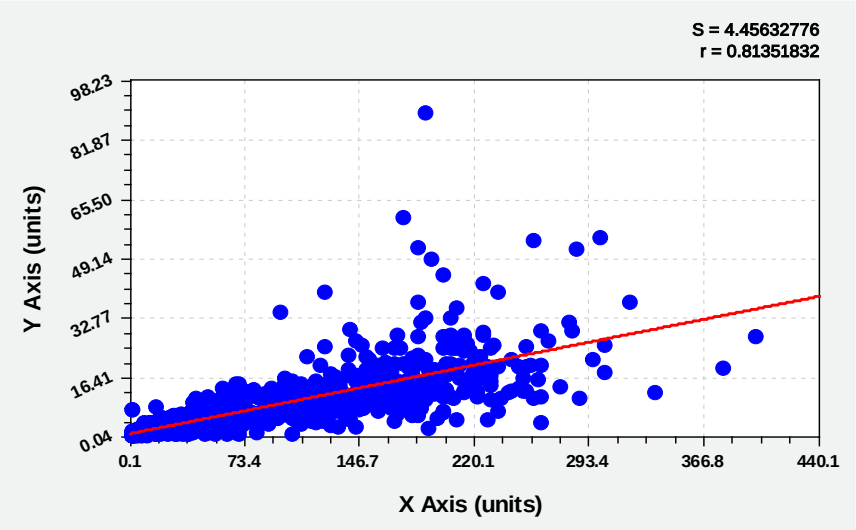

Annex 1.1: Flow regression of Koga with Gilgel Abay Rivers for a period of 1996-2005

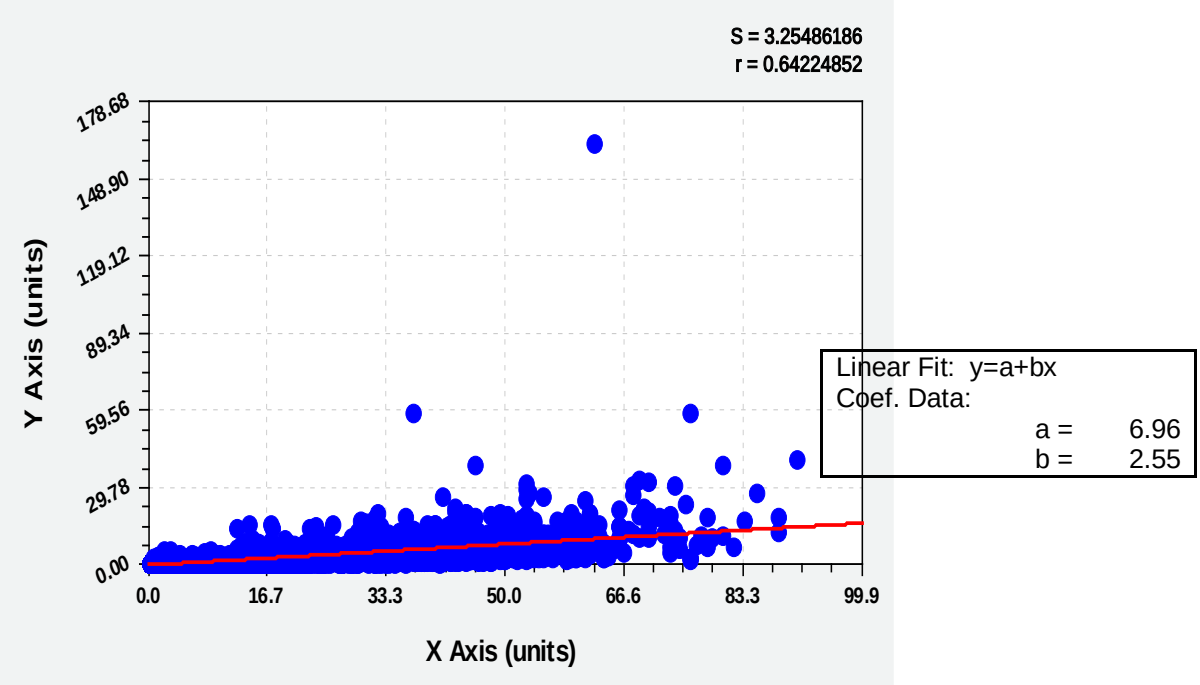

Annex 1.2: Flow Regression Equation for Guder with Indris Rivers for a Period of 1994-2005.

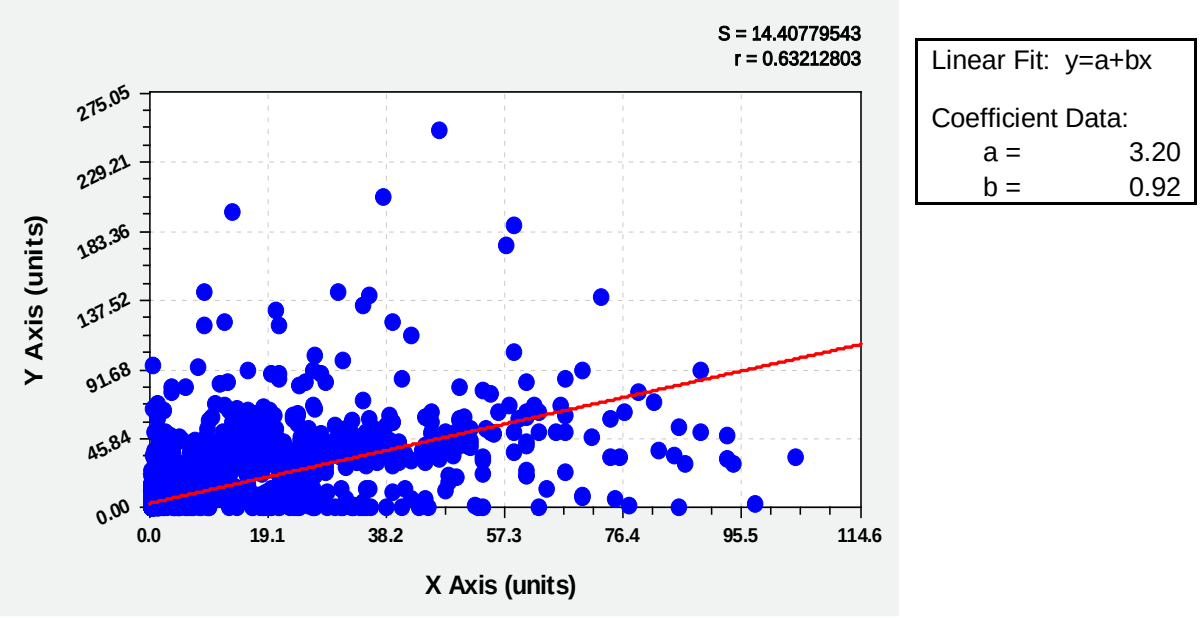

Annex 1.3: Flow Regression Equation for Muger with Aleltu Rivers for a period of 1994-2004

Annex 2: *List of Common Parameter used for Sensitivity* Analysis

Annex 2.1 List of Common parameters used for sensitivity analysis, automatic model calibration and uncertainty analysis

Parameter Code	Rank	Parameter Description	File
CN2	1	Initial SCS CN II value	*.mgt
RCHRG_DP	2	Deep Aquifer percolation coefficient	*.gw
GWQMN	3	Threshold depth of water in the shallow aquifer req'd for return flow	*.gw
GW_REVAP	4	Groundwater revap coefficient	*.gw
CANMX	5	Maximum canopy storage	*.hru
SOL_AWC	6	Available water capacity	*.sol
ESCO	7	Soil evaporation compensation factor	*.hru
SLOPE	8	Average slope steepness	*.hru
SOL_Z	9	Soil depth	*.sol
SOL_K	10	Saturated hydraulic conductivity	*.sol
REVAPMN	11	Threshold water in the shallow aquifer for revap to occur	*.gw
ALPHA_BF	12	Baseflow alpha factor	*.gw
GW_DELAY	13	Groundwater delay	*.gw
BIOMIX	14	Biological mixing efficiency	*.mgt
CH_K2	15	Channel effective hydraulic conductivity	*.rte
SURLAG	16	Surface runoff lag time	*.bsn
SOL_ALB	17	Moist soil albedo	*.sol
SLSUBBSN	18	Average slope length	*.hru
BLAI	19	Sub Maximum potential leaf area index	*.crp
EPCO	20	Plant uptake compensation factor	*.hru
CH_N	21	Manning's n value for main channel	*.rte

Parameters	Change method	Descriptions for the method
Cn2	3	1 Replacement of parameter by value
Alpha_Bf	1	2 Adding value to initial parameter
Sol_Awc	3	3 Multiplying initial parameter by value
Gwqmn	2	
Revapmn	2	
Canmx	1	
Blai	1	
Sol_Z	3	
Esco	1	
Gw_Revap	2	
Slope	3	
Ch_K2	1	
Sol_K	3	
Epco	1	
Gw_Delay	2	

Annex 2.2: Sensitivity results with their MRS Value for all Catchments according to their rank

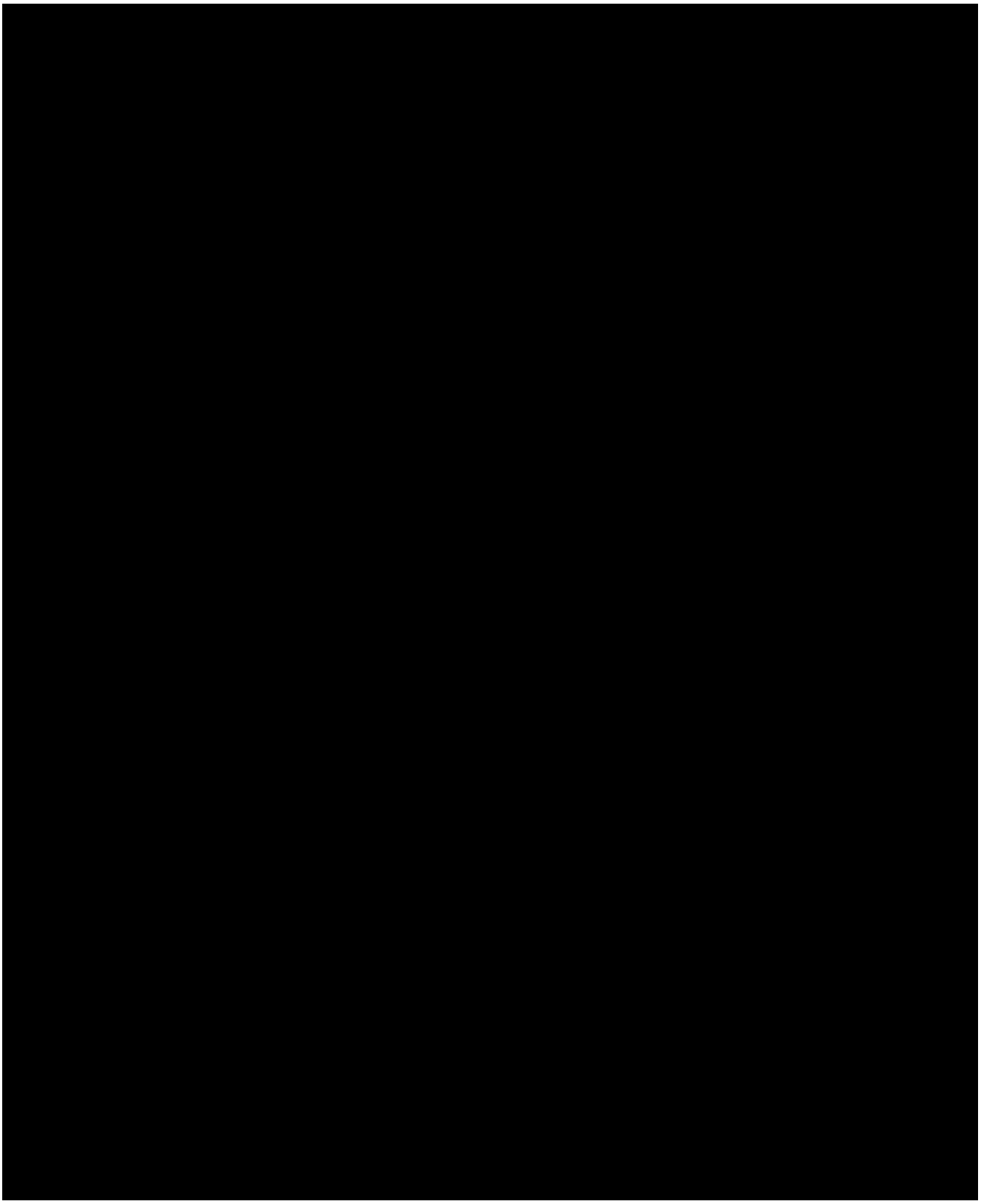

Annex 3: Graphs describe the observed and simulated streamflow during Calibrations and Verifications.

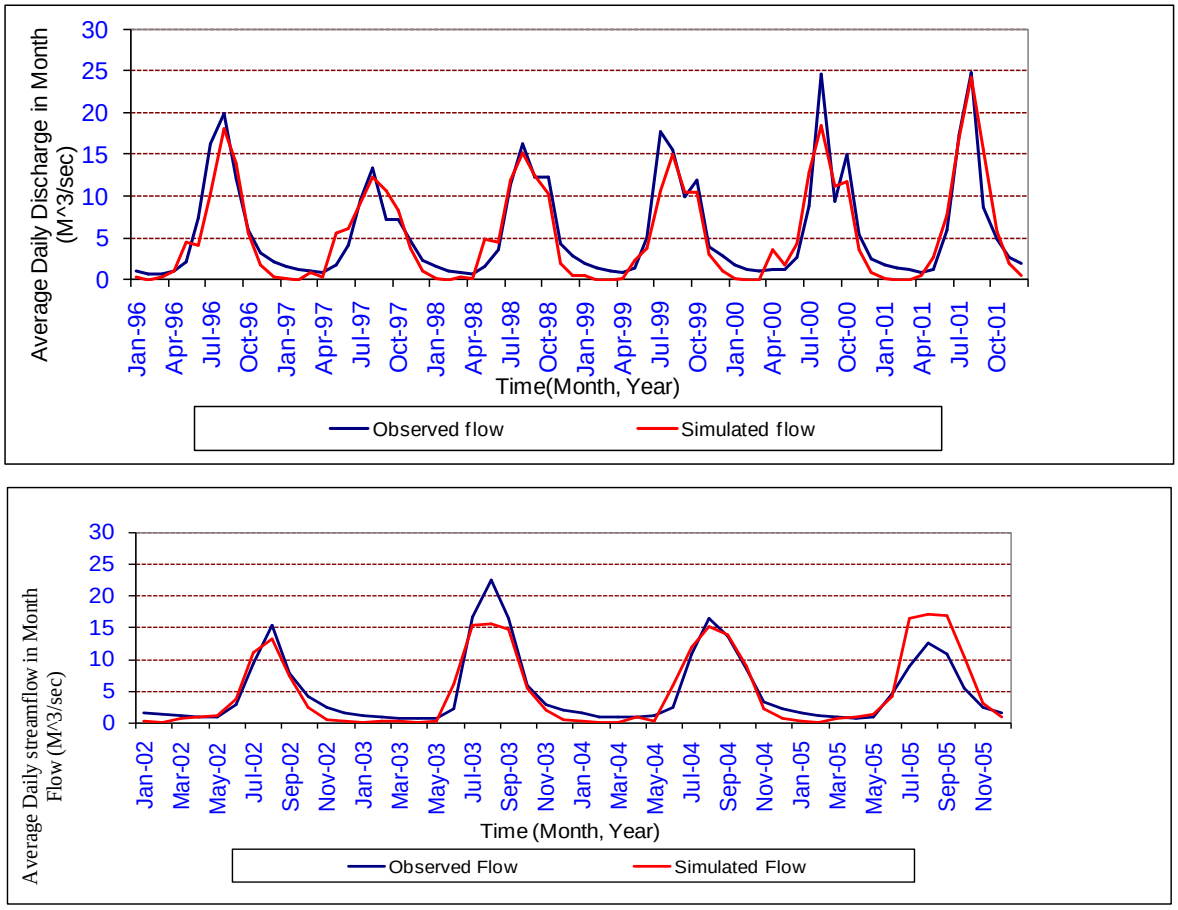

Annex 3.1: Average daily calibration and Validation results in month at the outlet of Koga River at Merawi. (At top: Calibration (1996-2001) and at bottom: Validation (2002-2005))

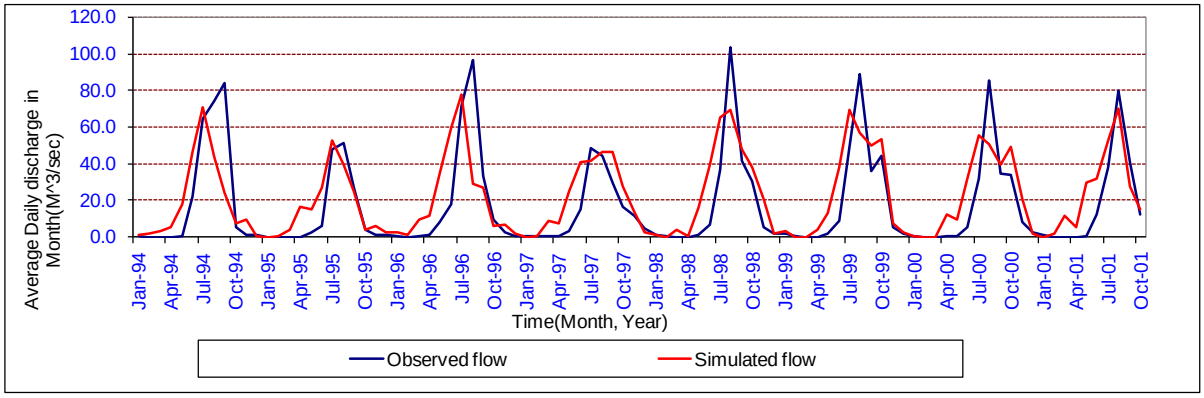

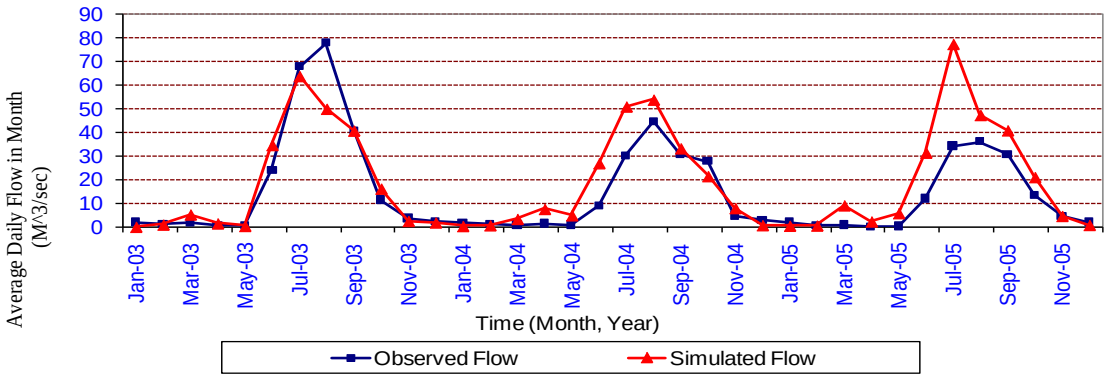

Annex 3.2: Average daily Calibration and Validation results in month at the outlet of Birr River near Jiga. (At top: Calibration (1994-2001) and at bottom: Validation (2003-2005))

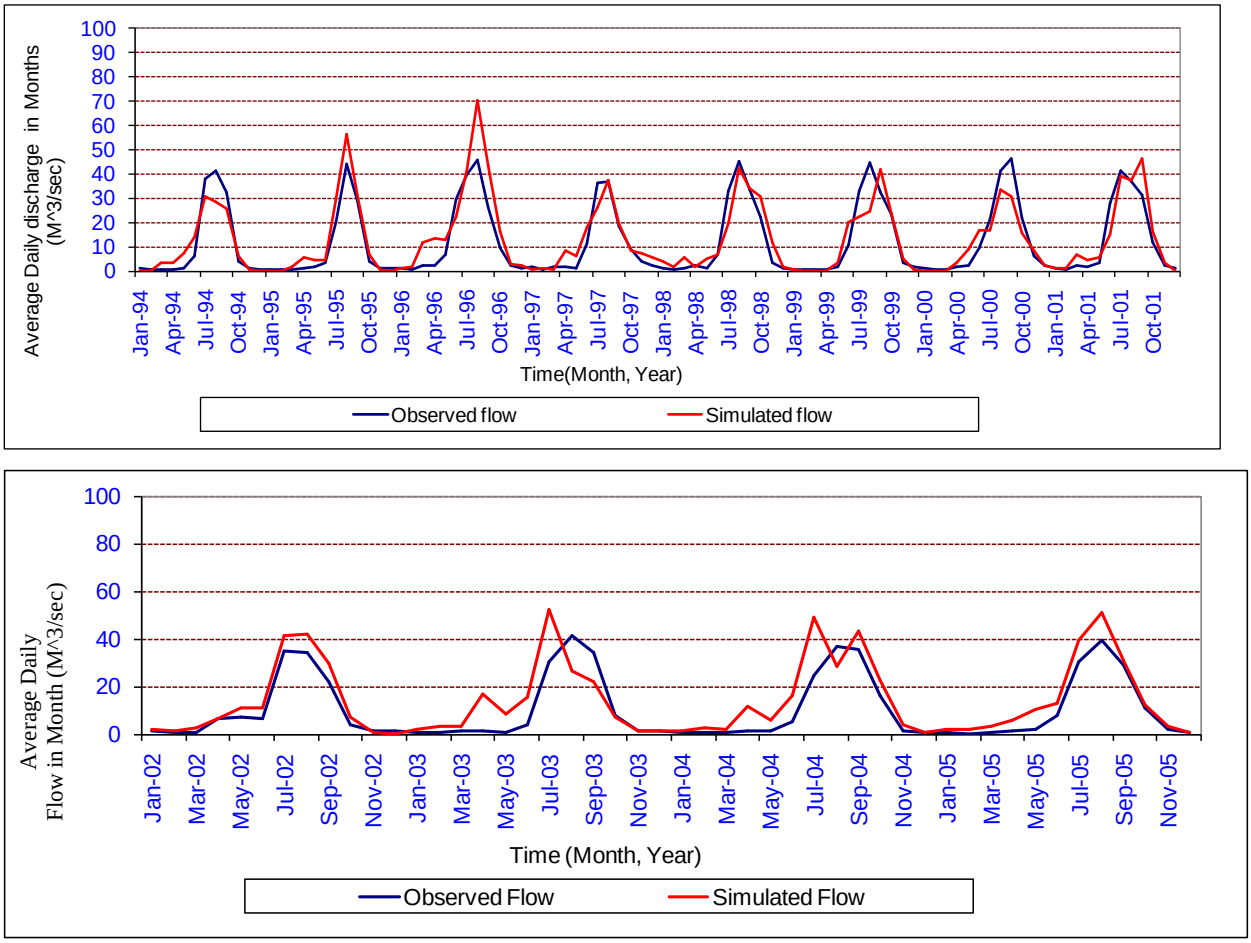

Annex 3.3: Average daily Calibration and Validation results in month at the outlet of Guder River at Guder. (At top: Calibration (1994-2001) and at bottom: Validation (2002-2005))

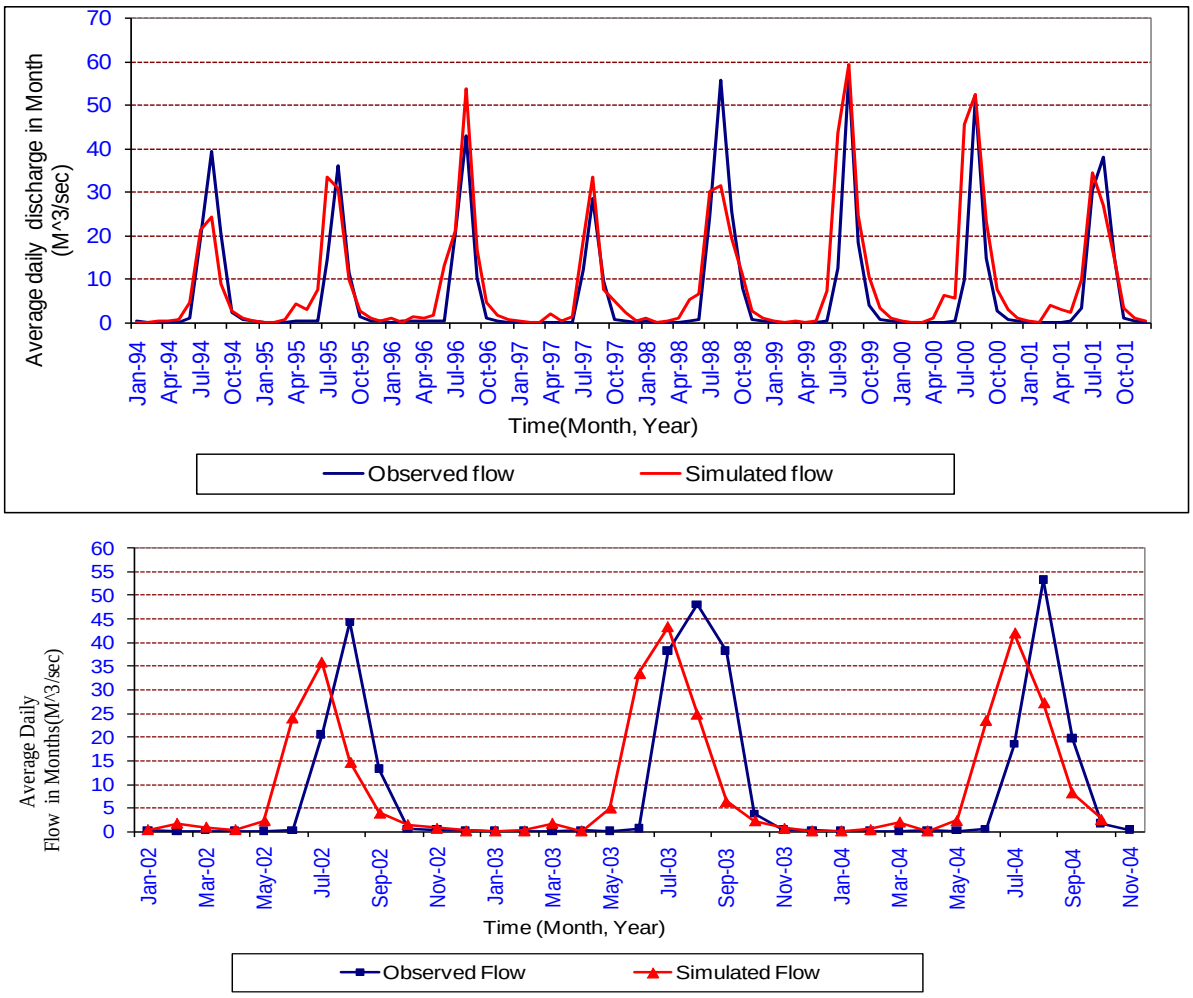

Annex 3.4: Average daily Calibration and Validation results in month at the outlet of Muger River near Chancho. (At top: Calibration (1994-2001) and at bottom: Validation (2002-2004))

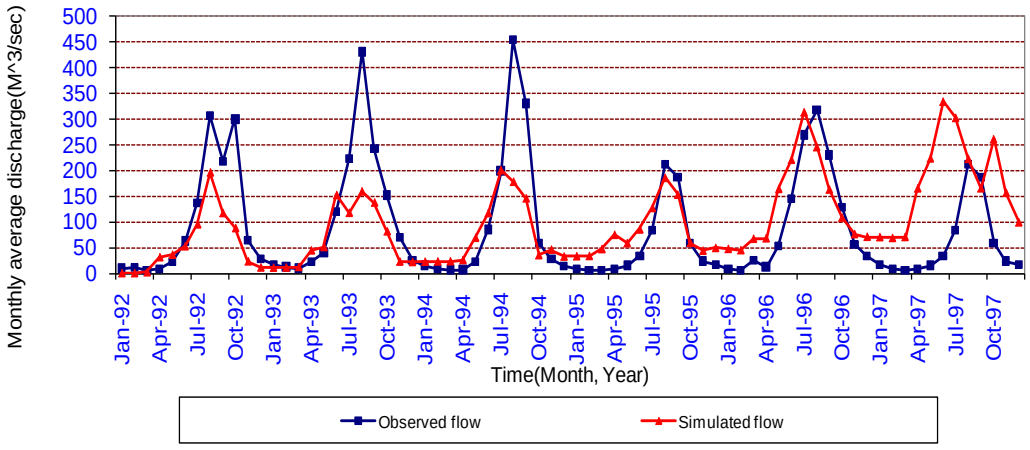

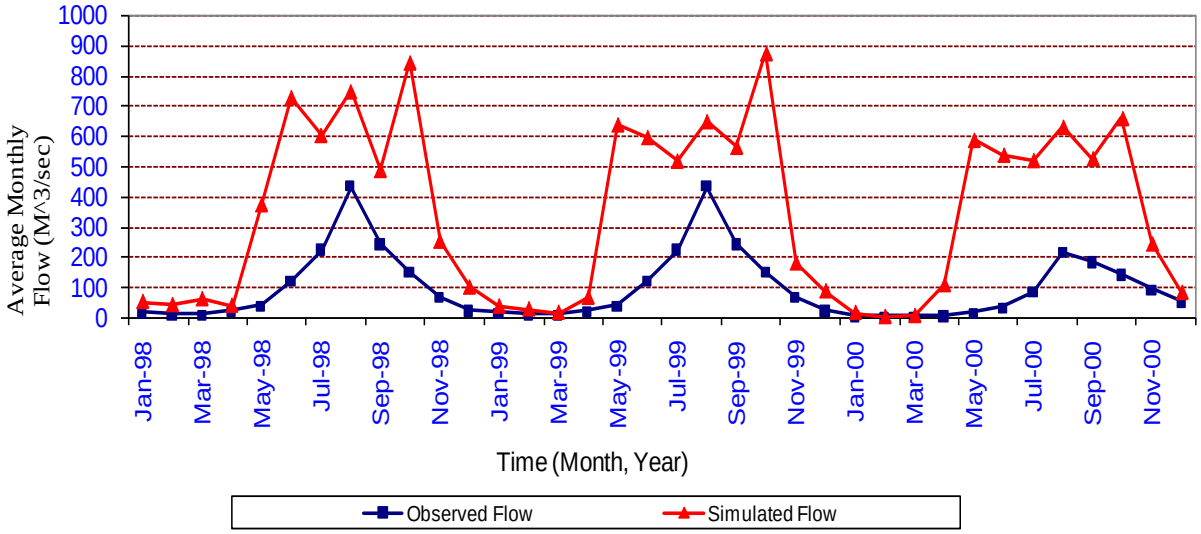

Annex 3.5: Average daily Calibration and Validation results in month at the outlet of Didessa River at Arjo. (At top: Calibration (1992-1997) and at bottom: Validation (1998-2001))

Annex 4: Graphs describe the consistency check for rainfall stations.

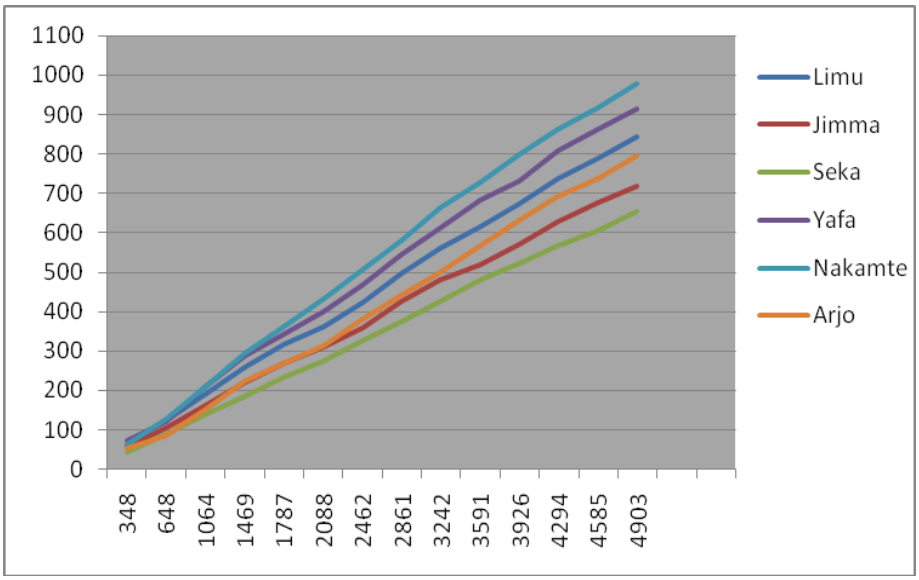

Annex 4.1 Consistency check of percipitation stations used in Didessa Catchments.

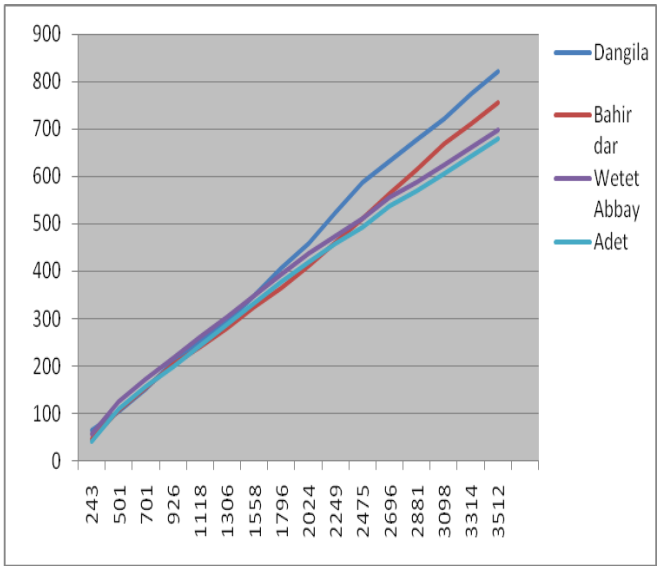

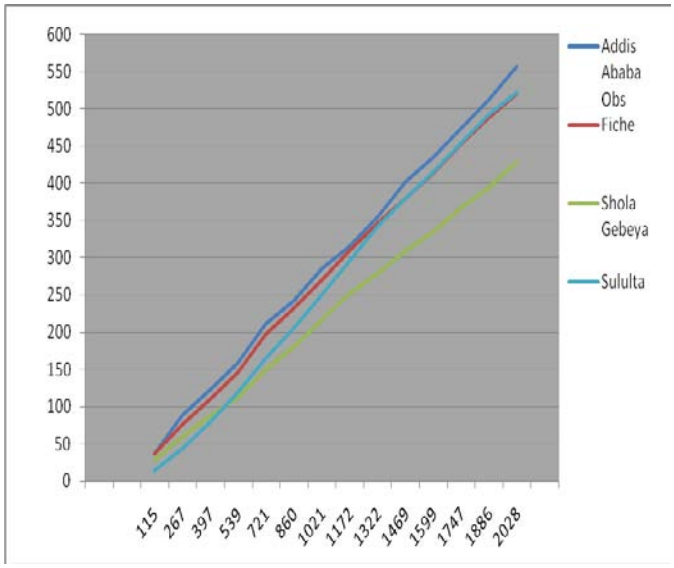

Annex 4.2 Consistency check of percipitation stations used in Koga Catchments(at left) and Muger(at right).

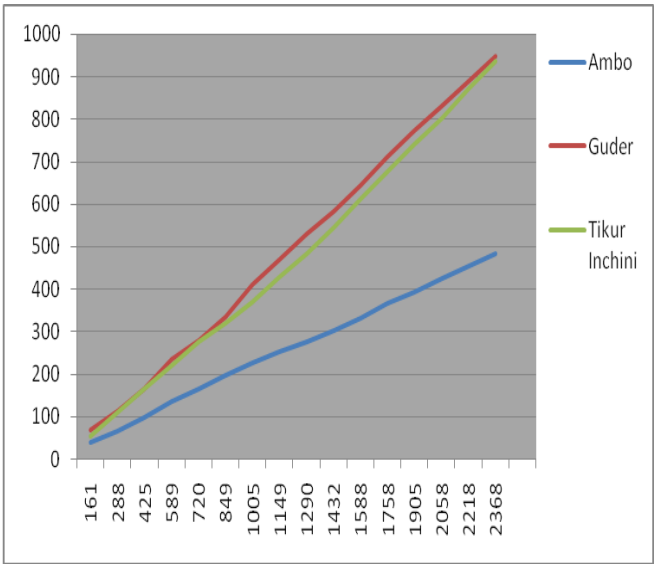

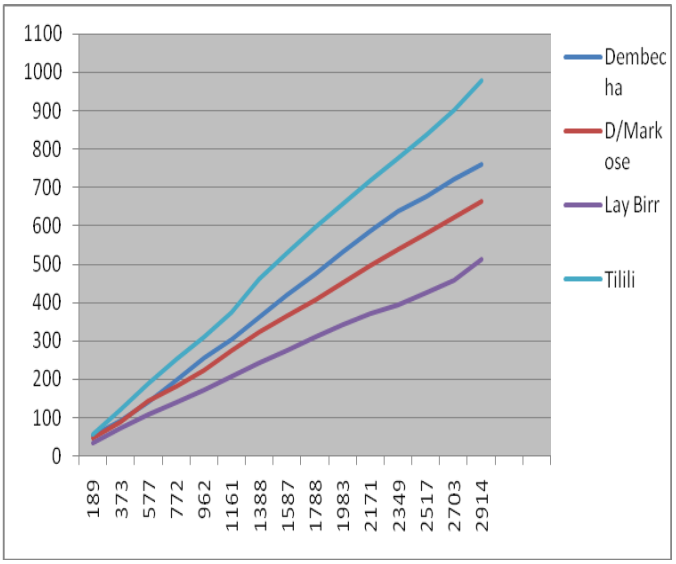

Annex 4.3 Consistency check for percipitation stations used in Guder Catchments(at left) and Birr(at right).